2009-06-23

Intestinal HCO3- Secretion in Fish: A Widespread Mechanism with Newly Recognized Physiological Functions

Josi R. Taylor
University of Miami, jtaylor@rsmas.miami.edu

UNIVERSITY OF MIAMI

INTESTINAL HCO_3^- SECRETION IN FISH:

A WIDESPREAD MECHANISM WITH NEWLY RECOGNIZED PHYSIOLOGICAL FUNCTIONS

By

Josi R. Taylor

A DISSERTATION

Submitted to the Faculty
of the University of Miami
in partial fulfillment of the requirements for
the degree of Doctor of Philosophy

Coral Gables, Florida

June 2009

UNIVERSITY OF MIAMI
A dissertation submitted in partial fulfillment of
the requirements for the degree of
Doctor of Philosophy

INTESTINAL HCO_3^- SECRETION IN FISH:

A WIDESPREAD MECHANISM WITH NEWLY RECOGNIZED PHYSIOLOGICAL FUNCTIONS

Josi R. Taylor

Approved:

_____ Martin Grosell, Ph.D. Professor of Marine Biology	_____ Terri A. Scandura, Ph.D. Dean of the Graduate School
_____ Douglas L. Crawford, Ph.D. Professor of Marine Biology	_____ M. Danielle McDonald, Ph.D. Professor of Marine Biology
_____ Joseph E. Serafy, Ph.D. Professor of Marine Biology	_____ Su Sponaugle, Ph.D. Professor of Marine Biology
_____ W. Gary Anderson, Ph.D. Professor of Biology University of Manitoba	

TAYLOR, JOSI R. (Ph.D., Marine Biology)

Intestinal HCO_3^- Secretion in Fish: A Widespread Mechanism with Newly Recognized Physiological Functions (June 2009)

Abstract of a dissertation at the University of Miami.

Dissertation supervised by Professor Martin Grosell.
No. of pages in text. (202)

Intestinal HCO_3^- secretion and the excretion of resultant $CaCO_3$ precipitates have become a recognized characteristic of seawater osmoregulation in teleosts; however, this is the first report of this osmoregulatory strategy outside of teleosts and also includes evidence for its use in green turtles, *Chelonia mydas*. Furthermore, the effects of feeding on intestinal HCO_3^- secretion were newly investigated in teleosts. Intestinal base secretion via apical Cl^-/HCO_3^- exchange was found to increase following feeding, at a magnitude sufficient to offset the “alkaline tide” commonly associated with digestion. Intestinal HCO_3^- secretion in marine teleosts draws HCO_3^- from both endogenous (via hydration of intracellular CO_2) and serosal (blood) sources, of which serosal HCO_3^- was found to contribute a greater proportion to the elevated postprandial intestinal base secretion measured in gulf toadfish, *Opsanus beta*. The mechanism by which this serosal HCO_3^- crosses the basolateral membrane for subsequent secretion into the intestinal lumen was confirmed in toadfish to be a basolateral Na^+/HCO_3^- co-transporter, tfNBCe1. Furthermore, the isolated intestinal tissue was found to have a high metabolic rate in both control and

postprandial toadfish, with respect to that of the whole animal, and shows a considerable specific dynamic action (SDA) response to feeding. Overall, this dissertation provides evidence for the widespread use of intestinal HCO_3^- secretion as a strategy of marine osmoregulation across aquatic taxa, and also for its newly recognized involvement in postprandial acid-base balance.

TABLE OF CONTENTS

LIST OF FIGURES

Chapter 6

LIST OF TABLES

Chapter 1:

Introduction

Salt and water balance is essential at all levels of life, and most animals have a constant, impeccably regulated intracellular environment in order to maintain basic cellular functions. In contrast, the extracellular fluids are subject to environmental influence by diffusion across body surfaces, particularly those of respiratory organs with characteristically high surface areas. Salt and water balance is particularly challenging for aquatic animals, considering the high potential for osmotic and ionic diffusion between an animal and its fluid environment. This diffusion occurs predominantly across the large gill surface area (Goss *et al.* 1998; Evans *et al.* 2005; Kidder *et al.* 2006) dictated by the low O_2 content of aquatic environments.

Teleost fish, like mammals, regulate their extracellular fluids at approximately 300 mOsm l^{-1} (Takei 2000; Marshall and Grosell 2005). Thus, seawater teleosts are subject to a constant diffusive salt gain and water loss to the environment, with an opposite scenario in freshwater teleost fish. Marine teleosts use a well-orchestrated, multi-organ response to offset this continual dehydration with active ingestion of seawater. Marine teleosts drink seawater at rates of 1-5 ml kg^{-1} h^{-1} (Smith 1930; Shehadeh and Gordon 1969; Takei 2000; Marshall and Grosell 2005; Scott *et al.* 2008), compared to the rates of < 1 ml kg^{-1} h^{-1} (Shehadeh and Gordon 1969; Scott *et al.* 2006) at which freshwater teleosts

ingest the environmental media. Ingested seawater (approx. 1000 mOsm l^{-1}) is desalinized in the esophagus, and enters the anterior intestine via the pyloric sphincter at approximately one-third to one-half the concentration of seawater (Ando *et al.* 2003; Marshall and Grosell 2005). Absorption of Na^+ and Cl^- along the intestinal tract drives water absorption and results in intestinal fluids low in Na^+ and Cl^- but containing Mg^{2+} and SO_4^{2-} at concentrations 3-5-fold those of seawater (Smith 1930; Shehadeh and Gordon 1969; Marshall and Grosell 2005). Because the intestinal epithelium is largely impermeable to these divalent ions, high rates of intestinal H_2O absorption lead to their concentration along the intestinal tract (Smith 1930; Shehadeh and Gordon 1969; Marshall and Grosell 2005). The intestinal fluids are also very high in HCO_3^-, owing to intestinal Cl^- absorption via apical Cl^-/HCO_3^- exchange (Wilson *et al.* 2002; Grosell *et al.* 2005; Grosell 2006). While intestinal NaCl absorption has historically been attributed exclusively to apical Na^+/Cl^- (NaCl) and $Na^+/K^+/2Cl^-$ (NKCC) cotransport (Frizzell *et al.* 1979; Musch *et al.* 1982; Loretz 1995), the last two decades have brought about the recognition of apical anion exchange (AE) as a mechanism contributing up to 70% to intestinal Cl^- and thereby fluid absorption in marine teleosts (Grosell *et al.* 2005).

The high intestinal fluid [HCO_3^-] and alkalinity resulting from intestinal HCO_3^- secretion facilitate the precipitation of Ca^{2+} (Smith 1930; Shehadeh and Gordon 1969; Wilson *et al.* 2002; Grosell 2006). The $CaCO_3$ formed in this reaction serves several interrelated purposes. First, the resultant reduction in intestinal fluid osmotic pressure enhances the osmotic gradient favoring H_2O

absorption across the intestinal epithelium (Wilson *et al.* 2002; Wilson and Grosell 2003; Grosell *et al.* 2005). Second, Ca^{2+} precipitation maintains low [Ca^{2+}] in the intestinal fluids, thereby inhibiting Ca^{2+} absorption across the leaky intestinal epithelium (Flik and Verbost 1993) and preventing any resultant accumulation of Ca^{2+} in the plasma and renal tubules where conditions may favor the detrimental formation of carbonate "kidney stones". Finally, the conversion of HCO_3^- to $CaCO_3$ maintains a gradient favoring continued HCO_3^- secretion to the intestinal fluids, thereby facilitating Cl^- and H_2O absorption across the intestinal epithelium (Wilson *et al.* 2002; Wilson and Grosell 2003; Grosell *et al.* 2005).

Intestinal HCO_3^- secretion and the excretion of resultant $CaCO_3$ precipitates have become a recognized characteristic of seawater osmoregulation in teleosts (Wilson *et al.* 2002; Marshall and Grosell 2005; Grosell *et al.* 2005; Grosell 2006); however, the use of this osmoregulatory strategy outside of teleosts has not yet been investigated. Early Chondrostean fishes, including sturgeon, are also known to osmoregulate in seawater (Bemis and Kynard 1997; Rodriguez *et al.* 2002). Indeed, even the most primitive jawed vertebrates, lamprey, are shown to have some seawater osmoregulatory ability (Brown *et al.* 2005). Furthermore, several elasmobranch species, traditionally categorized as osmoconformers, have recently been shown to ingest seawater on exposure to acute salinity increase (Anderson *et al.* 2002), suggesting these animals are capable of some degree of osmoregulation. The first objective (Chapter 2) of my dissertation is to address these questions by sampling intestinal fluids and blood plasma from non-teleost fishes. Analysis of the fluids

from these compartments in a range of marine animals will allow ion gradients to be determined, particularly for HCO_3^- which is secreted against its transepithelial concentration gradient in marine teleost fish. Comparison of HCO_3^- concentrations with those of other ions, particularly Cl^- and Na^+, will also allow prediction of the intestinal mechanisms involved in osmoregulation.

Inquiry of the evolutionary origins of intestinal HCO_3^- secretion as a mechanism of salt and water balance has brought about additional interest in the specific factors by which it is regulated. Concentration of the environmental media has become widely accepted as a potent stimulator of intestinal HCO_3^- secretion in marine fish (Shehadeh and Gordon 1969; Walsh *et al.* 1991; Wilson *et al.* 2002; McDonald and Grosell 2006; Genz *et al.* 2008), and has led to the recognition of intestinal HCO_3^- secretion as an osmoregulatory mechanism. The role of intestinal HCO_3^- secretion in Ca^{2+} handling has inspired investigation of intestinal HCO_3^- secretion rate regulation by intestinal [Ca^{2+}] (Wilson and Grosell 2003). This idea of stimulation by Ca^{2+} led to the consideration of natural circumstances in which intestinal [Ca^{2+}] may vary. The objective of Chapter 3 of this dissertation accordingly was to investigate the effects of the ingestion and subsequent processing of a high [Ca^{2+}] (i.e. fish) vs. a low [Ca^{2+}] (i.e. squid) meal in a seawater teleost, the gulf toadfish (*Opsanus beta*). Although many fish species are relatively continual feeders, research of homeostatic fish physiology is typically carried out on “control” fish from which food has been withheld for at least 72 h prior to experimentation. As such, the use of feeding as a means to investigate this marine teleost osmoregulatory mechanism is novel and

represents a promising vantage point from which fish physiology can be interpreted. The finding during these investigations of high postprandial (post-feeding) intestinal fluid [HCO_3^-], concomitant with low [Cl^-] and unchanged [Na^+], in toadfish fed both diets formed the basis for the remaining objectives of this dissertation.

The remaining chapters of this dissertation serve to characterize the mechanistic details by which intestinal HCO_3^- secretion is up-regulated following feeding. Fortunately, a great deal has been deduced about the mechanism of intestinal HCO_3^- secretion during the last two decades and has laid a sturdy groundwork for the remaining objectives. The reliance of intestinal HCO_3^- secretion on apical anion exchange has been deduced (Grosell *et al.* 2001); however, aspects of the specific mechanisms underlying the sources of energy and HCO_3^- for apical anion exchange are still being revealed. Basolateral Na^+/K^+-ATPase (NKA) is a driving force for many cellular transport processes, including intestinal HCO_3^- secretion (Wilson *et al.* 2002; Grosell 2006). The efflux of 3 Na^+ in exchange for 2 K^+ defines the low Na^+, electrically negative intracellular environment, in contrast to the relatively high Na^+, electrically positive extracellular environment. This electrochemical gradient favors Na^+ uptake by the epithelial cell and is thereby also a well-recognized driving force for apical NaCl and NKCC co-transporters (Loretz 1995; Grosell 2007). The source of HCO_3^- for apical anion exchange is two-fold (Wilson *et al.* 2002; Grosell 2006). First, endogenous CO_2 is hydrated in a reaction facilitated by the enzyme carbonic anhydrase (CA), resulting in HCO_3^- and H^+ formation. HCO_3^- is secreted across

the apical membrane into the intestinal fluids in exchange for Cl^-, while basolateral extrusion of the H^+ formed during this reaction maintains cellular acid-base balance. Basolateral H^+ extrusion occurs in exchange for Na^+ (Wilson *et al.* 2002; Grosell and Genz 2006) which is driven into the cell by the electrochemical gradient created by basolateral NKA. As such, NKA indirectly fuels the secretion of endogenously originating HCO_3^- to the intestinal fluids. The second source of HCO_3^- for apical AE is the blood (serosa), although the mechanism by which transepithelial intestinal HCO_3^- secretion is achieved has been less well-characterized than that by which endogenous CO_2 contributes to apical AE. It has been postulated that basolateral entry of HCO_3^- to the epithelial cell from the serosa occurs in cotransport with Na^+ (Wilson *et al.* 2002; Grosell 2006; Grosell and Genz 2006) and is thereby also driven by NKA. However, this mechanism has only relatively recently received attention for its role in intestinal HCO_3^- secretion and requires further characterization to ascertain its contribution to marine teleost osmoregulation. Due to the reliance of intestinal HCO_3^- secretion on the movement of acid/base equivalents between fluid compartments and ultimately between the fish and its environment, deducing the mechanistic specifics of these transport processes is essential to the understanding of salt-water and acid-base balance in fish.

While the importance of intestinal HCO_3^- secretion to marine teleost osmoregulation has become widely accepted over recent decades, its impact on acid-base balance has received relatively little attention. A handful of studies suggest that base efflux via intestinal HCO_3^- secretion is completely

compensated by branchial acid efflux under control (Wilson and Grosell 2003; Genz *et al.* 2008), high intestinal Ca^{2+} (Wilson and Grosell 2003), and high salinity (Genz *et al.* 2008) conditions. However, the result of significant elevation in toadfish intestinal fluid [HCO_3^-] post-feeding has motivated an investigation of the potential role of intestinal HCO_3^- secretion in postprandial acid-base balance. Feeding in most animals including fishes results in a range of notable consequences for homeostatic physiology (thus the rationale for withholding food for ≥ 72 h to achieve "control" conditions). These physiological consequences include challenges to (1) salt and water balance resulting from the influx of inorganic and organic nutrients to the gastrointestinal tract and bloodstream, (2) acid/base balance, resulting from gastric acid secretion and the associated "alkaline tide" (Hersey and Sachs 1995; Niv and Fraser 2002), and (3) energy balance, based on the metabolic rate increases (specific dynamic action, SDA)(Jobling 1981; Mccue 2006; Secor 2009) associated with feeding. While most physiological challenges associated with meal processing can be broadly classified under one of these three categories, the homeostatic mechanisms by which each category is regulated are very much interrelated.

The objectives of Chapter 3 were largely an investigation of the salt and water balance consequences associated with feeding, and also comprised a survey of blood chemistry. Accordingly, Chapter 4 serves a more in-depth investigation of postprandial consequences for whole fish acid-base balance and blood chemistry. The occurrence of alkaline tide in any fish has not, to the best of my knowledge, been investigated prior to the onset of my dissertation research.

As such, the objectives of Chapter 4 were to quantify (1) gastric acidification, (2) branchial acid/base flux, and (3) plasma and gastrointestinal fluid chemistry, under control and postprandial conditions in euryhaline European flounder, *Platichthys flesus*, acclimated to both freshwater and seawater. Intestinal HCO_3^- secretion has not been shown in freshwater teleosts (Wilson *et al.* 2002; Grosell 2006); therefore, the use of a euryhaline teleost in these experiments allows investigation of the possibility of different postprandial acid-base balance regulatory strategies between freshwater and seawater animals. These objectives serve to quantify any changes in plasma chemistry indicative of alkaline tide or respiratory compensation, of which none were found. Furthermore, mass-balance calculations of acid-base equivalents suggest incomplete compensation of gastric acid secretion via branchial base efflux. However, intestinal fluid chemistry again suggests elevated postprandial HCO_3^- secretion and has inspired subsequent investigation of the source of this HCO_3^- and the mechanism by which it is transported into intestinal fluids.

The hypothesis emergent from Chapters 3 and 4 of my dissertation research is that intestinal HCO_3^- secretion serves not only marine fish osmoregulation, but may play a role in postprandial acid-base balance by offsetting alkaline tide. This hypothesis shaped Chapters 5 and 6 of this dissertation to characterize two mechanisms, transepithelial HCO_3^- transport and endogenous CO_2 production, respectively, by which intestinal HCO_3^- secretion may offset alkaline tide. Mechanistic investigations of transepithelial HCO_3^- secretion in toadfish focused on the basolateral component of HCO_3^- transport,

hypothesized to entail cotransport with Na^+ (Wilson *et al.* 2002; Grosell 2006). Accordingly, Chapter 6 served to quantify postprandial changes in HCO_3^- secretion and oxygen consumption (as a proxy for endogenous CO_2 production) by the toadfish intestine. Monitoring these parameters in a parallel postprandial time course allowed for more accurate predictions of the source of high postprandial intestinal fluid [HCO_3^-] and thereby its possible contribution to dynamic regulation of acid-base balance.

In its entirety, this dissertation contributes, I believe, a number of important investigations to the field of fish physiology, and also has implications for tangential fields. Chapter 2 provides a more complete picture of the prevalence and evolution of intestinal HCO_3^- secretion as an osmoregulatory strategy than had even been considered at the onset of these investigations. Chapter 3 is the first study to look at the effects of feeding on intestinal HCO_3^- secretion in fish, with Chapter 4 proposing that postprandial intestinal HCO_3^- secretion serves a newly recognized role in acid-base balance. Chapter 5 is the first study to undertake the characterization of the basolateral mechanism by which transepithelial intestinal HCO_3^- secretion proceeds in fish; and Chapter 6 is the first, to my knowledge, to quantify metabolic rate of the isolated marine teleost intestine. This collection of complementary research objectives combine to provide further evidence of the mechanism by (and the extent to) which intestinal HCO_3^- secretion may contribute to a newly recognized function in osmoregulatory and digestive physiology of fish.

Chapter 2:

Evolutionary aspects of intestinal bicarbonate secretion in fish

Summary

Experiments compared intestinal HCO_3^- secretion in the intestine of the marine teleost Gulf toadfish, *Opsanus beta*, to representatives of early chondrostean and chondrichthyan fishes, the Siberian sturgeon, *Acipenser baerii*, and White-spotted bamboo shark, *Chiloscyllium plagiosum*, respectively. As seen in marine teleosts, luminal HCO_3^- concentrations were 10-fold plasma levels in all species when exposed to hyperosmotic conditions. While intestinal water absorption left Mg^{2+} and SO_4^{2-} concentrated in intestinal fluids up to four-fold ambient seawater concentrations, HCO_3^- was concentrated up to 50 times ambient levels as a result of intestinal HCO_3^- secretion. Reduced luminal Cl^- concentrations in the intestine of all species suggest that HCO_3^- secretion also occurs via Cl^-/HCO_3^- exchange in chondrostean and chondrichthyan fishes**.** Sturgeon began precipitating carbonates from the gut after only three days at 14‰, a mechanism utilized by marine teleosts to reduce intestinal fluid osmolality and maintain calcium homeostasis. Analysis of published intestinal fluid composition in the cyclostome *Lampetra fluviatilis* reveal that this species likely also utilizes intestinal HCO_3^- secretion for osmoregulation. Analysis of existing cyclostome data and the present results indicate that intestinal Cl^-/HCO_3^- exchange plays an integral role in maintaining hydromineral balance not only in teleosts, but in all fish (and perhaps other animals) with a need to drink seawater.

Background

Despite early reports of high HCO_3^- and CO_3^{2-} concentrations in the gut fluid of marine teleosts (Smith 1930; Shehadeh and Gordon 1969), intestinal anion exchange was largely overlooked until recently. HCO_3^- secretion occurs in the intestine of marine teleosts via Cl^-/HCO_3^- exchange across the apical membrane and contributes up to 50-70% to Cl^-/fluid absorption (Grosell *et al.* 2005). It is well documented that marine fish must drink seawater to combat diffusive water loss to a hyperosmotic environment. As imbibed seawater passes through the gut, Na^+ and Cl^- absorption occurs via Na^+:Cl^- and Na^+:K^+:$2Cl^-$ cotransporters, in addition to apical Cl^-/HCO_3^- exchange. Water follows this salt absorption, leaving behind Mg^{2+} and SO_4^- at concentrations often more than three times those of seawater. In contrast, HCO_3^- is present in the gut of marine teleosts at values up to 50 times seawater levels as a result of apical Cl^-/HCO_3^- exchange within the intestine (Grosell *et al.* 2005). Bicarbonate secretion may also play a role in calcium homeostasis, inhibiting intestinal Ca^{2+} absorption by precipitating $CaCO_3$ (Wilson *et al.* 2002; Wilson and Grosell 2003) which is subsequently excreted. Carbonate precipitation concomitantly promotes water absorption, lowering osmolality by removing Ca^{2+} and CO_3^{2-} from solution (Wilson *et al.* 1996; Wilson *et al.* 2002; Marshall and Grosell 2005).

Secondary active intestinal HCO_3^- secretion arises from endogenous CO_2 and derives its energy indirectly from the Na^+ gradient created by Na^+,K^+-ATPase (Grosell and Genz 2006). Endogenous CO_2 hydration is mediated in part by

carbonic anhydrase and yields HCO_3^- and H^+; reversal of this reaction is prevented by H^+ extrusion across the basolateral membrane (Grosell *et al.* 2001; Grosell *et al.* 2005). Grosell and Genz (2006) found that in Gulf toadfish, *Opsanus beta*, H^+ extrusion occurs by a Na^+/H^+ exchange mechanism (NHE), although the mechanism of H^+ extrusion may vary among species (Marshall and Grosell 2005). Meanwhile, HCO_3^- is secreted across the apical membrane into the intestinal lumen in exchange for Cl^- absorption.

A fish's capacity to adapt to different environmental salinities is ultimately determined by its ability to regulate ion uptake and excretion, and to maintain hydromineral balance (Rodriguez *et al.* 2002). The uncertainty whether vertebrates evolved in a freshwater or marine environment (or an intermediate salinity for that matter) may be clarified by looking at the osmoregulatory physiology of modern-day relatives of ancestral fishes. The ability of ancestral fishes to adapt to different salinities utilizing the same mechanisms as modern teleosts may elucidate the origin of these mechanisms or provide evidence of convergent evolution. Little is known about the osmoregulatory mechanisms of anadromous sturgeon, one of the most ancient Osteichthyan fishes (Bemis and Kynard 1997; Rodriguez *et al.* 2002). In addition to gaining insight to the evolution of intestinal Cl^-/HCO_3^- exchange as a marine osmoregulatory mechanism, the importance of sturgeon in aquaculture creates an added advantage to learning how, if at all, the physiological strategy of these fish differs from that of modern teleosts. Even marine elasmobranch fishes, which maintain blood plasma osmolality iso-osmotic or slightly hyperosmotic to seawater (Smith

1931), have a need to osmoregulate when faced with a salinity challenge. Anderson et al. (2002) subjected *Scyliorhinus canicula* and *Triakis scyllia* to an acute salinity increase from 80% to 100% seawater and measured a significant although transient increase over basal drinking rates. Wilson et al. (2002) suggested that the physiological processes involved in HCO_3^- secretion must have appeared early in the evolutionary history of teleosts that can inhabit seawater. Interestingly, although all osmoregulating marine fish have a need to drink seawater, intestinal HCO_3^- secretion has thus far only been acknowledged in teleosts. Given the need that these fish have to drink in a hyperosmotic environment and the significant role of intestinal Cl^-/HCO_3^- exchange in all marine teleosts examined to date, a similar mechanism is hypothesized for all seawater-ingesting animals, regardless of phylogenetic position.

The present study investigates the role of the intestine, in particular apical Cl^-/HCO_3^- exchange, in the evolution of marine osmoregulation. A series of experiments compare the marine teleost Gulf toadfish, *Opsanus beta*, to representatives of early chondrostean and chondrichthyan fishes, the Siberian sturgeon, *Acipenser baerii*, and White-spotted bamboo shark, *Chiloscyllium plagiosum*, respectively, to determine the presence of intestinal anion exchange as a means of osmoregulatory balance.

Materials and methods

Gulf toadfish, Opsanus beta

Gulf toadfish, *Opsanus beta*, were obtained as bycatch from local shrimp fishermen on Virginia Key, FL, US. Following transport to the University of Miami (RSMAS), fish were subject to a prophylactic treatment against ecto parasites as described previously (McDonald *et al.* 2003) and held in 75 L tanks receiving a flow-through of natural seawater of ambient temperature and salinity (26 ± 2.0 ºC, 35 ± 2.0 ‰) for approximately three weeks. All fish were starved 12 days prior to sampling to ensure the absence in the gut of any carbonate remains from dietary items. Five fish (mass 79.9 ± 9.70 g) were euthanized by a Tricaine Methane Sulfonate overdose (5 g L^{-1} MS-222, pH 8.0) after which a blood sample (300-500 µL) was obtained by caudal puncture into a heparinized syringe fitted with a gauge 22 needle, and placed on ice. The entire gastrointestinal tract was then carefully removed and ligated with silk ligatures into anterior, middle, posterior, and rectal segments as previously described (Grosell *et al.* 2004). Each section was removed and intestinal fluids were drained into 2-mL plastic microcentrifuge tubes for later analysis.

Siberian sturgeon, Acipenser baerii

Siberian sturgeon, *Acipenser baerii*, were transported from Rokaviar Sturgeon Farm, Homestead, FL, US, in an isotonic (approx. 9‰) mixture of fresh and seawater to minimize stress. Once at RSMAS, fish were transferred to 200 L recirculating tanks (22 ± 2.0 ºC) and salinity was gradually lowered until aquaria

contained dechlorinated tapwater. Following acclimation to laboratory conditions, an initial blood sample was taken (n = 5, mass 95.7 ± 17.02 g) as described above to establish freshwater baseline conditions. A target hyperosmotic salinity of 14‰ was identified based on observations of diminished health and some mortality at salinities over 17‰, consistent with findings by Rodríguez et al. (2002). Daily water changes gradually increased salinity to 14‰ over the course of 14 days during which fish were fed a pellet diet (provided by Rokaviar aquaculture facility) at ~3% body mass every other day. Fish were allowed to acclimate to 14‰ for five days, and were starved three days, prior to sampling. Eight fish (mass 70.5 ± 4.83 g) were euthanized via Tricaine Methane Sulfonate overdose (5 g L^{-1} MS-222, pH 8.0) and a blood sample was immediately taken as for toadfish. The entire gastrointestinal tract was then carefully removed and ligated with silk ligatures into stomach, small intestine, and spiral valve intestine segments. Each section was removed and fluid drained into 2-mL plastic microcentrifuge tubes for later analysis.

White-spotted bamboo shark, Chiloscyllium plagiosum

Natively Indo-Pacific White-spotted bamboo sharks, *Chiloscyllium plagiosum*, were obtained from Sea World, Orlando, FL, US. Following transport to RSMAS, sharks were held in a 2200 L covered outdoor flow-through seawater aquarium (28 ± 2.0 ºC) and starved 30 days prior to experimentation. During this time resting blood samples were taken as above by caudal puncture with a heparinized syringe. To induce drinking, seawater flow was discontinued and

salinity was increased to 140% seawater by adding an aerated brine solution of 30 kg Instant Ocean to the existing 34‰ seawater to raise salinity to 48‰ over the course of 30 min. After eight to ten hours of exposure to these hyperosmotic conditions, sharks (n = 3, standard length 83.0 ± 4.71 cm) were euthanized via Tricaine Methane Sulfonate overdose (5 g L^{-1} MS-222, pH 8.0) and a blood sample was immediately taken as described above. The stomach and spiral valve intestine were carefully removed and fluid drained into 15-mL Falcon tubes for analysis.

Sample analysis

All blood samples were analyzed for hematocrit and then centrifuged and plasma was retained in addition to intestinal fluid samples for immediate analysis of pH (Accumet pH electrode connected to a Radiometer PHM220 pH meter). Total CO_2 was analyzed using a Corning 965 Carbon Dioxide Analyzer and osmolality was measured by a vapor pressure osmometer (Wescor Vapro 5520). Samples were stored at -20 ºC for subsequent analysis of inorganic anions (Dionex DX-120) and cations (Fast Sequencial Atomic absorption spectrophotometry, Varian FS220) after appropriate dilution.

Results

Gulf toadfish, Opsanus beta

In concurrence with previous reports of marine teleost intestinal Cl^-/HCO_3^- exchange, HCO_3^- equivalents in the alkaline gut fluid of Gulf toadfish were about

10-fold those measured in the plasma and up to 33-fold seawater levels (Fig. 2.1b, Table 2.1). Meanwhile SO_4^{2-} and Mg^{2+} were concentrated two to four times above seawater values (Fig. 2.1a) as a result of water absorption across the intestinal epithelium. The Na^+ and Cl^- concentrations from all gut sections (Fig. 2.1a) were lower than plasma values and thus consistent with absorption of these ions across the intestinal epithelium.

Fig. 2.1. (a) Osmolality and concentrations of the most common seawater ions (Cl^-, Na^+, Mg^{2+} and SO_4^{2-}) in 35‰ seawater (SW) and Gulf toadfish, *Opsanus beta*, intestinal fluids from anterior (ANT), middle (MID), posterior (POST) and rectal (REC) segments. (b) HCO_3^-, Ca^{2+} and K^+ concentrations in seawater and toadfish intestinal fluids. Mean ± SEM (n = 10).

a.

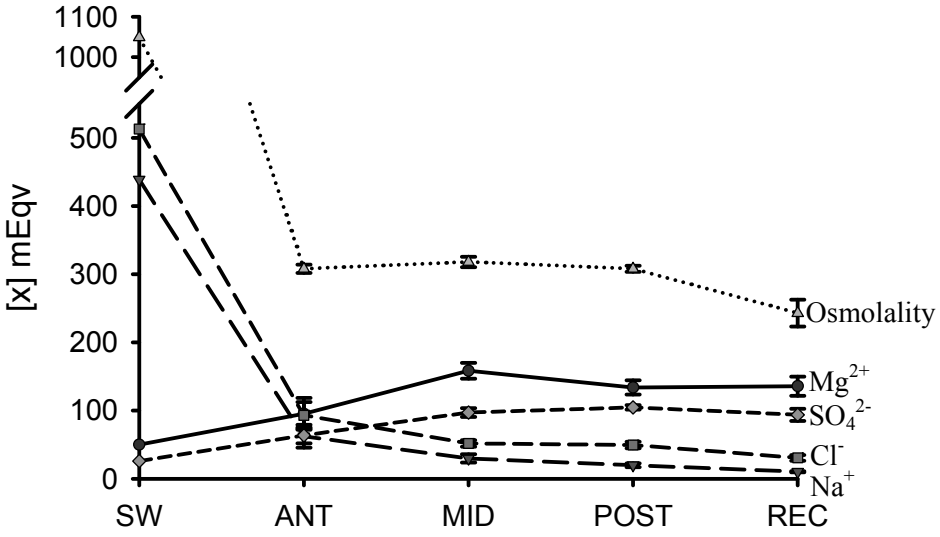

b.

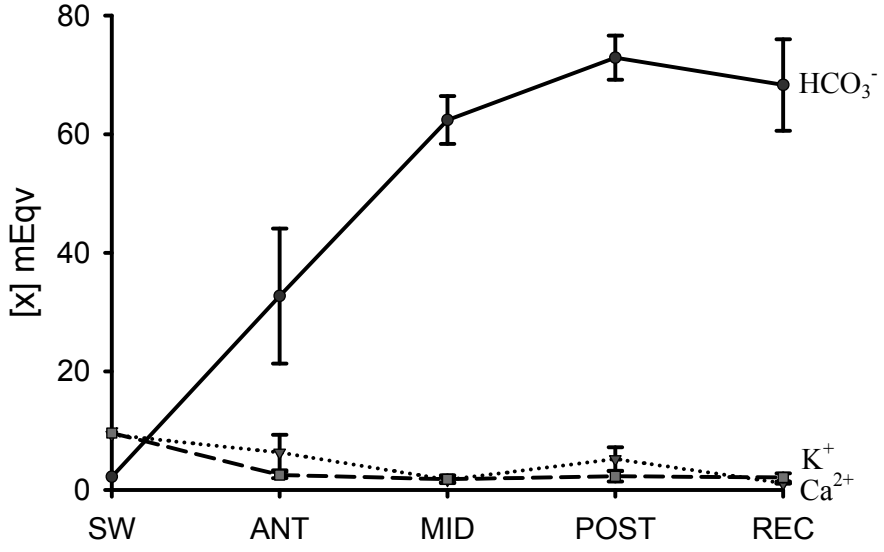

Table 2.1. Plasma chemistry of Gulf toadfish (*Opsanus beta*) in seawater (n = 10), Siberian sturgeon (*Acipenser baerii*) in 14‰ seawater (n = 8) and freshwater (n = 5), and White-spotted bamboo shark (*Chiloscyllium plagiosum*) in seawater (n = 3) and 140% seawater (n = 3). Data displayed as mean (SEM).

	pH	Total CO_2 (mM L^{-1})	Osmolality (mOsm L^{-1})	Hematocrit (%)	Cl^- (mM L^{-1})	K^+ (mM L^{-1})	Na^+ (mM L^{-1})	Ca^{2+} (mM L^{-1})
Gulf toadfish								
Seawater	7.7 (0.04)	5.2 (0.59)	310 (2.4)	26.3 (2.26)	118.5 (1.44)	2.5 (0.15)	143.6 (2.95)	2.0 (0.14)
Siberian sturgeon								
14‰ Seawater	7.6 (0.04)	4.0 (0.23)	305 (6.5)	24.6 (1.96)	113.4 (16.44)	2.8 (0.10)	153.0 (11.61)	2.3 (0.04)
Freshwater	7.9 (0.02)	6.8 (0.29)	252 (2.0)	22.1 (1.66)	98.1 (2.13)	2.5 (0.13)	117.6 (3.04)	1.3 (0.09)
Bamboo shark								
Seawater	7.8 (0.06)	3.8 (0.30)	968 (22.9)	15.3 (1.56)	221.3 (4.01)	5.8 (0.31)	194.9 (2.11)	3.0 (0.05)
140% Seawater	7.8 (0.03)	5.9 (0.91)	1149 (18.0)	21.1 (3.45)	271.5 (9.65)	9.1 (0.71)	232.4 (10.17)	3.9 (0.07)

Siberian sturgeon, Acipenser baerii

Juvenile Siberian sturgeon tolerated salinities between zero and 14‰ well, although with a significant (Student's t-test, $P < 0.001$) increase in plasma osmolality at 14‰ (Table 2.1). After just three days of exposure to 14‰ seawater, excreted $CaCO_3$ precipitate was visible in sturgeon holding aquaria. Sample analysis revealed intestinal fluid composition (Fig. 2.2) similar to that of modern teleosts, with pH 8.3 (± 0.10) and intestinal HCO_3^- levels (Fig. 2.2b) approximately 10-fold those measured in the plasma (Table 2.1) and up to 50-fold HCO_3^- levels in 14‰ seawater. As in Gulf toadfish, SO_4^{2-} and Mg^{2+} were concentrated up to four-fold ambient levels and Na^+ and Cl^- concentrations indicated absorption of these ions across the intestine (Fig. 2.2a).

Fig. 2.2. (a) Osmolality and concentrations of the most prevalent seawater ions in 14‰ seawater (14‰), stomach fluid (ST), small intestine fluid (SI) and spiral valve fluid (SV) in 14‰ seawater- acclimated Siberian sturgeon, *Acipenser baerii*. (b) HCO_3^-, Ca^{2+} and K^+ concentrations in 14‰ seawater and sturgeon gastrointestinal fluids. Mean ± SEM (n = 8)

a

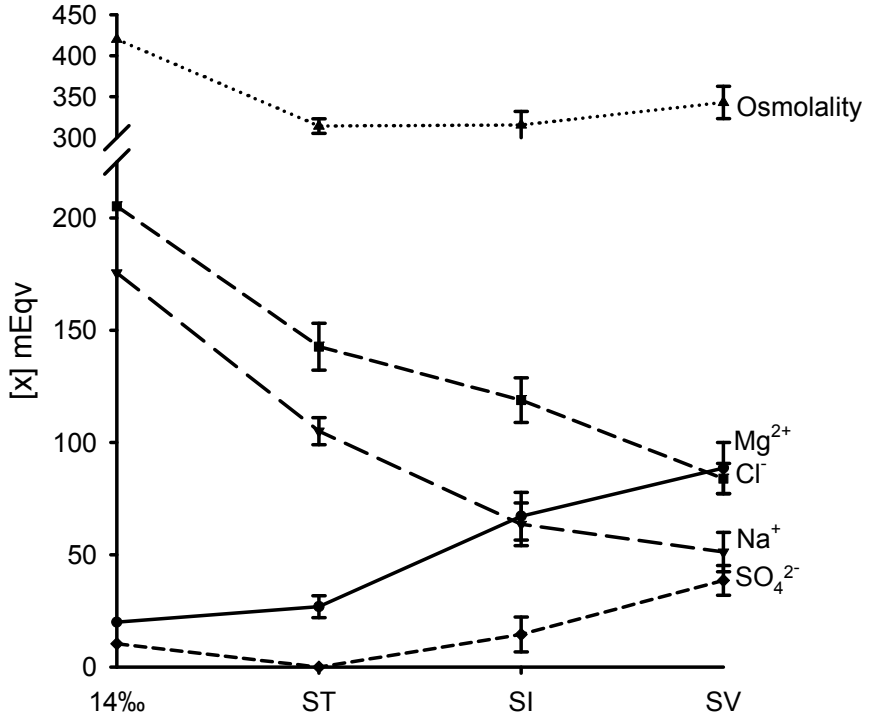

b

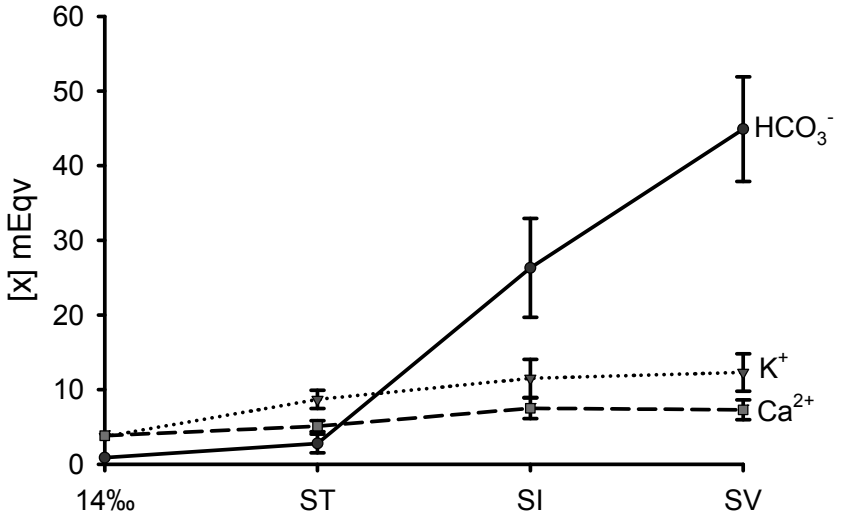

White-spotted bamboo shark, Chiloscyllium plagiosum

Our method of inducing drinking by acute salinity increase adapted from Anderson et al. (2002) proved effective. Fish appeared dehydrated based on a nearly 19% increase in plasma osmolality (Table 2.1). A total of 5.3 (± 0.92) mL of fluid with very high osmolality (Fig. 2.3a) was recovered from the stomach and 2.5 (± 0.20) mL from the spiral valve intestine, yielding 7.8 mL over 8-10 h in these approximately 1 kg elasmobranchs suggesting apparent drinking rates comparable to teleosts (Marshall and Grosell 2005). Similarly to teleosts and sturgeon, HCO_3^- equivalents in the intestinal fluid were about 10-fold plasma levels, and 16-fold levels found in 140% seawater (Fig. 2.3b, Table 2.1). Also similarly to teleosts and sturgeon, Mg^{2+} and SO_4^{2-} were concentrated about 2-fold ambient levels, and Na^+ and Cl^- concentrations were consistent with absorption of these ions across the intestinal epithelium (Fig. 2.3a).

Fig. 2.3. (a) Osmolality and concentrations of the most common seawater ions in 140% seawater (140% SW), stomach fluid (ST) and spiral valve fluid (SV) from White-spotted bamboo sharks, *Chiloscyllium plagiosum*, exposed to an acute salinity increase. (b) HCO_3^-, Ca^{2+} and K^+ concentrations in 140% seawater and bamboo shark gastrointestinal fluids. Mean ± SEM (n = 3)

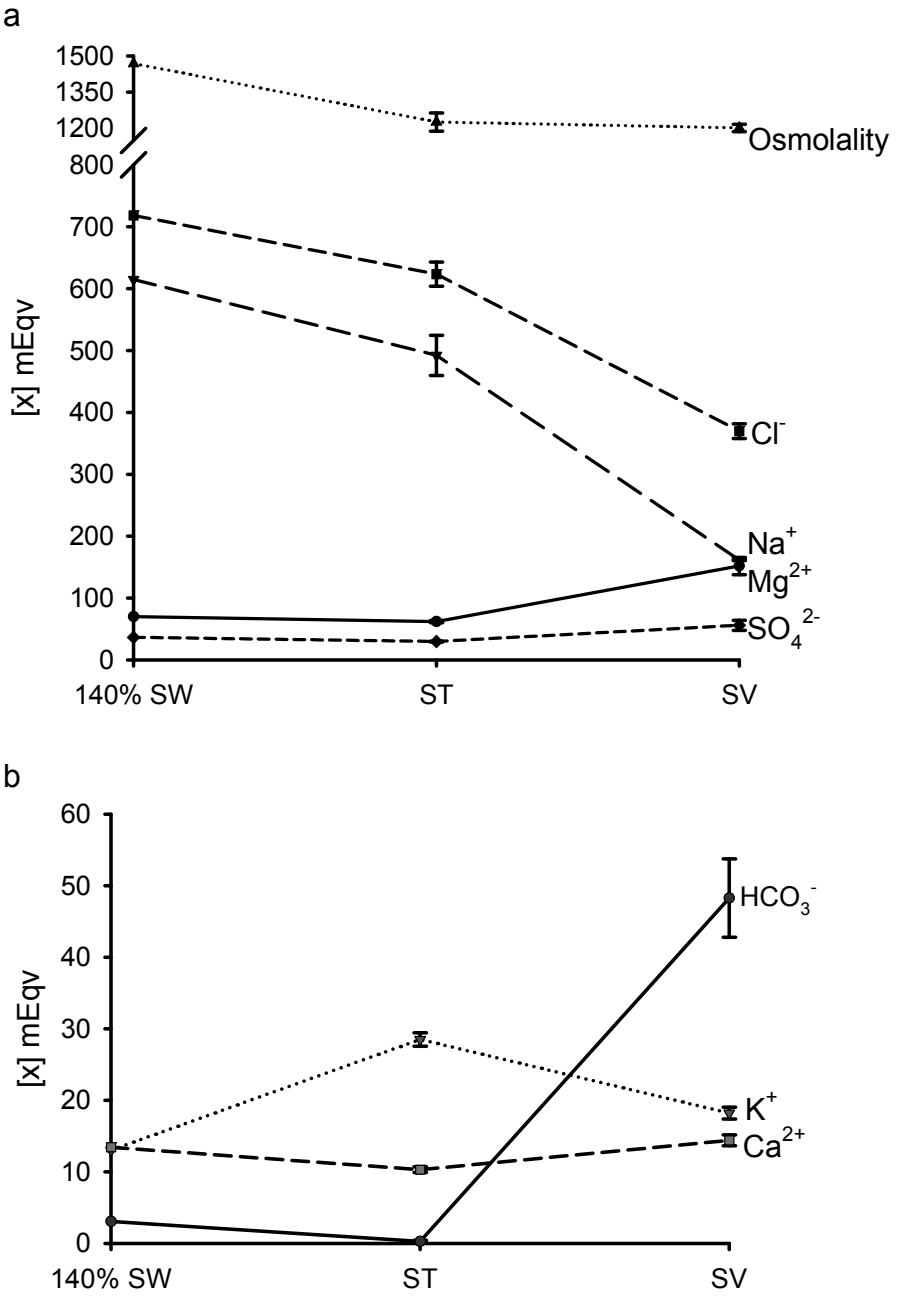

Conclusions

The osmoregulatory role of the intestine in non-teleosts

These results are the first to demonstrate the occurrence of intestinal HCO_3^- secretion in non-teleost fishes. Data also suggest the importance of Cl^-/HCO_3^- exchange in fishes that are not necessarily osmoregulators, but experience environmental salinity fluctuations. Thus, the hypothesis of a strong correlation between drinking rate and HCO_3^- secretion underscores the importance of intestinal anion exchange in osmoregulation. Smith (1930) was the first to show that marine teleosts swallow relatively large quantities of seawater. Most of the ingested water, Na^+, K^+ and Cl^- are absorbed across the intestinal epithelium leaving in the lumen a fluid that is rich in divalent ions Mg^{2+} and SO_4^{2-} and approximately isotonic with the blood (Smith 1930). The present results support evidence for differential intestinal ion transport in all osmoregulating marine fish. In all fishes tested, intestinal Mg^{2+} and SO_4^{2-} were concentrated up to four times over ambient seawater levels, indicating water absorption rates similar to those suggested for teleosts based on phenol red methods (Smith 1930). Accordingly, Na^+ and Cl^- were absorbed, with part of the Cl^- absorption attributed to anion exchange. Having these estimations of hydromineral absorption and HCO_3^- secretion rates allows us to predict the fate of imbibed Ca^{2+}.

Implications for Ca^{2+} homeostasis

As Shehadeh & Gordon speculated in 1969, recent findings indicate that intestinal Ca^{2+} absorption is modest in marine teleosts (Wilson and Grosell 2003; Marshall and Grosell 2005). Under these conditions, if no $CaCO_3$ precipitation were assumed, luminal Ca^{2+} might be expected to behave similarly to Mg^{2+} and SO_4^{2-} and reach concentrations up to 38 mmol L^{-1}. However, in contrast to Mg^{2+} and SO_4^{2-} which are left highly concentrated after water absorption, intestinal fluid Ca^{2+} concentrations of 2.1 (± 0.22) mmol L^{-1} were measured, nearly five-fold less than seawater levels (Fig. 2.1b). This indicates the importance of $CaCO_3$ precipitation, observed in all segments of the Gulf toadfish intestine. Wilson and Grosell (2003) working on the European flounder found that precipitate formation can account for 30-65% of the ingested Ca^{2+}, with the renal system secreting any absorbed Ca^{2+}. In contrast to low Ca^{2+} concentrations found in marine teleost intestinal fluid, measurements of Ca^{2+} in Siberian sturgeon small intestine and spiral valve intestine fluid (Fig. 2.2) are elevated compared to those in plasma (Table 2.1) and also are nearly twice the levels found in 14‰ seawater (Fig. 2.2), despite elevated HCO_3^- concentrations (Fig. 2.2) and visible $CaCO_3$ precipitates. However, considering Mg^{2+} and SO_4^{2-} concentrations which are elevated about four-fold, the only two-fold elevation of Ca^{2+} in the intestinal fluids indicates that alkaline Ca^{2+} precipitation is important also in sturgeon. Whether the relatively high Ca^{2+} concentrations in the intestinal fluids of sturgeon is associated with higher intestinal Ca^{2+} uptake rates and thus high demand for renal secretion remains to be investigated. It is worth mentioning that drinking rates in these

sturgeon might be unusually high at 14‰ (enough fluid was recovered from the stomach for analysis) due to slight dehydration resulting from imperfect marine osmoregulation, which could contribute to elevated intestinal Ca^{2+} concentrations.

Bamboo shark intestinal Ca^{2+} concentrations were not significantly different (Students t-test, $P = 0.41$) from levels in their ambient 140% seawater medium. Considering that Mg^{2+} and SO_4^{2-} were concentrated about two-fold as a result of water absorption, it is surmised that half of the ingested Ca^{2+} must have been either absorbed or precipitated within the intestine. Indeed plasma Ca^{2+} concentrations were found to be significantly (Students t-test, $P < 0.001$) elevated over basal levels following exposure to 140% seawater. Precipitates were not observed in the intestinal fluid, which might be attributed to the acute nature of the osmoregulatory period in these fish. As yet, the amount of time required for intestinal $CaCO_3$ precipitation following an osmoregulatory challenge is undescribed.

Intestinal HCO_3^- secretion in cyclostomes?

The present study has demonstrated that intestinal Cl^-/HCO_3^- exchange is not a characteristic unique to modern teleosts, but rather may be utilized in the osmoregulatory strategy of most if not all marine fishes that drink seawater in response to a hyperosmotic environment. In addition to the ancestral groups sampled, there is strong evidence that lamprey, and a suggestion that even the traditionally osmoconforming hagfishes, are able to utilize intestinal Cl^-/HCO_3^-

exchange in marine osmoregulation. Because apical Cl^-/HCO_3^- exchange is stimulated by the ingestion of seawater in all hypo-osmoregulating fish examined to date, HCO_3^- secretion might be expected in all animals that drink seawater. The renin-angiotensin system (RAS) plays a central role in control of body fluid balance (Kobayashi and Takei 1996) and hence drinking, and has been described in the majority of vertebrate groups including teleost fish (Kobayashi and Takei 1996), and more recently in elasmobranchs (Takei *et al.* 1993; Anderson *et al.* 2001) and lamprey (Rankin *et al.* 2004; Takei *et al.* 2004; Brown *et al.* 2005). Lampreys, being effective osmoregulators in marine environments, drink seawater (Morris 1958; Rankin 2002). Furthermore, isolated intestine experiments by Pickering and Morris (1973) indicate that in marine osmoregulating lamprey, Cl^- is transported across the epithelium at rates approximately twice those of Na^+. The authors even speculate that this difference in transport rates might be explained by a sodium-independent Cl^-/HCO_3^- exchange mechanism (Pickering and Morris 1973). Additionally, lamprey rectal fluid cation and anion concentrations (Table 2.2) from Rankin (1997) indicate a charge imbalance consistent with the magnitude of HCO_3^- secreted into the lumen of marine teleost intestine, strongly suggesting that intestinal anion exchange contributes to osmoregulation also in this ancient group. Recent evidence by Cobb et al. (2004) suggests that RAS may also be present in Atlantic hagfish, *Myxine glutinosa*, indicating a potential for regulated drinking and intestinal anion exchange during water ingestion in a hyperosmotic environment or during hypovolemia-induced dehydration.

Table 2.2. Charge balance of rectal fluid from lampreys caught by eel fishermen in Ringkøbing Fjord on the west coast of Jutland, acclimated to sea water (composition: 944 mOsm kg^{-1}; Na^+ 471 mmol L^{-1}; K^+ 9.0 mmol L^{-1}; Ca^{2+} 10.6mmol L^{-1}; Mg^{2+} 54.2 mmol L^{-1}; SO_4^{2-} 26.5mmol L^{-1}) based on figure 4.3 from Rankin (1997). * K^+ value not given in Rankin (1997); estimated based on teleost data

Cation	mM L^{-1}	Ionic (+) charge	Anion	mM L^{-1}	Ionic (-) charge
Na^+	10	10	Cl^-	110	110
K^+	5*	5	SO_4^{--}	55	110
Ca^{++}	20	40	PO_4^{---}	--	--
Mg^{++}	135	270			
Total Charge		320			220

Intestinal HCO_3^- secretion in "non-fish" marine organisms

The prospect of seawater ingestion in all fish groups leads to the question whether intestinal HCO_3^- secretion is limited to osmoregulating marine fishes, or might be found in other animal groups known to imbibe seawater. Sea turtles have been shown to have drinking rates ranging from 13.3 ml kg^{-1} d^{-1} in unfed juvenile (93.9 ± 2.3 g) green turtles (Holmes and McBean 1964) and 15 ml kg^{-1} d^{-1} for a 50 kg turtle (Prange 1985), to 40 ml kg^{-1} d^{-1} in hatchling (approximately 20 g) loggerhead turtles (Bennett *et al.* 1986). These reported drinking rates are comparable to those in the order of 1-5 ml kg^{-1} h^{-1} recognized in marine teleosts (Marshall and Grosell 2005). Sea otters are the only marine mammals reported to possess the ability to actively consume seawater, at rates estimated up to 124 mL kg^{-1} d^{-1} (Costa 1982), and gain free water (Costa 1982; Ortiz 2001), thus representing an exciting link to mammalian ion transport mechanisms. A role of

the gut in osmoregulation has also been suggested in certain species of crustaceans that drink small amounts of seawater to maintain hydromineral balance (Mantel 1968; Chu 1987; do Carmo Fernandes Santos 2002). The uniquely high Ca^{2+} and Mg^{2+} conditions in crustacean gastrointestinal fluids, and variable internal $CaCO_3$ concentrations associated with ecdysis provide another point of curiosity. do Carmo Fernandes Santos (2002) found Ca^{2+} concentrations of approximately 50 mEq l^{-1} in gastric juice and suggested its application in rapid buffering to counter hemolymph acidosis. Additionally, high Mg^{2+} concentrations were measured in gut fluid, more than twice and five times levels in the 34 and 9 ‰ seawater media, respectively (do Carmo Fernandes Santos 2002), potentially indicating water absorption across the intestinal epithelium. As water absorption seems to occur proportionally to intestinal Cl^-/HCO_3^- exchange (Grosell *et al.* 2005) and is stimulated acutely and chronically by high Ca^{2+} levels in European flounder (Wilson *et al.* 2002), the ability of some crustaceans to use the gastrointestinal tract as a “storage reservoir” for Ca^{2+} and Mg^{2+} (do Carmo Fernandes Santos 2002) is intriguing.

An additional question arises of whether intestinal anion exchange might also be utilized in seawater and even freshwater fish to deal with an increased salt load resulting from a meal. The impact of feeding on basic fish physiology has been largely overlooked by comparative physiologists. Obviously feeding will have a significant impact on physiology, and consequently comparative physiologists generally control for this by starving fishes at least three days before experimentation. The huge influx of ions alone may be sufficient to

present postprandial osmoregulatory challenges. Based on observations that sturgeon were able to excrete carbonate precipitates after only three days at a salinity of 14‰, it is interesting to consider at what salinity, or what meal-induced salt load, HCO_3^- secretion begins to play a significant role in osmoregulation. Walsh et al. (1991) noted that no carbonate precipitation was observed in Gulf toadfish acclimated to 25% seawater, while McDonald and Grosell (2006) measured significantly increased intestinal fluid HCO_3^- levels in Gulf toadfish at salinities as low as 5‰ when compared to 2.5‰ and found a general trend between increasing salinity and increasing intestinal HCO_3^- secretion between 2.5 and 70‰. Furthermore, freshwater teleosts have luminal HCO_3^- concentrations similar to, or much lower than, corresponding plasma concentrations (Wilson 1999), compared to seawater teleosts which have luminal HCO_3^- concentrations approximately five to ten-fold plasma levels (Grosell *et al.* 2001). Additional research is essential to identify the extent of the role of intestinal anion exchange and its resultant carbonate precipitation in not only marine teleosts, but in all marine and freshwater fishes, and seawater ingesting animals.

Acknowledgments

Jimbo's Shrimp, Key Biscayne, FL, US, for providing Gulf toadfish; Rokaviar Sturgeon Farm, in Homestead, FL, US, for providing juvenile Siberian sturgeon; and Sea World in Orlando, FL, US, for providing White-spotted bamboo sharks. Also T. Capo and T. Laberge-MacDonald for animal care

assistance. This work was supported by a University of Miami Fellowship to J.R. Taylor and by a National Science Foundation Grant to M. Grosell (NSF-IBN 0416440).

Chapter 3:

Feeding and osmoregulation: dual function of the marine teleost intestine

Summary

Experiments on Gulf toadfish, *Opsanus beta*, demonstrate how feeding impacts osmoregulation in the marine teleost intestine. A high Ca^{2+} diet of Pilchards, *Sardina pilchardus* ([Ca^{2+}] 404.2 mmol kg^{-1}) was compared to a low Ca^{2+} diet of Common squid, *Loligo forbesi* ([Ca^{2+}] 1.3 mmol kg^{-1}), as high [Ca^{2+}] has been shown to stimulate intestinal anion exchange. Gastrointestinal fluids and blood plasma were collected in a time course from pre-feeding to 216 h post feeding. Following food intake, monovalent ions were largely absorbed across the intestinal epithelium, leaving a fluid rich in divalent ions which have a lower osmotic coefficient and effectively reduce osmotic pressure in the lumen to allow for enhanced fluid absorption. Concentrations of Cl^- and HCO_3^- in fluid along the gastro-intestinal tract of fish fed both diets, particularly one and two days post-feeding, demonstrate that apical Cl^-/HCO_3^- exchange plays a vital role in postprandial Cl^- and water absorption. Postprandial acid-base balance disturbance as indicated by plasma alkalinization was limited or absent indicating compensation for gastric acid secretion in this teleost fish. Plasma osmolality peaked 12 h post-feeding in toadfish fed squid, but was not accompanied by a significant increase in inorganic ion concentrations. Transient fluid secretion by the gastrointestinal tract was evident from reduced luminal Mg^{2+} and SO_4^{2-} concentrations for 24-48 h post feeding. Discrepancy between the sum of

inorganic osmolytes and measured osmotic pressure was attributed to organic osmolytes which occurred at high concentrations in the stomach and anterior intestine for up to 24 h post feeding.

Background

Feeding and subsequent nutrient absorption provide life-sustaining energy to all animals, and are inevitably accompanied by physiological consequences. Most comparative physiology studies of fishes in the last century have been done on animals starved at least 72 h to control for physiological variability resulting from a meal. Although significant work has been done regarding the effects of feeding on physiology in other vertebrate groups, similar studies of fishes have been less comprehensive or are specifically designed to meet aquaculture goals. Dabrowski et al. (1986) found that feeding in seawater and freshwater drastically changes the ionic balance in the euryhaline fish intestine, even though the salt intake that accompanies drinking in seawater fish largely surpassed dietary intake (Shehadeh and Gordon 1969; Dabrowski *et al.* 1986). The acute nature of dietary salt intake may in itself induce an osmoregulatory challenge for the gastro-intestinal tract. Marshall and Grosell (2005) note that a large meal for a piscivorous fish, for example, will provide a substantial K^+ and Ca^{2+} load (from prey intracellular K^+ and bone phosphate, respectively), consequences of which remain to be examined. Additional intestinal salt load and systemic fluid loss might also result from bile, pancreatic and gastric secretions. Biliary secretions can carry Na^+ concentrations of over 300 mM (Grosell *et al.* 2000b), pancreatic

secretions in many species contain HCO_3^- concentrations up to 140 mM (Novak 2000; Steward *et al.* 2005), and gastric parietal cells are capable of secreting Cl^- into the mammalian gastric lumen at rates up to 70 mM min^{-1} (Thomas and Machen 1991). In addition to potential osmoregulatory consequences of salt intake and gastrointestinal secretions, postprandial disruption to acid-base balance as a result of gastric acid secretion is possible, as occurs in many higher vertebrates. The “alkaline tide” phenomenon recognized in amphibians, reptiles and mammals (Wang *et al.* 2001) was recently demonstrated in an elasmobranch (Wood *et al.* 2005), representing the first instance of alkaline tide reported in fishes. The term alkaline tide refers to a significant alkalinization of the blood following gastric acid secretion. The rate of gastric apical H^+ secretion into the lumen is countered by basolateral efflux of HCO_3^- (metabolic base) via Cl^-/HCO_3^- exchange, which prevents alkalosis of the acid-secreting oxyntic (mammals) or oxyntopeptic (non-mammalian vertebrates) cell. Basolateral Cl^-/HCO_3^- exchange provides Cl^- for gastric HCl secretion; H^+ and HCO_3^- are created in these gastric epithelial cells by CO_2 hydration, catalyzed by intracellular carbonic anhydrase (Niv and Fraser 2002).

In addition to digestion, the gastro-intestinal tract of marine fish plays an important role in osmo- and iono-regulation, as hypo-osmoregulating fish have long been known to drink seawater to replace water lost diffusively to their environment. Ingested seawater passes through the gastro-intestinal tract and ions must be differentially absorbed across the intestinal epithelium to facilitate water absorption. A large portion of Cl^- and water absorption in the intestine is

accomplished via apical Cl^-/HCO_3^- exchange (Grosell *et al.* 2005), making intestinal anion exchange an important addition to long-recognized cotransporters Na^+-Cl^- and Na^+-K^+-$2Cl^-$ in the marine teleost intestine. The HCO_3^- that is consequently secreted into the intestinal lumen is present at levels approximately five to ten-fold plasma concentrations (Wilson *et al.* 2002; Taylor and Grosell 2006a) in starved fishes, indicating an active transport mechanism (Grosell 2006).

Bicarbonate secretion also seems to play a role in calcium homeostasis, inhibiting intestinal Ca^{2+} absorption by precipitating $CaCO_3$ which is subsequently excreted (Wilson *et al.* 2002; Wilson and Grosell 2003). This carbonate precipitation in itself also promotes water absorption by lowering osmolality in removing Ca^{2+} and CO_3^{2-} from solution (Wilson *et al.* 1996; Wilson *et al.* 2002; Marshall and Grosell 2005). High Ca^{2+} concentrations alone (Wilson *et al.* 2002) and elevated ambient salinity (Walsh *et al.* 1991; McDonald and Grosell 2006; Taylor and Grosell 2006a) have been shown to stimulate HCO_3^- secretion, which is not surprising considering the role of intestinal anion exchange in Cl^- and water absorption (Grosell *et al.* 2005; Grosell 2006).

In designing experiments, consideration was given to the potential of high salinity in general, and high Ca^{2+} concentrations specifically, to stimulate Cl^-/HCO_3^- exchange, along with the great osmoregulatory challenge imagined to be associated with ingesting a large meal and associated salts. The effects of a high Ca^{2+} and a low Ca^{2+} diet (and feeding in general) on intestinal HCO_3^- secretion and osmoregulation in Gulf toadfish, *Opsanus beta,* have been examined. By

investigating the effects of feeding on gastrointestinal fluid chemistry, and thereby gaining more information about intestinal anion exchange, a better understanding of the function, regulation, and mechanism(s) of apical Cl^-/HCO_3^- exchange may be achieved. Gastrointestinal fluids and blood plasma were sampled in a detailed time course post feeding to reveal the timeline for organic and inorganic nutrient absorption across the intestine for differing diet composition. In addition, a detailed time course of blood plasma chemistry allowed for investigation of the possibility of postprandially-disturbed acid/base balance and osmoregulatory compromise.

Materials and methods

Animal care

Gulf toadfish, *O. beta*, were obtained as bycatch from local shrimp fishermen based on Virginia Key, FL, US. Following transport to the University of Miami (RSMAS), fish were subject to a prophylactic treatment against ectoparasites as described previously (McDonald *et al.* 2003). Toadfish were held in aerated, 75 L tanks receiving a flow-through of natural seawater at ambient temperature and salinity (26 ± 2.0 ºC, 35 ± 2.0 ‰, mean and range) and fed their respective experimental diet (see below) to satiation once weekly, for approximately three weeks prior to experimentation.

General experimental procedures

Two natural experimental diets were determined based on knowledge of Ca^{2+}-induced HCO_3^- secretion in European flounder. A squid diet (*Loligo forbesi*, see Table 3.1 for inorganic ion composition) represented a low Ca^{2+} meal, while a fish diet (*Sardina pilchardus*, see Table 3.1 for inorganic ion composition) corresponded to a relatively high Ca^{2+} meal. Both experimental diets represent realistic meals for *O. beta*. Gulf toadfish were starved 12 days prior to feeding to ensure resting conditions. In the initial experiment, 60 fish (mass 64 ± 3.5 g, mean and SEM) were fed one of the two experimental diets to satiation (all uneaten food was removed after 30 min) and terminally sampled in groups of five fish pre-feeding (12 d following their last meal), 1, 2, 3, 6 and 9 days after feeding. Based on the results of this first experiment, follow-up sampling was done on another 50 toadfish (mass 80 ± 3.5 g) fed the same two diets and sampled in groups of five fish pre-feeding (again 12 d following their last meal), 3, 6, 12 and 24 hours after feeding. The final data set comprises timepoints 0, 3, 6, 12, 24, 48, 72, 144 and 216 h post-feeding. Data reported in the 24 h timepoint were taken exclusively from the second experiment as sample time was monitored more precisely in this more detailed trial. Experimental fish were euthanized by a Tricaine Methane Sulfonate overdose (5 g L^{-1} MS-222, pH 8.0) after which a blood sample (200-400 µL) was obtained by caudal puncture into a heparinized syringe fitted with a gauge 22 needle, and placed on ice. The entire gastrointestinal tract was then carefully removed and ligated with silk ligatures into stomach, anterior, mid, posterior, and rectal segments as previously

described by Grosell et al. (2004). Each section was removed and contents were drained into 2 mL plastic microcentrifuge tubes (15 ml Falcon tubes for stomach contents) for analysis. At the 3 h timepoint, while most of the ingested meal remained in the stomach, contents were weighed to estimate meal size relative to body mass. Experimental design was such that fish sampled at each timepoint (n = 5) were taken exclusively from one 75 L tank containing only these fish. Thus, any effects of dominance/hierarchy on food intake would have revealed themselves amongst the five fish from each diet sacrificed at 3 h post-feeding and used to estimate meal size.

TABLE 3.1.
Mean (SEM) composition of experimental diets (per kg wet weight), pilchards, *Sardina pilchardus* (n = 3), and Common squid, *Loligo forbesi* (n = 3).

	$[Mg^{2+}]$ mmol kg^{-1}	$[Ca^{2+}]$ mmol kg^{-1}	$[Na^{+}]$ mmol kg^{-1}	$[K^{+}]$ mmol kg^{-1}	$[Cl^{-}]$ mmol kg^{-1}	$[SO_4^{2-}]$ mmol kg^{-1}
Loligo forbesi	21.0 (0.73)	1.3 (0.21)	121.1 (5.54)	61.0 (3.33)	141.2 (2.87)	4.9 (0.39)
Sardina pilchardus	30.2 (2.33)	404.2 (24.8)	123.3 (4.44)	70.2 (3.89)	116.6 (7.54)	4.6 (0.22)

Sample analysis

All blood samples were promptly analyzed for hematocrit and then centrifuged (2 min at 13,000 rpm). Plasma was retained in addition to gastro-intestinal fluid samples (only the supernatant of gastro-intestinal fluid samples was retained after centrifugation to eliminate reaction with solid meal remains) for immediate analysis of pH (Accumet pH electrode connected to a Radiometer PHM220 pH meter). Total CO_2 was analyzed using a Corning 965 Carbon Dioxide Analyzer and osmolality was measured using a vapor pressure

osmometer (Wescor Vapro 5520). Samples were stored at -20ºC for subsequent analysis of inorganic anions (Dionex DX-120) and cations (Fast Sequencial atomic absorption spectrophotometry, Varian FS220) after appropriate dilution.

Osmotic coefficient calculation

Osmotic coefficients of representative monovalent (NaCl) and divalent ($MgSO_4$) solutions were calculated by making, in triplicate, 150mM solutions of each and measuring osmolality using a vapor pressure osmometer (Wescor Vapro 5520). The osmotic coefficient was calculated by dividing the measured osmotic pressure of each solution by 300 mOsm (the expected osmotic pressure assuming an osmotic coefficient = 1).

Statistical analyses

Due to variable amounts of fluid present in each gastro-intestinal segment at different stages after a meal, means were generally comprised of five samples (except for the control timepoint, in which up to 10 samples were collected for each parameter), but at times, some samples were too small to be analyzed for every parameter. Of a total 720 means, 8% (59) contained 10 samples; 3% (19) contained 9 samples; < 1% (2) contained 8 samples; 63% (455) contained 5 samples; 17% (119) contained 4 samples; 5% (36) contained 3 samples, 3% (21) contained 2 samples, 1% (8) contained 1 sample, and < 1% (1) means were omitted because no samples contained sufficient fluid for analysis. Data are presented as Mean ± 1 SEM. In analyses of organic nutrient absorption, total

inorganic ion concentration was calculated from the inorganic ion concentrations measured in each sample for each time point (including only samples in which sufficient fluid was collected to measure every ion). This provides a conservative estimate of osmotic pressure exerted by inorganic ions by assuming an osmotic coefficient of one. Because data were not normally distributed, Kruskal-Wallis one way analysis of variance (ANOVA) on ranks was used to evaluate all data, followed, where applicable, by comparisons of each parameter at each time point to control values by Dunn's method. When only two groups were compared, a Mann-Whitney Rank Sum test was used to determine statistically significant differences. Means were considered significantly different at $P<0.05$. For the sake of clarity, significant differences are not noted in figures or tables but rather are described in detail in the Results section.

Results

The meal sizes of toadfish fed the two experimental diets were not significantly different when fed to satiation. Toadfish fed sardines ingested an estimated 9 ± 2% of their body mass (n = 5), and toadfish fed squid consumed an estimated 9 ± 1% of their body mass (n = 5; based on the mass of stomach contents in fish sampled 3 h after feeding). Feeding to satiation ensured that adequate food was available to all fish, and no signs of hierarchy were observed during feeding events. The ingested meal was found to be cleared completely from the stomach between 24 and 48 hours after feeding for both diets.

Postprandial intestinal Cl^-/HCO_3^- exchange

In both high and low Ca^{2+} diets, pH (Fig. 3.1) and total CO_2 (HCO_3^- equivalents, Fig. 3.2) levels in gastro-intestinal fluids indicated that postprandially increased HCO_3^- secretion acted as a buffer for H^+ secreted and subsequently released from the stomach with chyme. Between 3 and 24 h post-feeding, intestinal fluid HCO_3^- equivalents were reduced to as little as 50% of control levels (Fig. 3.2, Table 3.2), a decrease that was statistically significant only in the mid intestinal fluid 3 h after feeding a squid diet. Luminal pH was also slightly depressed at these timepoints, especially in the anterior and mid intestinal fluid (Fig. 3.1, Table 3.2), where pH was significantly reduced from control levels 3 h after feeding sardines. Correspondingly, 48 h after feeding (once stomach secretions were presumably neutralized), a dramatic increase in HCO_3^- equivalents was measured relative to control levels. Bicarbonate equivalents on average were present at 231 and 204% control levels in the anterior intestinal fluid 48 h after feeding fish and squid diets, respectively (Fig. 3.2, Table 3.2), although limited sample sizes prohibited statistical significance. This rise over control HCO_3^- concentrations was most dramatic in the anterior intestine of both diets 48 h post feeding, and was sequentially less pronounced in the more posterior sections, indicating that postprandial HCO_3^- secretion might be prevalent in the anterior intestine. Notably, these HCO_3^- measurements are based exclusively on intestinal fluid concentrations, and neglect to account for any additional increases in HCO_3^- concentration accounted for by $CaCO_3$

precipitation. Overall, HCO_3^- concentrations of intestinal fluids ranged from 4 to 20-fold control plasma levels (Tables 3.2 and 3.3, respectively).

Postprandial luminal Cl^- concentrations (Fig. 3.3, Table 3.2) in both diets support an increase in intestinal Cl^-/HCO_3^- exchange post-feeding. Intestinal fluid Cl^- concentrations were reduced from control levels between 3 and 48 h post-feeding in both squid and sardine diets. This difference from control conditions was statistically significant in the anterior, mid, and posterior intestinal fluid between 6 and 24 h post-feeding in toadfish fed a squid diet, and at 12 h and 24 h timepoints in toadfish fed sardines. Additionally, a slight (though not statistically significant using Kruskal-Wallis one-way ANOVA on ranks) increase in plasma Cl^- concentration over control levels was measured between 12 and 48 h post feeding in toadfish fed squid (Table 3.3).

TABLE 3.2. Chemistry and inorganic ion composition of intestinal fluid from *O. beta* fed squid (A) and sardines (B); mean (±1 SEM), sample sizes vary as detailed in text.

A.

Squid Diet	pH	Total CO_2 (mM)	$[Cl^-]$ (mM)	$[Na^+]$ (mM)	$[Ca^{2+}]$ (mM)	$[K^+]$ (mM)	$[Mg^{2+}]$ (mM)	$[SO_4^{2-}]$ (mM)
Pre-feeding (0 h)								
Anterior	8.51	32.7	93.0	62.3	2.5	6.2	95.3	63.7
	(0.155)	(11.38)	(19.47)	(16.74)	(0.52)	(2.99)	(23.38)	(11.71)
Mid	8.50	62.4	51.9	29.8	1.8	1.7	158.5	97.1
	(0.120)	(4.03)	(4.82)	(6.07)	(0.65)	(0.43)	(11.69)	(6.44)
Posterior	8.70	72.9	49.4	19.8	2.3	5.2	133.9	104.7
	*	(3.72)	(4.83)	(2.78)	(0.86)	(1.99)	(10.41)	(3.19)
Rectal	8.78	68.3	30.7	10.4	2.1	1.1	135.8	93.8
	(0.013)	(7.71)	(4.22)	(0.79)	(0.69)	(0.04)	(14.04)	(8.96)
3 h post-feeding								
Anterior	8.14	20.6	36.0	71.9	4.0	7.0	34.4	26.8
	(0.096)	(3.63)	(8.28)	(9.12)	(0.48)	(1.02)	(5.31)	(1.40)
Mid	8.33	29.2	35.3	83.0	3.6	3.9	62.0	41.1
	(0.042)	(4.47)	(8.72)	(17.77)	(1.25)	(0.56)	(18.03)	(11.34)
Posterior	8.47	54.9	38.0	48.2	3.4	3.1	144.2	83.9
	(0.081)	(3.73)	(5.76)	(8.44)	(0.49)	(0.52)	(16.15)	(8.59)
Rectal	8.80	59.0	28.7	17.7	3.1	1.8	127.5	78.7
	(0.032)	(9.26)	(6.64)	(6.12)	(0.99)	(0.22)	(18.39)	(11.94)

6 h post-feeding								
Anterior	8.08	50.5	23.7	64.7	10.3	3.6	66.0	48.3
	(0.119)	(10.05)	(8.34)	(14.02)	(3.56)	(0.37)	(16.87)	(8.18)
Mid	8.27	55.2	13.5	71.0	6.9	2.7	80.7	56.4
	(0.112)	(14.72)	(3.77)	(19.40)	(2.84)	(0.26)	(30.47)	(15.01)
Posterior	8.37	65.2	19.5	56.6	3.4	2.9	73.2	77.2
	(0.025)	(18.11)	(6.54)	(18.96)	(0.79)	(0.32)	(14.34)	(19.24)
Rectal	8.74	55.1	15.5	16.2	5.5	1.4	106.0	78.5
	(0.141)	(11.27)	(6.97)	(5.90)	(0.36)	(0.14)	(22.94)	(16.07)
12 h post-feeding								
Anterior	7.99	34.4	37.3	85.3	9.6	4.5	77.1	36.1
	(0.021)	(2.11)	(5.07)	(14.23)	(0.37)	(0.42)	(7.32)	(2.79)
Mid	8.39	49.0	13.7	39.2	9.7	2.0	111.4	55.6
	(0.024)	(3.86)	(1.47)	(6.62)	(1.56)	(0.15)	(13.46)	(4.27)
Posterior	8.44	48.6	15.6	21.5	8.5	1.9	108.8	56.5
	(0.036)	(4.56)	(2.00)	(3.70)	(1.81)	(0.05)	(13.65)	(6.47)
Rectal	8.16	62.0	24.5	9.6	3.9	1.0	78.6	60.7
	(0.575)	(36.60)	(9.36)	(4.17)	*	(0.10)	(32.74)	(26.26)
24 h post-feeding								
Anterior	7.81	42.1	29.9	54.3	13.0	5.0	100.4	67.1
	(0.084)	(5.63)	(3.41)	(22.00)	(1.55)	(0.26)	(18.64)	(8.21)
Mid	8.06	41.7	14.4	64.6	15.6	3.6	91.5	84.9
	(0.035)	(3.66)	(2.18)	(16.76)	(2.09)	(0.26)	(16.50)	(4.62)
Posterior	8.24	44.4	18.5	40.4	11.9	2.8	115.7	76.0
	(0.101)	(5.44)	(2.18)	(11.86)	(2.16)	(0.24)	(12.75)	(5.81)
Rectal	8.56	50.4	13.6	8.5	6.7	1.9	81.5	56.4
	(0.113)	(5.99)	(2.33)	(2.97)	(1.87)	(0.35)	(22.49)	(8.07)
48 h post-feeding								
Anterior	8.20	66.5	53.6	37.6	7.7	2.1	140.6	109.1
	(0.162)	(5.22)	(10.56)	(4.54)	(0.80)	(0.36)	(3.02)	(6.39)
Mid	8.14	69.1	41.9	37.1	7.8	1.8	167.4	137.2
	(0.204)	(5.68)	(10.95)	(4.78)	(1.68)	(0.19)	(5.29)	(10.16)
Posterior	8.36	74.1	37.5	38.7	7.6	2.9	166.5	129.4
	(0.122)	(7.19)	(8.63)	(10.14)	(1.37)	(0.57)	(10.33)	(10.17)
Rectal	8.41	63.0	21.7	20.7	8.1	1.8	167.2	131.5
	(0.093)	(6.77)	(1.67)	(7.95)	(0.76)	(0.34)	(10.23)	(7.67)

72 h post-feeding								
Anterior	8.55 *	52.1 (9.82)	101.6 (14.66)	60.3 (18.21)	4.5 (1.05)	4.2 (1.28)	113.9 (17.75)	73.1 (17.80)
Mid	8.66 (0.020)	71.3 (6.75)	76.0 (10.20)	27.5 (7.43)	5.9 (1.08)	3.1 (0.45)	141.5 (12.96)	79.3 (9.39)
Posterior	8.73 *	79.1 (4.07)	82.2 (8.67)	33.9 (7.76)	4.0 (1.43)	4.4 (0.98)	159.5 (14.06)	98.0 (10.42)
Rectal	8.80 (0.035)	78.4 (5.26)	49.8 (8.25)	13.9 (1.24)	4.1 (0.93)	1.2 (1.05)	133.1 (15.50)	87.8 (10.50)
144 h post-feeding								
Anterior	8.61 (0.046)	60.0 (3.18)	81.6 (4.10)	31.4 (3.44)	4.1 (0.69)	3.9 (1.09)	119.3 (7.70)	69.6 (7.86)
Mid	8.64 (0.045)	81.4 (5.71)	57.6 (5.53)	22.3 (4.28)	2.6 (0.61)	2.5 (0.83)	147.6 (19.78)	72.9 (15.93)
Posterior	8.62 *	84.8 (4.45)	71.1 (10.80)	23.3 (2.48)	3.3 (1.32)	1.5 (0.47)	173.0 (8.27)	90.9 (5.42)
Rectal	8.76 (0.055)	83.7 (8.13)	41.4 (5.38)	12.7 (1.65)	1.3 (0.37)	0.3 (0.09)	158.0 (19.43)	81.4 (11.04)
216 h post-feeding								
Anterior	8.68 (0.035)	78.5 (8.12)	78.5 (7.32)	41.9 (6.35)	3.4 (0.70)	5.1 (1.00)	132.5 (12.93)	38.1 (22.66)
Mid	8.68 (0.027)	77.5 (12.36)	63.8 (11.49)	28.8 (4.18)	2.7 (0.87)	2.6 (0.85)	158.6 (14.51)	75.2 (9.93)
Posterior	8.69 (0.027)	81.4 (10.47)	60.1 (7.66)	22.4 (2.46)	1.9 (0.73)	1.7 (0.47)	153.7 (9.92)	46.6 (15.97)
Rectal	8.72 (0.018)	89.0 (3.92)	53.2 (3.00)	18.4 (2.17)	2.9 (0.11)	0.9 (0.19)	170.9 (5.42)	58.8 (11.89)

B.

Sardine Diet	pH	Total CO_2 (mM)	$[Cl^-]$ (mM)	$[Na^+]$ (mM)	$[Ca^{2+}]$ (mM)	$[K^+]$ (mM)	$[Mg^{2+}]$ (mM)	$[SO_4^{2-}]$ (mM)
Pre-feeding (0 h)								
Anterior	8.47	34.0	101.2	91.0	2.4	6.5	52.2	45.4
	(0.047)	(13.00)	(8.19)	(13.84)	(0.63)	(1.08)	(22.33)	(13.33)
Mid	8.86	48.3	84.4	76.5	2.3	4.1	81.7	44.5
	(0.125)	(6.38)	(5.48)	(21.61)	(0.52)	(0.71)	(26.66)	(14.88)
Posterior	†	66.5	84.2	77.5	2.4	4.7	115.5	62.3
		(17.50)	(9.61)	(32.29)	(1.31)	(0.98)	(34.43)	(18.81)
Rectal	8.86	54.2	43.2	15.1	1.0	1.7	133.3	65.2
	(0.079)	(9.06)	(11.10)	(3.31)	(0.23)	(0.07)	(37.83)	(16.46)
3 h post-feeding								
Anterior	7.19	18.2	72.3	88.9	17.3	10.1	56.9	41.7
	(0.202)	(2.75)	(7.80)	(17.21)	(5.94)	(1.40)	(10.56)	(4.89)
Mid	8.05	40.3	38.6	73.9	12.1	3.6	78.1	54.0
	(0.083)	(5.03)	(6.36)	(17.53)	(4.39)	(0.46)	(16.75)	(6.04)
Posterior	8.27	46.9	31.7	66.2	8.5	3.2	91.0	64.8
	(0.108)	(8.02)	(5.91)	(17.06)	(3.07)	(0.39)	(21.87)	(7.92)
Rectal	8.87	49.6	19.6	18.5	1.6	1.5	86.6	61.7
	(0.128)	(3.53)	(4.69)	(9.61)	(0.85)	(0.20)	(23.46)	(8.45)
6 h post-feeding								
Anterior	7.50	23.2	64.7	75.6	21.3	4.7	63.9	49.9
	(0.105)	(5.26)	(7.84)	(8.23)	(4.48)	(0.45)	(2.58)	(4.33)
Mid	8.29	41.6	30.4	58.5	14.6	2.8	94.5	67.7
	(0.047)	(3.01)	(4.57)	(6.14)	(1.20)	(0.17)	(3.66)	(3.26)
Posterior	8.54	49.7	25.9	44.8	10.9	2.6	127.1	76.0
	(0.061)	(4.63)	(4.47)	(6.66)	(1.72)	(0.23)	(15.13)	(7.34)
Rectal	8.82	68.7	24.3	17.2	2.9	1.6	125.5	70.7
	(0.054)	(10.02)	(5.32)	(5.10)	(1.44)	(0.24)	(25.18)	(13.57)

12 h post-feeding								
Anterior	7.79	32.8	40.1	92.2	19.3	5.2	68.0	22.6
	(0.146)	(4.44)	(6.11)	(12.26)	(5.27)	(0.64)	(14.24)	(8.77)
Mid	8.18	42.9	16.9	82.4	14.4	3.4	93.1	47.4
	(0.077)	(5.86)	(3.06)	(12.91)	(2.06)	(0.40)	(16.66)	(10.68)
Posterior	8.41	51.3	14.9	41.9	11.1	2.2	134.7	67.8
	(0.120)	(7.32)	(3.46)	(4.64)	(1.82)	(0.20)	(15.19)	(9.59)
Rectal	8.58	48.5	16.1	17.8	5.9	1.5	115.1	41.6
	(0.057)	(15.52)	(8.05)	(3.80)	(2.04)	(0.14)	(26.29)	(12.41)
24 h post-feeding								
Anterior	8.06	47.2	41.5	77.1	7.9	3.7	110.0	45.8
	(0.262)	(9.73)	(8.63)	(24.12)	(3.05)	(0.83)	(26.17)	(13.55)
Mid	8.24	51.1	15.6	64.5	11.4	2.8	140.0	83.2
	(0.151)	(9.09)	(7.17)	(17.36)	(2.07)	(0.44)	(19.30)	(6.35)
Posterior	8.49	47.0	19.9	73.0	10.1	2.9	131.3	76.6
	*	(8.29)	(3.25)	(22.63)	(3.62)	(0.48)	(26.75)	(10.33)
Rectal	8.37	32.7	8.3	26.7	12.2	2.0	129.6	72.8
	(0.048)	(7.82)	(5.37)	(7.81)	(2.65)	(0.09)	(18.20)	(12.03)
48 h post-feeding								
Anterior	8.59	78.6	76.7	57.2	2.8	2.3	112.5	72.4
	(0.138)	(15.15)	(16.06)	(21.84)	(0.06)	(0.82)	(30.06)	(14.26)
Mid	8.67	100.2	58.8	72.8	5.0	2.8	128.6	83.6
	(0.086)	(13.18)	(11.57)	(25.71)	(1.65)	(0.54)	(24.09)	(11.21)
Posterior	8.73	105.6	43.8	71.4	2.8	3.4	125.3	82.4
	(0.120)	(14.58)	(7.64)	(26.13)	(0.33)	(0.86)	(29.48)	(13.45)
Rectal	7.93	68.5	43.0	41.4	7.0	4.5	165.5	121.9
	(0.260)	(7.27)	(10.47)	(16.72)	(2.28)	(1.56)	(40.27)	(19.35)
72 h post-feeding								
Anterior	8.33	43.0	100.1	62.5	3.1	4.1	104.3	58.6
	*	(11.78)	(11.37)	(14.74)	(0.21)	(1.06)	(17.66)	(11.00)
Mid	8.66	68.9	74.1	32.5	2.7	4.5	145.7	83.7
	(0.114)	(5.53)	(3.17)	(1.77)	(0.39)	(1.84)	(4.40)	(2.85)
Posterior	8.90	82.8	62.9	26.2	2.5	2.5	149.3	86.8
	(0.087)	(4.34)	(2.00)	(1.84)	(0.37)	(1.06)	(4.50)	(2.79)
Rectal	8.77	84.3	45.5	19.1	3.6	0.7	197.5	123.6
	(0.064)	(8.13)	(4.42)	(1.35)	(1.08)	(0.10)	(1.11)	(7.87)

144 h post-feeding								
Anterior	8.69	52.6	100.6	63.7	4.6	7.1	98.3	52.3
	(0.030)	(9.61)	(5.94)	(14.71)	(0.41)	(1.36)	(17.44)	(9.36)
Mid	8.57	73.5	81.9	31.5	3.5	3.3	139.6	76.9
	(0.050)	(10.08)	(4.57)	(4.24)	(0.43)	(0.66)	(6.35)	(4.46)
Posterior	8.66	69.4	88.6	29.2	5.0	4.4	151.4	82.4
	*	(6.48)	(6.75)	(3.67)	(1.30)	(1.17)	(9.66)	(5.88)
Rectal	8.75	69.7	73.5	23.2	2.5	0.8	170.8	93.6
	(0.031)	(5.73)	(6.96)	(3.70)	(0.14)	(0.22)	(9.46)	(6.87)
216 h post-feeding								
Anterior	8.52	55.8	80.2	41.6	3.2	2.3	98.9	54.0
	(0.025)	(9.01)	(8.63)	(2.92)	(0.80)	(0.44)	(15.89)	(8.65)
Mid	8.69	77.4	63.9	29.3	3.1	1.8	156.7	86.3
	(0.040)	(5.41)	(5.39)	(4.57)	(0.63)	(0.48)	(11.03)	(6.43)
Posterior	8.56	78.5	62.9	22.1	1.9	1.8	162.4	90.7
	(0.020)	(6.95)	(3.44)	(1.26)	(0.54)	(0.35)	(6.58)	(3.20)
Rectal	8.63	65.3	59.7	15.1	2.7	0.9	163.7	84.9
	(0.050)	(13.96)	(10.33)	(1.30)	(1.25)	(0.34)	(14.63)	(6.69)

* n = 1

† n = 0

TABLE 3.3. Chemistry and inorganic ion composition of blood plasma from *O. beta* fed squid (A) and sardines (B); mean (±1 SEM), n = 10 for control samples, n = 5 for all others.

A.

Time after feeding (h)	pH	Osmolality (mOsm)	Hematocrit (%)	Total CO_2 (mM)	$[Cl^-]$ (mM)	$[Na^+]$ (mM)	$[K^+]$ (mM)	$[Ca^{2+}]$ (mM)
0 (Control)	7.74 (0.038)	310 (2.4)	34 (2.3)	5.2 (0.59)	118.5 (1.44)	143.6 (2.95)	2.5 (0.15)	2.0 (0.14)
3	7.96 (0.038)	319 (1.7)	23 (1.6)	3.3 (0.51)	116.2 (0.70)	134.9 (3.72)	2.6 (0.25)	1.5 (0.11)
6	7.75 (0.041)	318 (1.9)	27 (2.6)	4.7 (0.37)	118.1 (2.76)	137.5 (4.47)	3.2 (0.59)	2.3 (0.15)
12	7.86 (0.018)	326 (2.4)	31 (3.0)	5.5 (0.39)	126.4 (1.99)	141.7 (4.50)	3.8 (0.23)	2.4 (0.34)
24	7.84 (0.055)	315 (11.9)	31 (4.3)	4.7 (0.43)	124.1 (6.58)	140.6 (12.62)	4.0 (0.32)	2.5 (0.70)
48	7.87 (0.062)	292 (3.3)	28 (2.7)	4.6 (0.30)	132.1 (5.93)	143.7 (6.70)	2.8 (0.14)	1.5 (0.06)
72	7.94 (0.033)	287 (3.1)	33 (3.2)	5.0 (0.10)	115.2 (1.22)	131.9 (1.57)	2.7 (0.15)	1.7 (0.11)
144	8.03 (0.013)	267 (6.7)	24 (1.3)	5.2 (0.23)	109.0 (2.93)	123.7 (4.25)	3.8 (0.38)	1.7 (0.18)
216	7.91 (0.041)	286 (4.6)	23 (2.4)	4.6 (0.64)	111.2 (4.10)	133.7 (4.86)	2.4 (0.12)	1.8 (0.16)

B.

Time after feeding (h)	pH	Osmolality (mOsm)	Hematocrit (%)	Total CO_2 (mM)	$[Cl^-]$ (mM)	$[Na^+]$ (mM)	$[K^+]$ (mM)	$[Ca^{2+}]$ (mM)
0 (Control)	8.21 (0.022)	321 (5.5)	21 (0.5)	2.7 (0.21)	129.5 (4.14)	158.3 (5.45)	4.5 (0.13)	2.5 (0.28)
3	8.31 (0.029)	322 (4.0)	20 (2.4)	2.4 (0.19)	120.0 (1.64)	149.9 (3.25)	6.4 (0.14)	1.9 (0.20)
6	8.34 (0.040)	323 (2.9)	21 (1.0)	3.8 (0.23)	124.3 (1.42)	145.1 (1.61)	4.4 (0.34)	2.3 (0.06)
12	8.30 (0.032)	315 (2.5)	23 (1.3)	4.2 (0.46)	127.5 (1.52)	145.8 (1.81)	4.1 (0.15)	2.6 (0.09)
24	7.95 (0.033)	312 (3.9)	17 (1.9)	2.2 (0.50)	114.2 (2.46)	139.1 (3.60)	4.7 (0.30)	2.8 (0.58)
48	7.65 (0.015)	320 (2.1)	28 (2.8)	5.3 (0.25)	130.0 (2.18)	147.1 (1.75)	2.8 (0.19)	1.6 (0.12)
72	8.01 (0.047)	319 (1.2)	35 (1.2)	5.0 (0.24)	130.3 (1.39)	149.5 (1.68)	3.7 (0.18)	1.3 (0.03)
144	7.74 (0.063)	337 (4.2)	35 (1.6)	3.4 (0.68)	130.0 (2.06)	154.1 (2.20)	6.8 (1.41)	1.4 (0.08)
216	7.86 (0.043)	321 (3.6)	23 (3.1)	5.3 (0.47)	127.3 (2.45)	155.6 (3.66)	4.2 (0.09)	1.6 (0.13)

While luminal Cl^- concentrations were reduced post-feeding, no such trend was observed for Na^+ concentrations (Fig. 3.4, Table 3.2), yielding additional evidence for enhanced postprandial apical Cl^-/HCO_3^- exchange as opposed to Na^+-Cl^- cotransport.

Consequences of high dietary Ca^{2+} and K^+ loads

While unfed (control) toadfish maintained low intestinal Ca^{2+} concentrations, fed toadfish experienced up to a 10-fold postprandial increase in intestinal Ca^{2+} concentrations (Fig. 3.5, Table 3.2). In toadfish fed a squid diet, Ca^{2+} concentrations were significantly elevated over control conditions at 24 h post-feeding in the anterior intestine fluid, 12 and 24 h post-feeding in mid and posterior intestine fluid, and 48 h post-feeding in rectal fluid. In toadfish fed sardines, however, Ca^{2+} seemed to be liberated into the intestinal fluid sooner, as concentrations were significantly elevated at 6 and 12 h post-feeding in the anterior and mid intestine fluid, and 24 h post-feeding in the rectal fluid. A notable difference in diet composition was evident in stomach Ca^{2+} concentrations, which were significantly higher in fish fed sardines and maximal 12 h post-feeding (77.4 ± 6.52 mM) in these fish (Fig. 3.5B). In toadfish fed a squid diet, stomach Ca^{2+} concentrations were maximal 3 h post-feeding (6.8 ± 0.32 mM; Fig. 3.5A). Despite the intense Ca^{2+} load to the gastro-intestinal tract of toadfish fed sardines, no increase in plasma Ca^{2+} concentration was observed in fish fed either diet (Table 3.3).

Another difference in diets was suggested by the K^+ loads they carried to the gastro-intestinal tract. While K^+ levels of the two diets were similar (Table 3.1), mean K^+ concentrations in the stomach and anterior intestine of toadfish fed sardines were approximately 2 and 1.5 times those in squid-fed toadfish, respectively (Fig. 3.6). Additionally, a nearly 50% increase was seen in mean plasma K^+ concentrations 3 h post-feeding in toadfish fed sardines (Table 3.3B), although sample sizes were too small to gain statistical significance.

Fig. 3.1. pH in the stomach and anterior intestinal fluids of *Opsanus beta* fed squid (filled circles) and fish (open circles); means ± 1 SEM, n = 5 for most samples, as described in text.

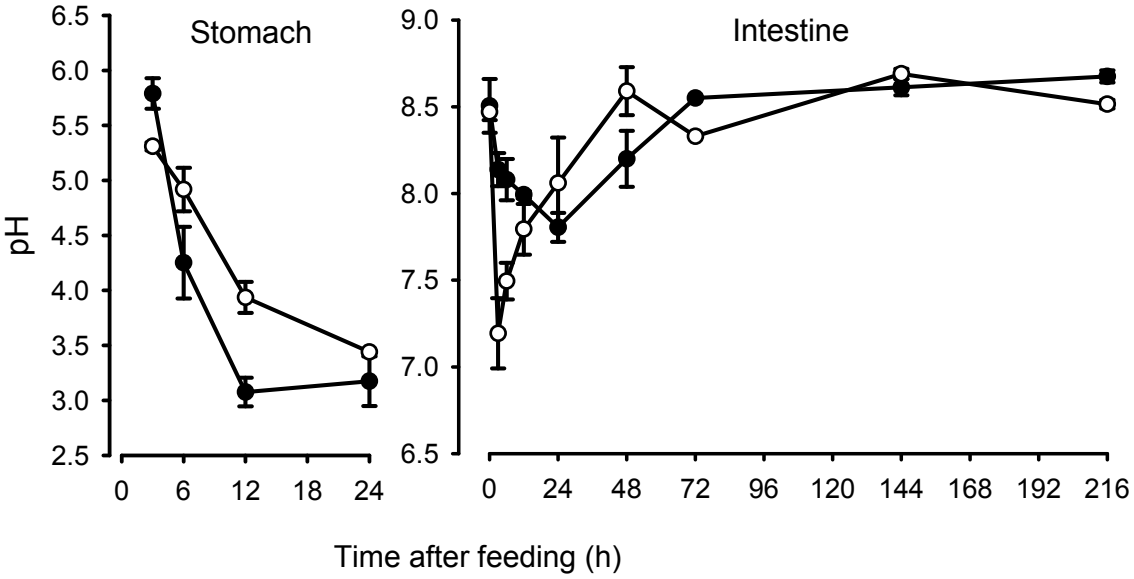

Fig. 3.2. Total CO_2 (HCO_3^- equivalents) in the stomach and anterior intestinal fluids of *Opsanus beta* fed squid (filled circles) and fish (open circles); means ± 1 SEM, n = 5 for most samples, as described in text.

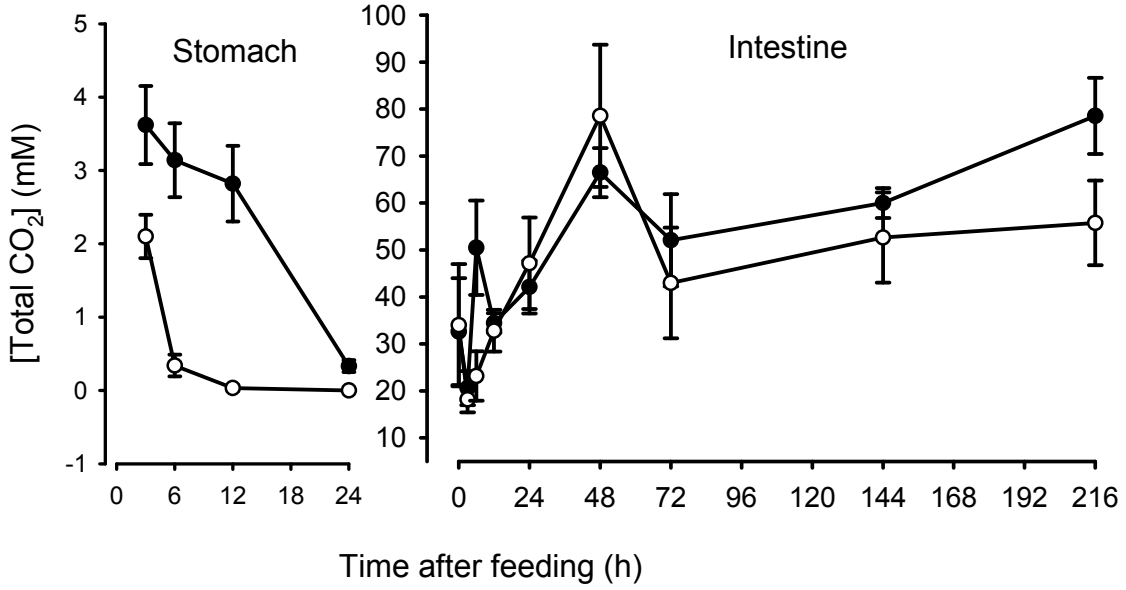

Fig. 3.3. Cl^- concentrations in the stomach and anterior intestinal fluids of *Opsanus beta* fed squid (filled circles) and fish (open circles); means ± 1 SEM, n = 5 for most samples, as described in text.

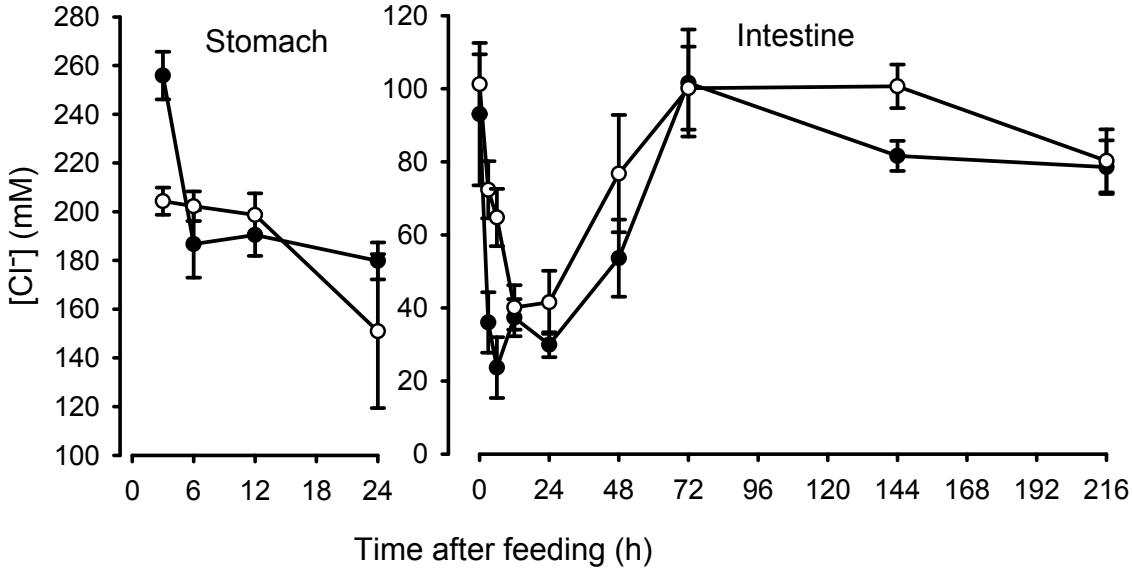

Fig. 3.4. Na^+ concentrations in the stomach and anterior intestinal fluids of *Opsanus beta* fed squid (filled circles) and fish (open circles); means ± 1 SEM, n = 5 for most samples, as described in text.

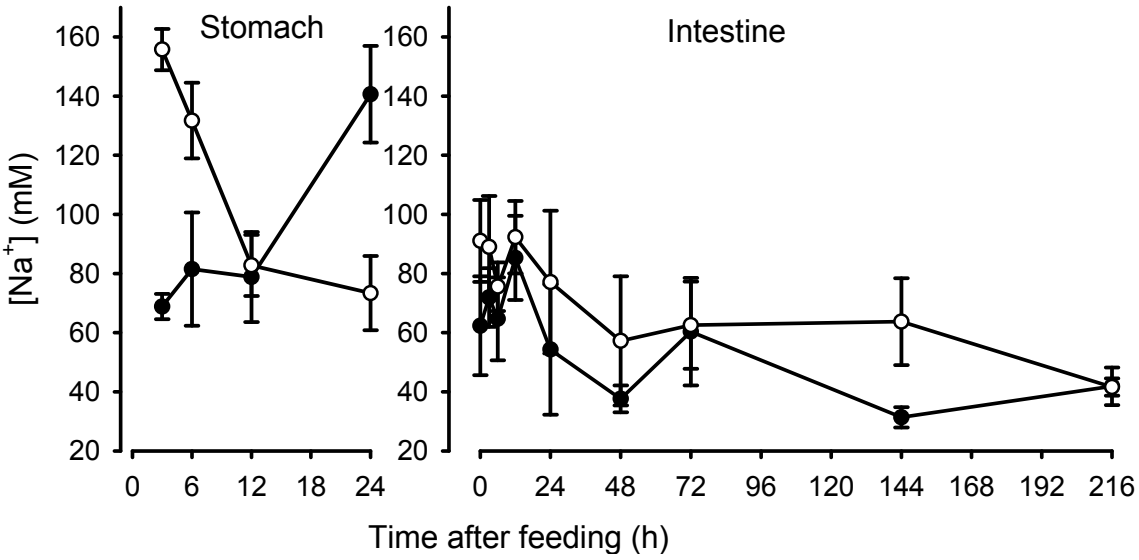

Fig. 3.5. Ca^{2+} concentrations in the stomach and anterior intestinal fluids of *Opsanus beta* fed squid (filled circles) and fish (open circles); means ± 1 SEM, n = 5 for most samples, as described in text.

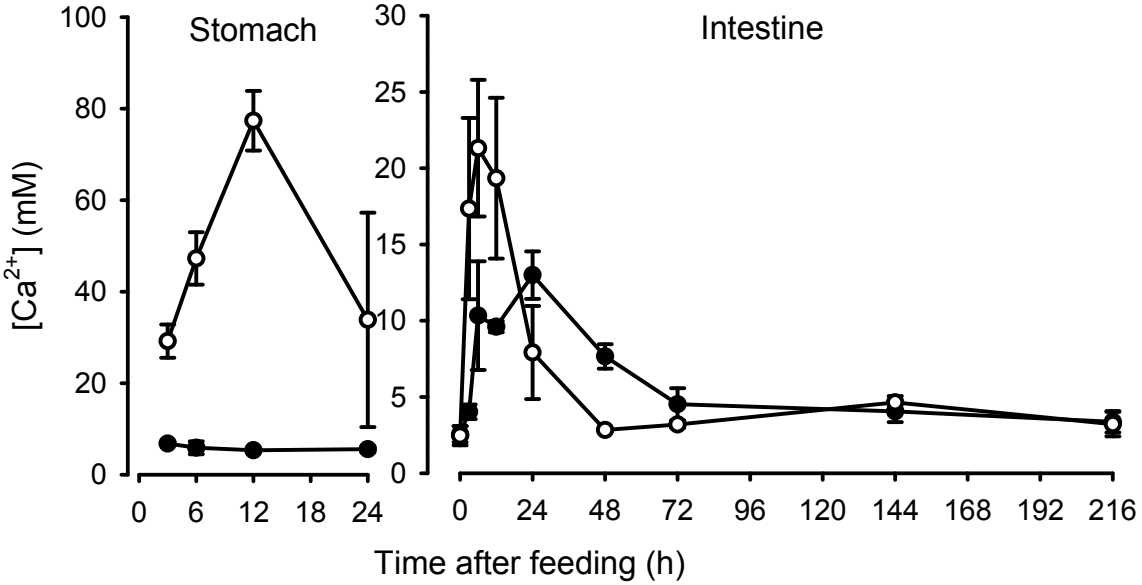

Fig. 3.6. K^+ concentrations in the stomach and anterior intestinal fluids of *Opsanus beta* fed squid (filled circles) and fish (open circles); means ± 1 SEM, n = 5 for most samples, as described in text.

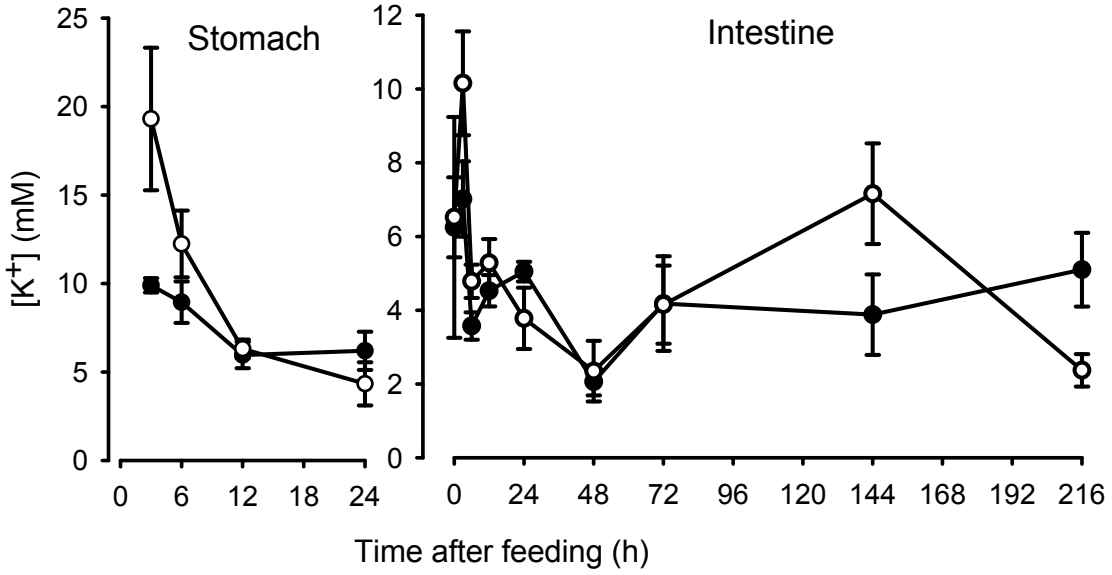

Fig. 3.7. Mg^{2+} concentrations in the stomach and anterior intestinal fluids of *Opsanus beta* fed squid (filled circles) and fish (open circles); means ± 1 SEM, n = 5 for most samples, as described in text.

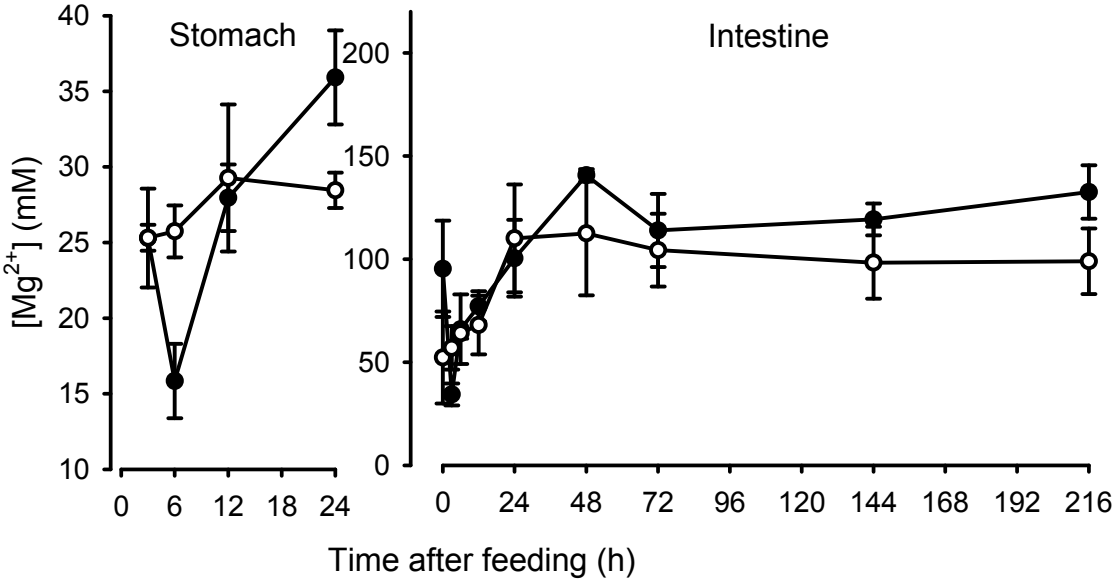

Fig. 3.8. SO_4^{2-} concentrations in the stomach and anterior intestinal fluids of *Opsanus beta* fed squid (filled circles) and fish (open circles); means ± 1 SEM, n = 5 for most samples, as described in text.

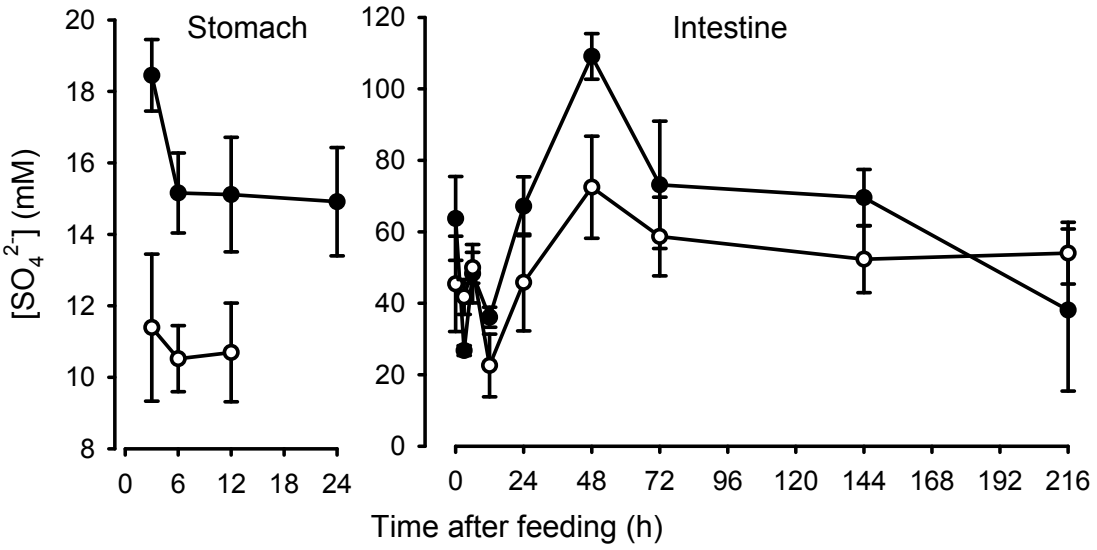

Intestinal water absorption and divalent ion concentration

Immediately following feeding, mean intestinal Mg^{2+} and SO_4^{2-} concentrations were reduced to as little as 36 and 42% control concentrations, respectively, in toadfish fed a squid diet (Figs. 3.7A and 3.8A, respectively, and Table 3.2). This decline in both Mg^{2+} and SO_4^{2-} concentrations was statistically significant only in the mid intestinal fluid 3 h post-feeding. A postprandial reduction in intestinal Mg^{2+} and SO_4^{2-} concentrations was also noted in toadfish fed sardines (Figs. 3.7B and 3.8B, respectively, and Table 3.2), though these ions were only reduced to as little as 65 and 50% control conditions, respectively, and exhibited no statistically significant differences from control concentrations. By 48 h post feeding, however, water absorption rather than secretion appears to

have resumed in full force as intestinal Mg^{2+} and SO_4^{2-} concentrations return to and even exceed their high levels in control fish.

Osmotic coefficients in monovalent and divalent solutions

Our experimental determination of divalent and monovalent solution osmotic coefficients yielded an osmotic coefficient of 0.91 (±0.002) for the monovalent solution NaCl, and an osmotic coefficient of 0.56 (±0.004) for the divalent solution $MgSO_4$. Thus a replacement along the gastro-intestinal tract of monovalent ions with divalent ions will facilitate water absorption by lowering osmotic pressure in the lumen.

Organic nutrient absorption

By calculating the difference between measured osmolality and the sum of inorganic ion concentrations in a given sample, a conservative prediction of the concentration (mEqv) of organic solutes present in the sample was made. Measured plasma osmolality is consistently significantly higher than the sum of inorganic ions (Fig. 3.9A) of fish fed both diets. In toadfish fed a squid diet (Fig. 3.9A.i.), there is a statistically significant rise in plasma osmolality 12 h post-feeding, but not a significant increase in the sum of inorganic ion concentration.

The very high stomach osmolality 3 h post-feeding in toadfish fed a squid diet comprises less than 45% inorganic ions (Fig. 3.9B.i.), while the stomach osmolality in toadfish fed sardines was significantly lower and composed of approximately 75% inorganic ions (Fig. 3.9B.ii.). The stomach of toadfish fed

sardines also held a significantly greater concentration of inorganic ions than did the squid diet. The gap between stomach osmolality and inorganic ion sum became progressively narrower as time after feeding increased, until most organics in the stomach were absorbed or passed on to the intestine by 24 h post feeding in toadfish fed squid, and 12 h in toadfish fed fish. In the stomach, this gap (thus the estimated concentration of organics) was statistically significant between 3 and 12 h after feeding in toadfish fed a squid diet, and between 3 and 6 h post-feeding in toadfish fed sardines. Along the intestine, osmolality exceeds total ion sum until 24-48 h post-feeding, when osmolality drops and total inorganic ion sum increases above the corresponding osmotic pressure as gastro-intestinal conditions return to baseline levels.

Fig. 3.9. Osmolality (solid line) and ion sum (dashed line) of plasma (A), stomach (B), anterior intestine (C), mid intestine (D), posterior intestine (E), and rectal (F) fluid of *Opsanus beta* fed squid (i) and fish (ii); means ± 1 SEM, n = 5 for most samples, as described in text.

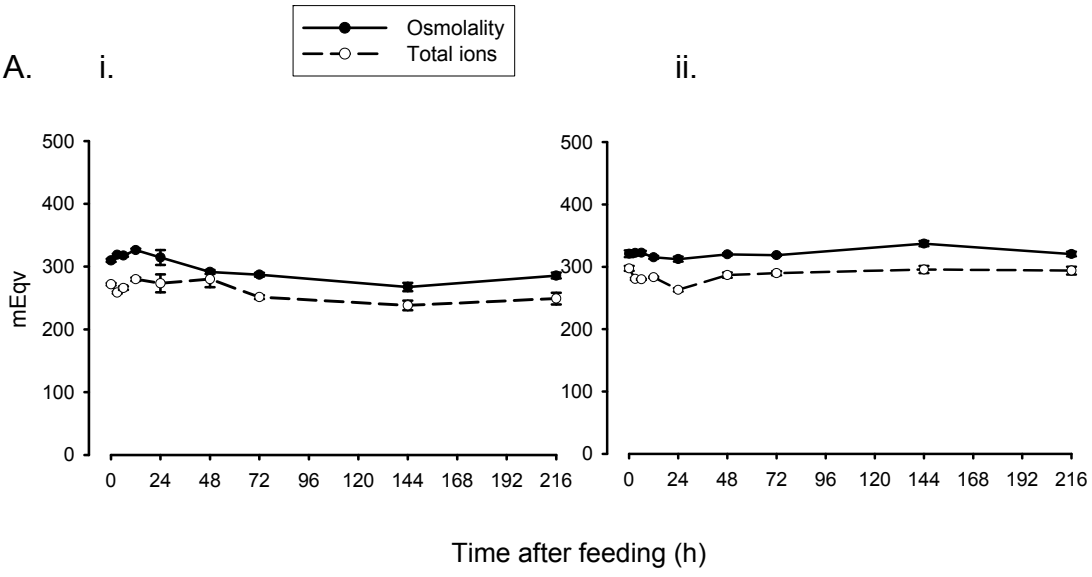

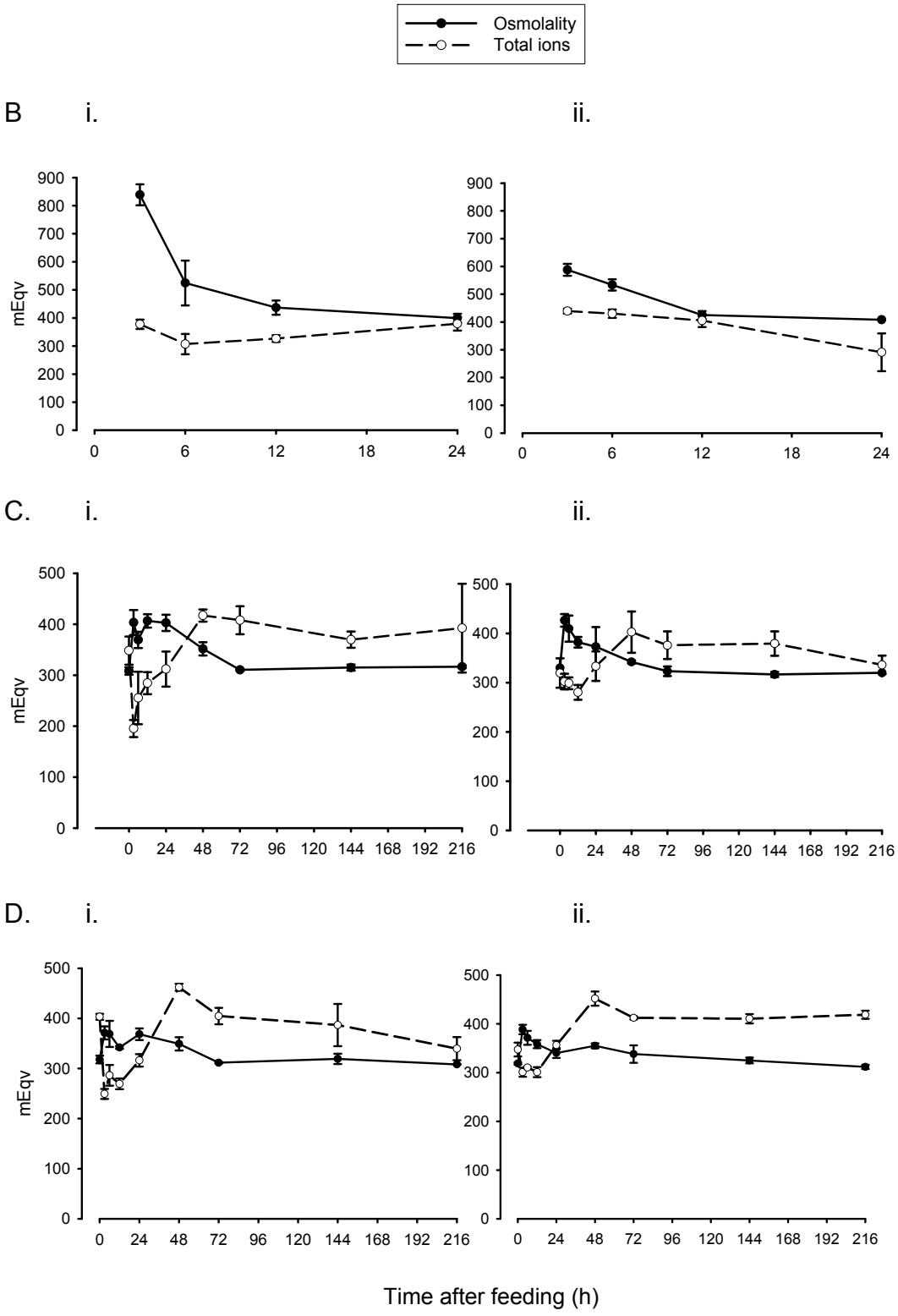
Osmolality
Total ions
B
i.
ii.
C.
i.
ii.
D.
i.
ii.
mEqv
Time after feeding (h)

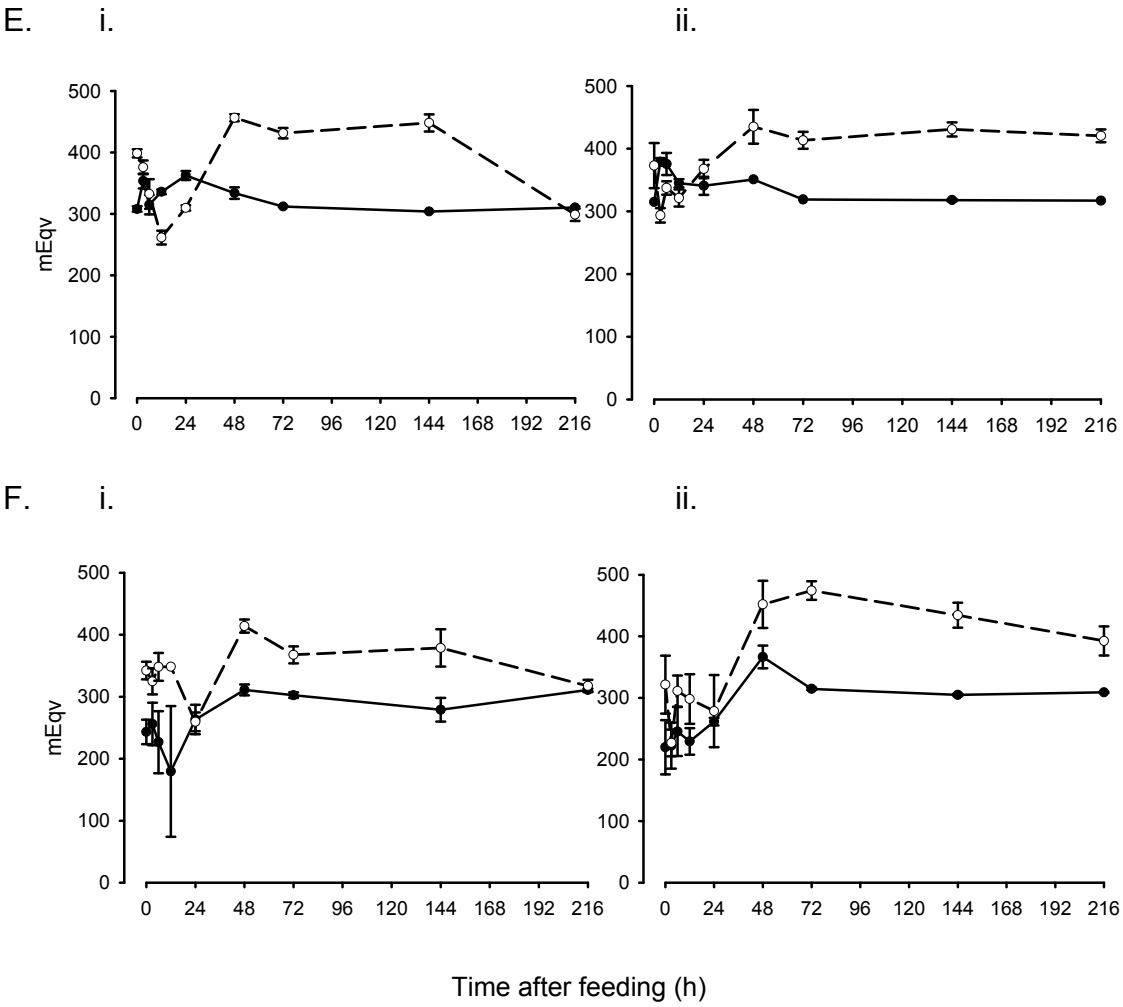

Disturbed acid-base balance?

Plasma pH (Table 3.3) did not exhibit strong trends in toadfish fed either diet, although it was significantly increased over control conditions at 3 h post-feeding in toadfish fed a squid diet. No statistically significant changes were seen in plasma pH of toadfish fed sardines. Also, no significant changes in plasma HCO_3^- (Table 3.3) were measured postprandially in either diet.

Conclusions

Feeding results in substantial changes in the ionic composition of intestinal fluids; notably, an acute influx of dietary salts prompts apparent transient changes in fluid absorption/secretion and stimulation of intestinal HCO_3^- secretion. The mechanisms of these intestinal transport properties (and changes therein) may be unique to digestive physiology or may be identical to mechanisms utilized to osmoregulate in a marine environment.

Postprandial intestinal Cl^-/HCO_3^- exchange

While influx of Cl^- to the anterior intestine was anticipated due to the passage of gastric HCl secretions, measured intestinal Cl^- concentrations markedly decreased immediately (by 3 h) following feeding and remained depressed for at least 48 h. Based on these reduced luminal Cl^- concentrations and on measurements of unchanged Na^+ concentrations between 3 and 48 h post-feeding, it is presumed that elevated levels of intestinal HCO_3^- at 48 h post-feeding cannot be accounted for by pancreatic-like secretion. Pancreatic secretions at least in higher vertebrates consist of a $NaHCO_3$ rich solution (Steward *et al.* 2005). Buffering of highly acidic chyme entering the intestine from the stomach to circumneutral and alkaline pH likely consumes much of the HCO_3^- secreted into the intestine. Increased apical Cl^-/HCO_3^- exchange may be stimulated postprandially either by a signal directly related to the act of feeding, by reduced luminal pH as has been shown in European flounder (Wilson and Grosell 2003), or by osmoregulatory challenges to the gastro-intestinal tract that

result from ingesting a large meal. Regardless of the mechanism of stimulation, intestinal Cl^-/HCO_3^- exchange appears beneficial both in neutralizing luminal pH and in serving Cl^- and water absorption across the intestinal epithelium between 3 and 48 h after feeding. Immediately (3 h) post-feeding, the anterior intestine of toadfish fed sardines becomes more acidified (Fig. 3.1) and has a higher Cl^- concentration (Fig. 3.3) than that of toadfish fed a squid diet. These observations together seem to indicate elevated gastric HCl secretion in fish fed sardines. Correspondingly, toadfish fed sardines experienced the highest intestinal HCO_3^- levels measured during these experiments at 48 h post-feeding (Fig. 3.2B, Table 3.2). While stomach pH was not significantly different between fish fed the two diets at any time point, it is presumed that a larger volume of acid would be required to acidify chopped fish (buffered by carbonate and phosphate salts characteristic of cycloid scales and bone) to a similar pH as chopped squid. In theory, increased gastric acid secretion and/or a prolonged gastric holding time may increase assimilation efficiency for a more difficult to digest meal (i.e., a fish diet containing scales and bone). This topic has only yet been discussed in reference to the potential of diet acidification to increase phosphorus (as bone phosphate in fish meal) assimilation in aquaculture as a means of reducing eutrophication by undigested P in these systems (Vielma and Lall 1997; Vielma *et al.* 1999; Sugiura and Hardy 2000). A review of the pylorus by Ramkumar and Schulze (2005) indicates that at least in mammals tested to date, the pylorus adjusts gastric outflow resistance to meet physiological needs as a function of chemical (acidification) and physical (mechanical) action by the stomach. The

release of chyme is presumably controlled by a similar mechanism in toadfish which, like most teleosts, possess a true stomach and pyloric sphincter. Notably, because fish were fed to satiation, the stomach of nearly all fish was so distended as to indicate the possibility that small amounts of chyme had entered the anterior intestine regardless of the state of contraction of the pyloric sphincter—a likely explanation for the immediate decrease in anterior intestine pH following feeding. Many ectothermic vertebrates also experience very large meals (often containing bone) at infrequent intervals; an exceptionally high volume of gastric acid secretion and long holding time are likely reasons for an especially pronounced alkaline tide response in these animals (Wang *et al.* 2001).

Intestinal HCO_3^- secretion may also act in part to regulate acute dietary Ca^{2+} influx. In addition to a larger influx of HCl to the intestine of toadfish fed sardines, maximal Ca^{2+} concentrations (reached 6 h post-feeding) in the anterior intestine were over two-fold those in fish fed a squid diet, yielding another possible reason for a larger peak of postprandial HCO_3^- levels in toadfish fed sardines. This may suggest an additional role of postprandial intestinal HCO_3^- secretion in leading to increased $CaCO_3$ precipitation to serve Ca^{2+} excretion during digestion of high calcium meals, as plasma Ca^{2+} concentrations were not increased postprandially in either diet (Table 3.3). Notably, Ca^{2+} concentrations in the posterior intestinal and rectal fluids never reached levels as high as those measured in the anterior and mid intestine fluid (Table 3.2). This difference could be accounted for by increased $CaCO_3$ precipitation, which was unaccounted for

by present measurements, and likely is a main route of Ca^{2+} excretion in the absence of major Ca^{2+} absorption to the extracellular fluid.

Disturbed acid-base balance?

The statistically significant yet transient increase in plasma pH measured 3 h post-feeding in toadfish fed a squid diet (Table 3.3A) indicates the possibility of a postprandial alkaline tide; however, the inconsistency in both control and treatment plasma pH values is a cause for reservation. The absence of plasma alkalinization in toadfish fed sardines (Table 3.3B), and unchanged plasma HCO_3^- concentrations in fish fed both diets (Table 3.3) suggest that feeding-induced acid-base balance disturbance is lacking in Gulf toadfish even when fed a 9% (of body mass) meal. Notably, due to the nature of the caudal puncture technique, blood samples may have contained a variable mixture of arterial and venous blood and may also have been influenced by tissue lactic acid release following anesthetic overdose. While the present measurements indicated the absence of acid-base balance disturbance, Wood et al. (2005) found that plasma pH and HCO_3^- concentrations were increased between 3 and 9 h after feeding in Pacific spiny dogfish, with virtually no evidence of respiratory compensation that is common among other vertebrate classes (Andrade *et al.* 2004). It has been shown in fishes that ventilatory adjustments have only a small effect on blood P_{CO2} levels (Perry and Wood 1989; Wood *et al.* 2005) and thus an alkaline tide would expectedly reveal itself exclusively in plasma pH and HCO_3^- concentrations as in the spiny dogfish (Wood *et al.* 2005). Additional experiments

are suggested to employ a more detailed time course, along with cannulation to provide for continual sampling, on a larger number of fish before concluding the presence or absence of a postprandial alkaline tide in Gulf toadfish. It is possible that plasma alkalinization might be absent or reduced by branchial base efflux, although this was not measured in the present experiments. Metabolic HCO_3^- is secreted by the gastric oxyntopeptic cell (gastric epithelial cells in non-mammalian vertebrates, secreting both HCl and pepsinogen) basolaterally into the extracellular fluid as a mechanism of alleviating cellular alkalosis. This HCO_3^- may be immediately transported across the gill, assumedly via either a Cl^-/HCO_3^- exchanger or Na^+-HCO_3^- cotransport (NBC) (Evans *et al.* 2005), thus no plasma alkalinization would be measured. If this is indeed the case, one may expect a more pronounced alkaline tide in freshwater fish, in which branchial anion exchange would presumably be limited by low environmental Cl^- concentrations. Another possible explanation for the lack of alkaline tide response lies in intestinal HCO_3^- secretion. As apical acid secretion by the gastric oxyntopeptic cell prompts basolateral secretion of metabolic HCO_3^- into the extracellular fluid, it is possible that this HCO_3^- provides additional substrate for intestinal Cl^-/HCO_3^- exchange which appears to be enhanced during digestion. This hypothesis however has several caveats. One involves the uncertainty of possible mechanisms responsible for transporting HCO_3^- to the intestine from the serosal side of the gastric oxyntopeptic cell. In fact, the mechanism transporting HCO_3^- to the systemic blood circulation thus creating an alkaline tide has not yet been described (Niv and Fraser 2002). A second caveat lies in the mechanism of

HCO_3^- entry into the intestinal epithelium cell. Recent reports show that the majority of HCO_3^- secreted into the intestinal lumen to serve osmoregulation arises from hydration of endogenous CO_2 in the epithelial cells of the intestine (Wilson *et al.* 2002; Grosell and Genz 2006; Grosell 2006). Therefore, it is presumed that HCO_3^- secreted basolaterally by the gastric parietal cells would have to either be dehydrated to CO_2 to enter the intestinal epithelium cell diffusively, or an additional transport pathway, such as basolateral NBC, must be supplying the intestinal epithelial cells with excess HCO_3^- during the period of postprandially stimulated HCO_3^- secretion. Clearly, postprandial acid-base balance in seawater and freshwater fishes deserves additional attention.

Gastro-intestinal water and monovalent ion absorption and divalent ion concentration

Intestinal Mg^{2+} and SO_4^{2-} concentrations are good markers for water absorption (Smith 1930), as these divalent ions see only very modest absorption across the intestinal epithelium, and are not known to precipitate to the extent that Ca^{2+} does in intestinal carbonate pellets (Walsh *et al.* 1991). A drop in luminal Mg^{2+} and SO_4^{2-} concentrations between 3 and 48 h after feeding presumably indicates an influx of gastric, biliary, intestinal and perhaps pancreatic secretions in addition to transient diffusive water gain. The intestinal lumen and certainly the stomach contents are hyperosmotic to the extracellular fluids which would facilitate diffusive water movement into the gastrointestinal tract. Additionally, seawater ingestion has been shown both prandially via

incidental intake and postprandially via drinking (Kristiansen and Rankin 2001). Together, it appears that these factors act to temporarily dilute the divalent ions that normally persist in marine teleost intestinal fluids (Marshall and Grosell 2005). An increase in Mg^{2+} and especially SO_4^{2-} concentrations over control levels at 48 h post-feeding, though not statistically significant, indicates the possibility of a period of highly increased intestinal water absorption. This is suitably the same time point at which intestinal HCO_3^- levels are maximal, luminal Cl^- concentrations are still reduced, and organic nutrients have been largely absorbed. Anterior intestinal fluid in both starved and fed fish is composed predominantly of monovalent ions Cl^- and Na^+, while a notable shift towards divalents Mg^{2+} and SO_4^{2-} occurs posteriorly. Based on the calculated osmotic coefficients for monovalent and divalent solutions, an intestinal fluid rich in divalent ions will act to facilitate water absorption in the posterior intestine by enhancing the transepithelial osmotic gradient by reducing the effective osmolality on the luminal side.

Organic nutrient absorption

Osmolality and inorganic ion sum measurements of gastro-intestinal fluids allow us to predict a timeline for organic nutrient absorption. Organic nutrient absorption seems to occur in the greatest magnitude in the stomach of toadfish fed a squid diet (Fig. 3.9B.i.), and be completed in all segments of the intestine by 48 h post feeding in both diets (Fig. 3.9C-F). In addition to diminishing over time, the amount of organic solutes in the fluids of each intestinal segment at any

given time is slightly reduced in progressively posterior intestinal sections. This not only indicates a consistent ability of the entire length of the intestinal epithelium to absorb organic nutrients, but also indicates that organic nutrients are truly being absorbed and not just passed along to posterior sections of the gastro-intestinal tract. In addition, a clear shift was seen in intestinal fluid composition between 24 and 48 h post-feeding in which osmolality decreases markedly and is exceeded by the sum of inorganic ions. This indicates a trend towards divalent ions, which have a lower osmotic coefficient than monovalents and thus account for the difference between inorganic ion sum (which assumes an osmotic coefficient of one) and actual osmolality. This difference between inorganic ion sum and actual osmolality is elevated progressively in posterior sections, indicating that in addition to organic nutrient absorption, water absorption also is consistent and cumulative along the intestine.

A transient but significant increase in plasma osmolality 12 h post-feeding in toadfish fed a squid diet in the absence of a significant increase in inorganic ion sum might be attributed to a high amino acid content in squid, although organics were not measured directly in these experiments.

Implications and future direction

Above all, these experiments have shown that feeding transiently and acutely alters the gastro-intestinal physiology of Gulf toadfish, and that these physiological changes are dependent upon diet composition. In addition to dramatically changing both the inorganic and organic ionic composition along the

gastro-intestinal tract, evidence for transient changes in water and solute secretion and absorption across the gastric and intestinal epithelia was also seen as time passed after feeding. By demonstrating a limited or lack of postprandial alkaline tide, questions have been raised about postprandial disruption to acid-base balance in seawater and freshwater fish, and the fate of metabolic HCO_3^- secreted basolaterally by gastric oxyntopeptic cells. The next question begging an answer is the regulation of intestinal HCO_3^- secretion. Considering the strong evidence that apical Cl^-/HCO_3^- exchange is stimulated in the intestine by feeding, regardless of the diet, it is possible that intestinal anion exchange is stimulated by parameters relating to ingestion of a meal itself and/or by the osmoregulatory and acid/base challenges that result. Conjecture might tie these questions of acid-base balance and anion exchange together by explaining the lack of an alkaline tide with increased intestinal HCO_3^- secretion, although this remains to be documented.

Acknowledgments

Jimbo's shrimp, Virginia Key, FL, USA, for providing toadfish for these experiments. Work was supported by a University of Miami fellowship to J.R. Taylor, and a National Science Foundation Grant to M. Grosell (NSF 0416440).

Chapter 4:

Postprandial acid-base balance and ion regulation in freshwater and seawater-acclimated European flounder, *Platichthys flesus*

Summary

The effects of feeding on both acid-base and ion exchange with the environment, and internal acid-base and ion balance, in freshwater and seawater-acclimated flounder were investigated. Following voluntary feeding on a meal of 2.5-5% body mass and subsequent gastric acid secretion, no systemic alkaline tide or respiratory compensation was observed in either group. Ammonia efflux rates more than doubled from 489 ± 35 and 555 ± 64 μmol kg^{-1} h^{-1} under control conditions to 1228 ± 127 and 1300 ± 154 μmol kg^{-1} h^{-1} post-feeding in freshwater and seawater-acclimated fish, respectively. Based on predictions of gastric acid secreted during digestion, net postprandial internal base gains (i.e., HCO_3^- secreted from gastric parietal cells into the blood) of 3.4 mmol kg^{-1} in seawater and 9.1 mmol kg^{-1} in freshwater-acclimated flounder were calculated. However, net fluxes of ammonia, titratable alkalinity, Na^+ and Cl^- indicated that branchial Cl^-/HCO_3^- and Na^+/H^+ exchange played minimal roles in counteracting these predicted base gains and cannot explain the absence of alkaline tide. Instead, intestinal Cl^-/HCO_3^- exchange appears to be enhanced after feeding in both freshwater and seawater flounder. This implicates the intestine rather than the gills as a potential route of postprandial base excretion in fish, to compensate for gastric acid secretion.

Background

Digestion is a necessary and nearly constant process in many animals; however, its effects on other physiological processes have been largely overlooked in comparative physiology studies of fishes. Indeed most studies of homeostasis in fish have deliberately withheld food to avoid the 'complicating' effects of feeding and post-prandial metabolic changes. Determining the effects of digestion on homeostatic processes, such as acid-base balance and osmoregulation, is likely to highlight important and frequently used mechanisms that may not be evident in unfed animals. Recent work suggests that feeding may induce osmoregulatory and acid-base balance challenges in fish (Wood *et al.* 2005; Bucking and Wood 2006; Taylor and Grosell 2006b). In fact, Wood et al. (2005) recently published the first and only report of alkaline tide in fish. The “alkaline tide” phenomenon recognized in ectothermic vertebrates (Wang *et al.* 2001) and mammals (Niv and Fraser 2002) refers to a significant alkalinization of the blood following gastric acid secretion during digestion. In brief, H^+ and HCO_3^- are created in the gastric acid-secreting oxyntic (mammals) or oxyntopeptic (non-mammalian vertebrates) cells by endogenous CO_2 hydration, catalyzed by intracellular carbonic anhydrase (Niv and Fraser 2002). Apical H^+ secretion into the gastric lumen is countered by an equivalent basolateral efflux of HCO_3^- (metabolic base) into the blood via Cl^-/HCO_3^- exchange. This anion exchange prevents alkalosis of the acid-secreting cell and provides Cl^- for gastric HCl secretion (Niv and Fraser 2002). This mechanism yields a net acid secretion into the stomach lumen and an equimolar metabolic base secretion into the blood,

causing the “alkaline tide” commonly observed at the onset of gastric digestion. The aforementioned study by Wood et al. (2005) shows increased plasma pH and HCO_3^- levels between 3 and 9 h post-feeding in an elasmobranch, the spiny dogfish, *Squalus acanthias*, in the absence of respiratory compensation (i.e. no increased P_{CO2} to counter elevated pH). Conversely, Taylor and Grosell (2006b) did not find a distinct alkaline tide at any point in a detailed time-course following feeding in a teleost, the seawater-acclimated Gulf toadfish, *Opsanus beta*, although blood samples in this study were taken via caudal puncture following natural feeding, rather than dorsal aortic cannulation in combination with force-feeding. Taylor and Grosell (2006b) did, however, measure a substantial postprandial increase in intestinal bicarbonate secretion via Cl^-/HCO_3^- exchange that alleviated luminal acidification (resulting from the influx of acidic chyme from the stomach) and aided in Cl^- and water absorption by the intestine.

In addition to digestion, the gastro-intestinal (GI) tract of marine fishes serves an important role in osmoregulation, with apical Cl^-/HCO_3^- exchange contributing up to 70% of Cl^- and water absorption under unfed experimental conditions (Grosell *et al.* 2005; Grosell 2006). While salt intake resulting from a feeding event has not been found to exceed daily intake from active drinking in a hypertonic environment (Shehadeh and Gordon 1969; Dabrowski *et al.* 1986), the acute nature of dietary salt intake (and subsequent gastric, pancreatic, and biliary secretions) may in itself induce diet-dependent osmoregulatory challenges in marine fishes (Taylor and Grosell 2006b). In contrast to the hydromineral situation of fish in a marine environment, freshwater fish presumably rely to some

extent on dietary salt intake for osmoregulation and may consequently require intestinal ion transport mechanisms similar to those utilized in marine teleost osmoregulation. Dietary salt intake in freshwater fishes may also transiently reduce the magnitude of branchial Na^+ and Cl^- uptake required for osmoregulation, thus reducing metabolic costs associated with active ion transport (Smith *et al.* 1989). This balance between branchial and dietary salt uptake will be inevitably dynamic based on food availability, and on abiotic environmental parameters dictating the efficiency of branchial ion uptake (Smith *et al.* 1989).

This study is the first to investigate the effects of feeding on acid-base balance and osmoregulation in seawater and freshwater-acclimated euryhaline fish. In choosing a euryhaline teleost, European flounder (*Platichthys flesus*), a closer examination of the postprandial relationship between osmoregulation and acid-base balance in two osmotically distinct media was facilitated. These experiments examined both acid-base exchange with the environment, and internal acid-base balance. The seawater environment provides a virtually unlimited supply of NaCl (>450 mM), while the low Na^+ and Cl^- concentrations of a freshwater environment (<1 mM) may limit branchial HCO_3^- and H^+ efflux (Iwama and Heisler 1991; Choe and Evans 2003; Evans *et al.* 2005). Branchial HCO_3^- excretion has long been linked to Cl^- uptake (Maetz and Romeu 1964; Garcia-Romeu and Maetz 1964; Evans *et al.* 2005), and may be capable of reducing or entirely alleviating alkaline tides in fishes. However, in a low Cl^- freshwater environment, it is hypothesized that branchial base efflux may be

limited, resulting in a more prominent alkaline tide in freshwater-acclimated fish than their seawater-acclimated counterparts. Additionally, branchial Na^+ uptake occurs across the apical membrane as H^+ are secreted (Evans *et al.* 2005). An inhibition of this mechanism, resulting in H^+ retention, may also compensate for a postprandial HCO_3^- load to the extracellular fluid.

Materials and Methods

Animal care

European flounder, *Platichthys flesus*, were obtained from fishermen local to southwest England, and transported back to Hatherly Laboratories at the University of Exeter, Exeter, UK. Flounder were held in a temperature controlled (14 °C) wetlab for approximately three weeks in plastic or fiberglass tanks with natural sand substrate, under respective flow-through dechlorinated freshwater or artificial seawater (33 ± 1 ‰) conditions prior to experimentation. Fish were fed ragworms *Nereis diversicolor* to satiation twice weekly prior to experimentation. All experiments were conducted with the approval of the University of Exeter Ethics Committee and under a UK Home Office license (PPL 30/2217).

General experimental procedure

A temperature-controlled (14 ± 1 °C) flux chamber system (volume ~500 l) was set up simultaneously in seawater and freshwater. Flux chambers were constructed from rectangular polypropylene containers with volumes set to

approximately 1 l (0.98 ± 0.033 l) by drilling a pluggable flow-through hole in the side of each chamber. Fish (mass 44.6 ± 3.6 g) were placed in individual flux chambers in each system and allowed to recover from handling stress for 12-24 h prior to beginning control flux measurements. In all feeding experiments each fish was offered a meal of live ragworms, *Nereis diversicolor*, maintained at 50% seawater (i.e. 16.5 ppt), at 5 % of its body mass. Uneaten worms were removed from the experimental chamber, weighed and recorded 30 min after being presented. Fish consuming less than half of the meal offered (12.5% of the experimental animals) were not included in analyses.

Titratable alkalinity and total ammonia fluxes

Titratable alkalinity and total ammonia were measured during fluxes in both freshwater (n = 12) and seawater (n = 12) flounder. Following a 12-24 h acclimation period, two approximately 12 h control fluxes were performed the day before feeding in all groups and post-feeding fluxes were carried out approximately 0-6, 6-12, 12-24, 24-36, 36-48, 48-60, and 60-72 h after feeding, during which initial and final water samples (25 ml) were taken from each flux chamber. Double endpoint titrations (Hills 1973; Wilson *et al.* 2002) were carried out on 5 ml sub-samples with 5 ml of deionized H_2O added to seawater samples and 5 ml of 450 mM NaCl added to freshwater samples prior to titration. These additions were made to increase the total volume for titration, fully submerge electrodes, and ensure identical ionic strength during titration of freshwater and seawater samples. Following 30 min of gassing the samples with CO_2-free gas

(nitrogen), 0.02 N HCl was added to each sample using a gas-tight glass micro-burette (Gilmont 2.0 ml micrometer burette), to lower pH to 3.80. Samples were allowed to equilibrate for 15 min while being continuously aerated with CO_2-free gas to remove all HCO_3^- and CO_3^{2-} as gaseous CO_2 during acidification, and to ensure stable pH measurement when returning to the starting pH (Wilson *et al.* 2002). Samples were then brought back to their initial (recorded) pH values by adding 0.02 N NaOH by gas-tight micro-burette. The volume of base addition was recorded and total titratable alkalinity of each sample was calculated from the difference in the number of moles of acid and base added. A 5 ml aliquot of the 25 ml water sample was frozen at -20 C for subsequent total ammonia assay. Ammonia assays were carried out using a micro-modification of the salicylate-hypochlorite assay based on Verdouw et al. (1978).

Na^+ and Cl^- uptake in freshwater

Rates of Na^+ and Cl^- uptake were determined radioisotopically in freshwater European flounder using ^{22}Na (n = 8) and ^{36}Cl (n = 8) in two separate fluxes of four fish each. Fluxes were carried out 24 and 12 h pre-feeding, and at approximately 6, 12 and 72 h post feeding, by adding 0.5 ml of the respective 1 μCi ml^{-1} isotope to each of four flux chambers (0.93 ± 0.014 L). The isotope was allowed to disperse for approximately 10 min before an initial water sample of 20 ml was taken. An intermediate water sample of the same volume was taken after 90 min, midway between initial and final samples. Sub-samples of the initial, intermediate and final water samples for ^{22}Na fluxes were counted in triplicate (1

ml each) using a gamma counter (Packard Cobra B5002), while ^{36}Cl samples (1 ml) were counted in triplicate after being combined with scintillation fluid (Emulsifier-Safe) in a 1:5 ratio using a liquid scintillation analyzer (Canberra Packard Tri-Carb 2500TR). Net Cl^- and net Na^+ concentrations were determined for these samples using a Cl^- assay based on the photometric method of Zall et al. (Zall *et al.* 1956) and a flame photometer (Corning 410), respectively. These measurements were used to calculate Na^+ and Cl^- influx, efflux, and net flux, as detailed by Grosell et al. (2000a).

Cl⁻ uptake kinetics in freshwater

Chloride uptake kinetics were determined in juvenile flounder (0.4 - 15.1 g) acclimated to freshwater for at least 7 days. Groups of five individuals were placed in plexiglass tanks containing 1 L of artificial freshwater (0.5 mM $CaSO_4$, 0.025 mM HCO_3^- as K_2CO_3 in deionized water). The NaCl level of the water was adjusted to nominal concentrations of 100, 200, 400, 800 and 2000 µM by addition of 1 M NaCl. Experiments were initiated by addition of 1 µCi ^{36}Cl (Amersham) to each tank. After a 10 min equilibration period and after 2 h, initial and final water samples were obtained for determination of exact Cl^- concentration and ^{36}Cl radioactivity. At the end of the 2 h incubation period, a liter of full strength seawater was added to effectively block ^{36}Cl uptake and fish were euthanized by an overdose of tricaine methane sulfonate (5 g ml^{-1} MS-222, neutralized to pH 8.0). Individual fish were rinsed, placed in individual pre-weighed plastic containers and weighed to the nearest 100 mg. A volume of 10%

HCl (v/v) equivalent to approximately 5 times the fish mass was added to each individual plastic container and fish were digested at 50 ºC overnight. The digests were centrifuged and a sample of the supernatant was pH neutralized by addition of an equal volume of 1.3 M $NaHCO_3$. Radioactivity arising from ^{36}Cl activity in water samples and neutralized fish digests was determined after addition of scintillation counting fluid as described above. No quenching was observed in any of the analyzed samples. The uptake rate of Cl^- was determined from the ^{36}Cl radioactivity accumulated in the fish, the specific activity of ^{36}Cl in the water and the incubation time as outlined previously (Grosell *et al.* 2000a). The affinity (K_m) and capacity (J_{max}) constants for the Cl^- uptake kinetics were determined using the non-linear regression function in SigmaPlot 8.0.

Postprandial blood and gastro-intestinal fluid sampling

Four freshwater fish (327 ± 120 g) and four seawater fish (234 ± 90 g) in individual chambers (approx. 7 l volume) were offered ragworms, *N. diversicolor,* at 5% of their body masses and allowed 30 min to feed, after which remaining worms were removed and their mass recorded. At 6 h post feeding fish were quickly blood sampled by caudal puncture, a sampling technique that allowed for natural feeding as opposed to the force-feeding that is generally required in cannulated fish. Blood samples (200-300 µl) were obtained with a chilled, heparinized 1 ml syringe fitted with a gauge 22 needle, with individual sampling times not exceeding 30 sec. Blood samples were quickly put on ice and centrifuged to obtain plasma, which was immediately analyzed for pH (Accumet

pH electrode connected to a Radiometer PHM220 pH meter), total CO_2 (Mettler Toledo 965 Carbon Dioxide Analyzer) and osmolality (Wescor Vapro 5520 vapor pressure osmometer). Plasma samples were stored at -20 °C for later analysis of cation and anion concentrations. To minimize pre-feeding stress, control blood samples were taken 72 h after feeding in each fish, at which time the flux measurements described above indicated the return of all feeding-induced changes to control levels. Blood samples were obtained and analyzed as described above. The group of freshwater fish was then moved to seawater, and *vice versa*, to allow for paired statistical analyses of differences in plasma chemistry. Following a 72 h acclimation to the new salinity, the experiment was repeated.

Three days after control blood samples were obtained from the second 6 h postprandial blood sampling experiment, the same (post salinity transfer) four freshwater fish (234 ± 90 g) and four seawater fish (327 ± 120 g) in individual chambers were prepared for terminal gastro-intestinal fluid and blood sampling. Flounder were again allowed 30 min to eat 5% of their body mass, after which remaining worms were removed from the chambers and their masses recorded. Fish that had ingested at least half of the offered meal were quickly blood sampled 6 h post feeding by caudal puncture as above. Fed fish were then euthanized by an overdose of MS-222 (as above) and the entire gastrointestinal tract was subsequently removed and the stomach, anterior, middle, posterior, and rectal segments ligated as described by Grosell et al. (2004). Contents of each segment were collected individually into 2 ml plastic microcentrifuge tubes

and centrifuged (2 min at 15 700 *g*), with the resulting fluid phase analyzed immediately for pH, total CO_2 and osmolality and retained at -20 °C for subsequent cation and anion analysis as described above. Three new fish were added to each group of experimental animals (one in each group did not feed and was thus re-used) to again give a potential sample size of four in each group. Masses were 211 ± 142 g and 62 ± 14 g in seawater and freshwater, respectively. The experiment was carried out as above, except samples were taken at 12 h rather than 6 h post-feeding.

The Henderson-Hasselbalch equation was used to calculate PCO_2 for all blood samples as follows:

$$PCO_2 = \frac{[\text{Total } CO_2]}{\alpha_{CO2} * (1 + 10^{(pH-pK_{app})})}$$

with α_{CO2} = 0.056 mmol l^{-1} $mmHg^{-1}$ and pK_{app} = 6.08, estimated based on Boutilier et al. (1984).

Titration of ragworm diet

In order to estimate *in vivo* stomach acid secretion, four ragworms (mass 0.34 ± 0.05 g), *N. diversicolor*, were individually homogenized with 2 ml deionized water using a tissue homogenizer (IKA, Ultra-Turrax T25). Following complete homogenization, 6 ml of 450 mM NaCl was added to the homogenate to increase sample volume and to stabilize the electrode without affecting buffering capacity during titration. The mixture was titrated using 0.02 N HCl to decrease the pH from approximately neutral, stepwise (by 0.5 pH units) to pH 2.5, with the added

volume of acid recorded at each step. *In vivo* gastric acid secretion was estimated from measured stomach pH and ragworm titration results.

Statistical analyses

Data are presented as means ± 1 SEM. Since data were not normally distributed, non-parametric repeated measures analyses were made using Friedman's test (two-way analysis of variance by ranks), followed where applicable by Dunn's post-hoc procedure. When only two groups were compared, a Mann-Whitney Rank Sum test or a Wilcoxon paired-sample test was used as the non-parametric equivalent to the two-sample and paired-sample *t* tests, respectively. Means were considered significantly different at $P < 0.05$. Significant differences from control values are denoted in figures by an asterisk, while significant differences between seawater and freshwater values are shown by a cross.

Results

Titratable alkalinity and total ammonia fluxes

Background titratable alkalinity efflux (Fig. 4.1a) was calculated for each group by averaging two pre-feeding control fluxes and a 72 h postprandial flux. Seawater-acclimated flounder tended to have a slight but not statistically significant higher background apparent base efflux (319 ± 63 μmol kg^{-1} h^{-1}) than freshwater-acclimated flounder (208 ± 52 μmol kg^{-1} h^{-1}). This was followed by a significantly higher apparent base efflux measured between 0 and 6 h

postprandially in seawater as compared to freshwater-acclimated flounder (Fig. 4.1a). Fish at both salinities displayed maximal apparent base efflux rates that were significantly higher than control rates, between 6 and 12 h post-feeding (1040 ± 171 μmol kg^{-1} h^{-1} in seawater, and 755 ± 62 μmol kg^{-1} h^{-1} in freshwater). In freshwater, apparent base efflux was still significantly elevated over control conditions between 12 and 48 h after feeding, while seawater fish had returned to values not significantly different from their control efflux, and significantly lower than those of freshwater-acclimated flounder between 12 and 24 h post-feeding (Fig. 4.1a). However, integration of apparent base efflux over the first 48 h after feeding in freshwater and seawater indicates similar values in freshwater- (14.2 mmoles kg^{-1}) and seawater-acclimated (13.5 mmoles kg^{-1}) flounder. Postprandial adjustments in the exchange of acid-base equivalents with the environment appeared to be complete by 48 h post-feeding.

Control total ammonia efflux (Fig. 4.1b) was calculated as above, and yielded similar baseline efflux at both salinities (489 ± 35 μmol kg^{-1} h^{-1} in freshwater and 555 ± 64 μmol kg^{-1} h^{-1} in seawater). Postprandial total ammonia flux measurements revealed ammonia efflux of similar magnitude in both salinities (Fig. 4.1b), but with maximal output occurring during the first 6 h post-feeding in seawater-acclimated fish (1300 ± 154 μmol kg^{-1} h^{-1}) and between 6 and 12 h post-feeding in freshwater flounder (1228 ± 127 μmol kg^{-1} h^{-1}). Both seawater and freshwater-acclimated flounder excreted ammonia at levels significantly increased over control efflux between 0 and 6 h after feeding, while in freshwater fish these significantly elevated levels of total ammonia excretion

persisted 24 h after feeding (Fig. 4.1b). The magnitude of total ammonia efflux in both groups (Fig. 4.1b) very closely matched the magnitude of apparent base efflux (Fig. 4.1a). This trend confers no significant changes in postprandial net acid flux (Fig. 4.1c), calculated as the difference between apparent titratable alkalinity and total ammonia fluxes. Again, while magnitude and duration of increased total ammonia efflux varied slightly between freshwater and seawater-acclimated fish, an integration of the postprandial change in total ammonia efflux (between 0 and 48 hours post-feeding, based on Fig. 4.1) in freshwater (14.5 mmoles kg^{-1}) and seawater (10.3 mmoles kg^{-1}) indicates that the net amount of total ammonia excreted into the environment as a result of feeding is similar in both groups. This integrated postprandial total ammonia excretion very closely matches the integrated change in apparent base efflux in seawater and freshwater-acclimated flounder.

Fig. 4.1. Apparent titratable alkalinity (a), total ammonia (b), and net acid (c) flux under control conditions (time 0 h and carried across in reference lines) and post-feeding conditions in seawater- (open circles, dashed line) and freshwater-acclimated (closed circles, solid line) flounder; n = 11, mean ± SEM. Negative flux values indicate excretion; * denotes significant differences from control values, and † denotes significant differences between freshwater and seawater values.

a.

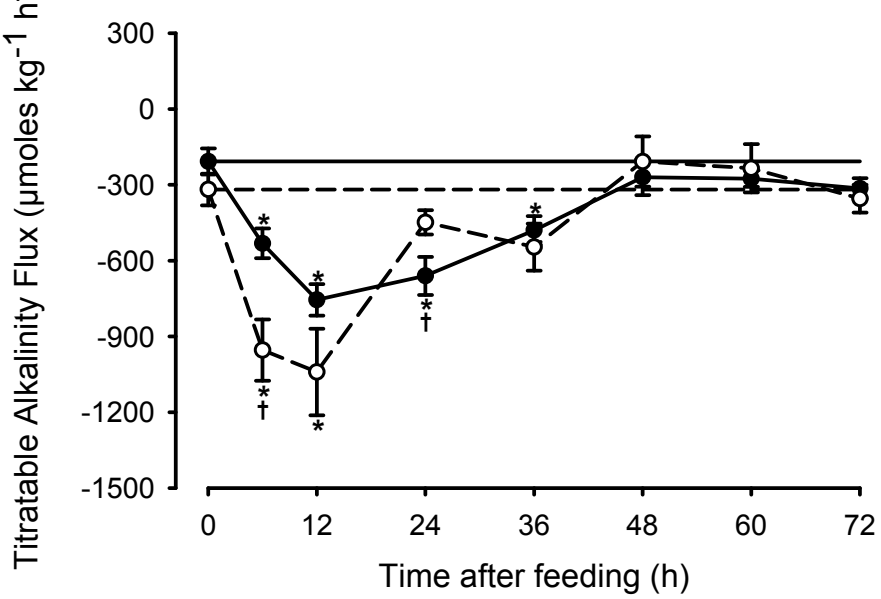

b.

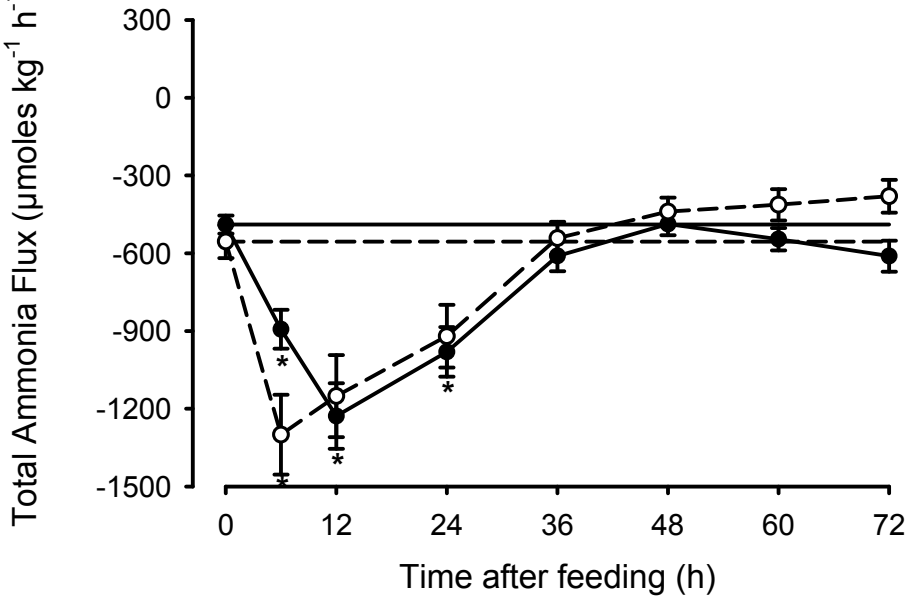

c.

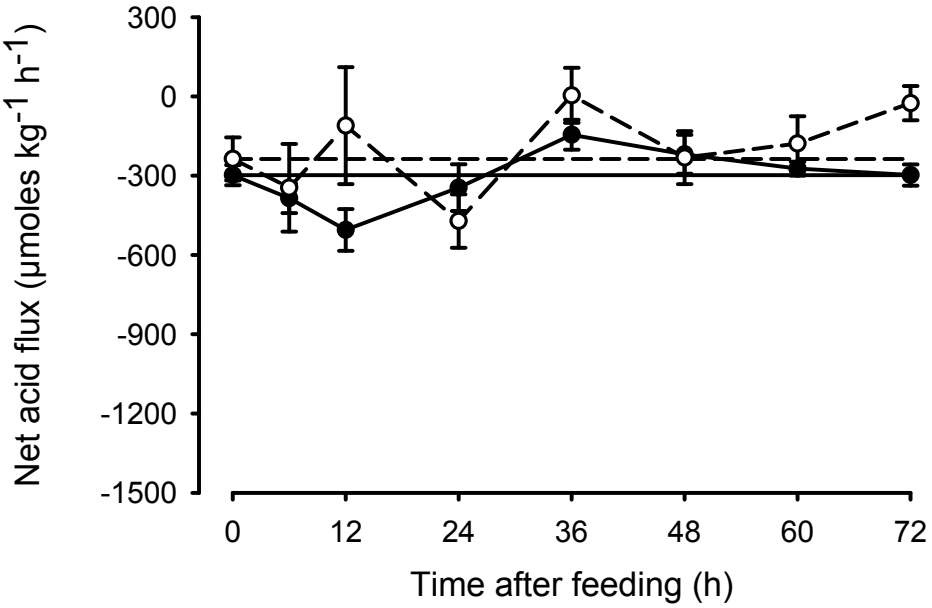

Na^+ and Cl^- uptake in freshwater

Baseline Na^+ and Cl^- influx were calculated as above, by averaging two pre-feeding control fluxes and a 72 h postprandial flux. No statistically significant differences were measured between control and postprandial Na^+ or Cl^- uptake (Fig. 4.2), efflux, or net flux. However, Na^+ uptake was slightly depressed 12 h after feeding, a trend that follows the prediction of reduced proton excretion at the gills (via Na^+/H^+ exchange) to counteract the alkaline tide. The magnitude of Cl^- influx was more than 3-fold smaller than the corresponding apparent base efflux (Fig. 4.1a), while Na^+ influx approximated the magnitude of resting control total ammonia and apparent base efflux.

Fig. 4.2. Na^+ (hatched bars) and Cl^- (solid bars) uptake in freshwater-acclimated flounder under control conditions (time 0 h and carried across in reference lines) and post-feeding conditions; n = 8 and 7 in Na^+ and Cl^-, respectively, mean ± SEM.

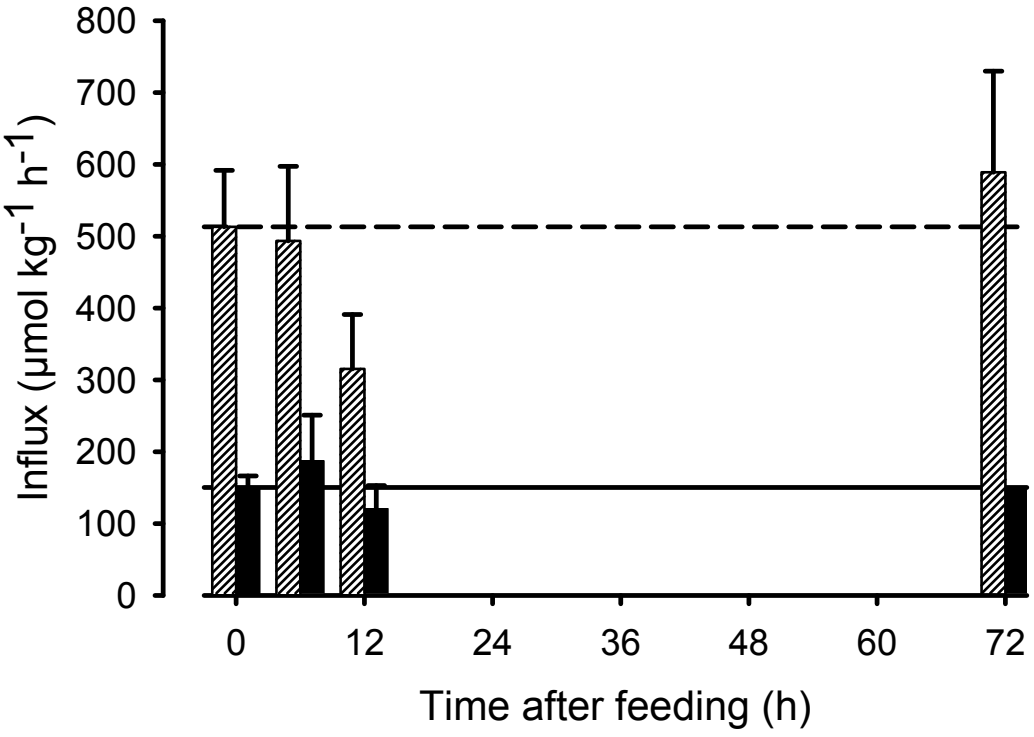

Cl⁻ uptake kinetics in freshwater

The relationship between branchial Cl^- uptake and ambient freshwater Cl^- concentrations (Fig. 4.3) displayed saturation-type kinetics characterized by a J_{max} of 198 ± 10 µmol kg^{-1} h^{-1} and K_m of 658 ± 79 µM Cl^- (r = 0.99). The freshwater used in the experimental chambers during the other treatments contained ~800 µM Cl^-, or approximately 60% of J_{max}.

Fig. 4.3. Chloride uptake was measured in juvenile flounder at several Cl^- concentrations and displayed saturation-type kinetics as detailed in the text (mean ± SEM, n = 5 per concentration).

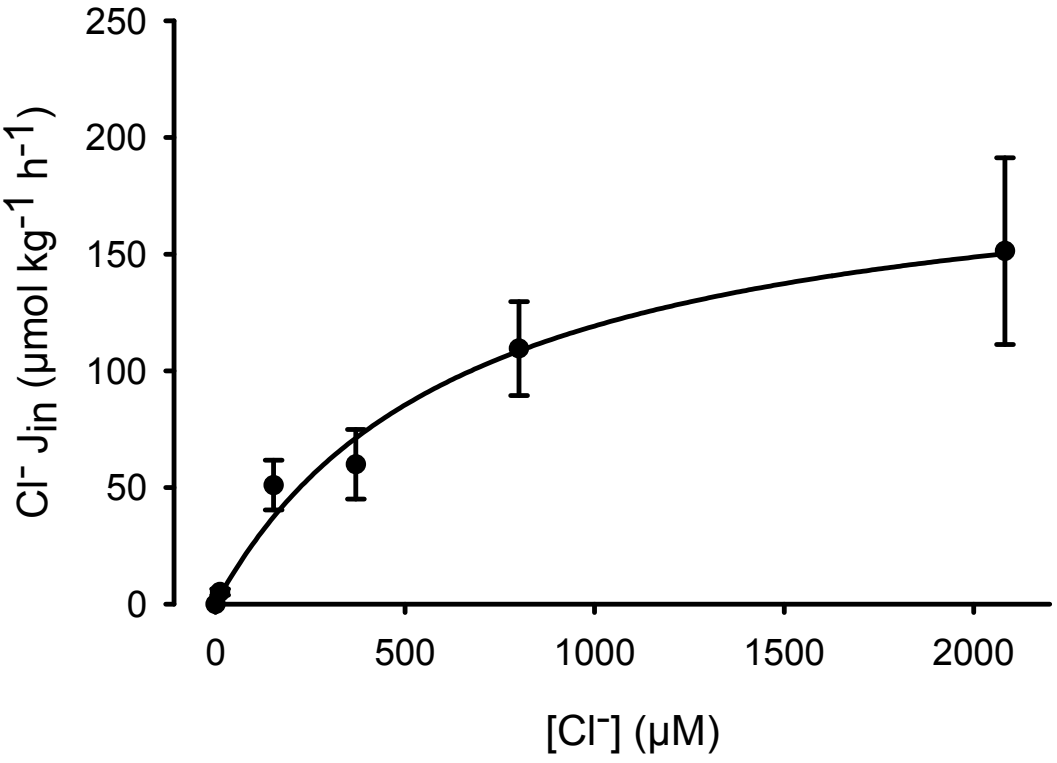

Postprandial blood and gastro-intestinal fluid sampling

At 6 and 12 h after feeding, few significant differences from the control samples were measured in blood plasma chemistry of flounder in either freshwater or seawater (Table 4.1). Plasma osmolality is the only parameter that consistently differed with salinity, and was significantly greater in seawater-acclimated flounder at all timepoints; however, no significant differences were measured between post-prandial and control samples within each salinity group. The higher plasma osmolality in seawater-acclimated fish was due predominantly to NaCl concentrations, which were consistently higher in seawater fish than

freshwater fish, a difference that was statistically significant 12 h post-feeding (Table 4.1). The significant difference in plasma osmolality between seawater and freshwater-acclimated flounder after a 72 h salinity acclimation period suggests that extracellular fluid chemistry in these fish changes quickly in response to salinity adjustments. In both freshwater and seawater-acclimated flounder, intestinal fluid HCO_3^- concentrations were elevated over plasma HCO_3^- concentrations within 6 h following feeding (with statistical significance in the mid and posterior intestinal fluid in FW, and in the posterior intestinal fluid in SW), after which concentrations dropped as this HCO_3^- was presumably titrated by acidic chyme moving into the intestine 12 h after feeding (Table 4.2). While anterior and mid intestinal fluid HCO_3^- concentrations dropped to near zero 12 h post-feeding in freshwater-acclimated flounder, seawater flounder appeared to maintain HCO_3^- concentrations in excess of those required for acidic chyme titration (although sample sizes were not large enough to give a statistically significant difference from plasma values), suggesting that HCO_3^- secreted by the intestine during digestion is likely additional to that secreted as a part of marine osmoregulation. Intestinal fluid Cl^- concentrations tended to correlate negatively with HCO_3^- concentrations, supporting a role of anion exchange in postprandial intestinal HCO_3^- secretion. In seawater-acclimated flounder, high Mg^{2+} and SO_4^{2-} concentrations in the distal intestinal fluids confer a high rate of water absorption at both 6 and 12 h after feeding; however, comparably high Mg^{2+} and SO_4^{2-} concentrations were not measured until 12 h post-feeding in the distal intestinal fluids of freshwater-acclimated flounder, suggesting that water absorption in

freshwater flounder becomes more important as chyme moves into the intestine. Unfortunately, small sample sizes precluded statistical significance of these trends, identifying intestinal water absorption as an interesting area of digestive physiology for further comparisons

Table 4.1. Blood plasma chemistry measurements in seawater and freshwater-acclimated flounder 6 and 12 h post-feeding, and under control conditions, mean (SEM). Statistically significant differences between seawater and freshwater measurements at each timepoint are indicated by a cross; no statistically significant differences from controls were measured for any parameter within either salinity group.

	N	pH	Total CO_2 (mM)	PCO_2 (torr)	Osmolality (mOsm)	Cl^- (mM)	Na^+ (mM)	K^+ (mM)	Ca^{2+} (mM)	Mg^{2+} (mM)
Seawater										
Fasted	8	7.94 (0.03)	6.5 (0.5)	1.6 (0.1)	311 (4)†	122.8 (4.9)	152.0 (5.2)	2.7 (0.1)	2.3 (0.1)	1.1 (0.3)
6 h	11	7.97 (0.03)	8.4 (0.5)	1.9 (0.2)	309 (3)†	121.9 (5.4)	158.7 (4.8)	3.0 (0.3)	2.4 (0.1)	1.6 (0.5)
12 h	4	[a]	8.2 (0.1)	[a]	310 (2)†	136.5 (3.5)†	154.0 (3.3)†	4.4 (0.4)	2.4 (0.1)	0.7 (0.1)
Freshwater										
Fasted	8	7.95 (0.06)	8.0 (0.7)	1.9 (0.1)	296 (3)†	119.3 (5.0)	142.9 (3.8)	2.2 (0.2)	2.3 (0.1)	1.1 (0.4)
6 h	11	7.93 (0.03)	8.3 (0.5)	2.1 (0.1)	293 (3)†	117.5 (5.3)	144.1 (3.1)	2.7 (0.2)	2.3 (0.1)	0.4 (0.1)
12 h	3	[a]	6.3 (0.1)	[a]	290 (2)†	119.7 (5.5)†	132.7 (8.7)†	4.2 (0.3)	2.2 (0.2)	0.5 (0.0)

[a] n = 0 due to electrode malfunction

Table 4.2
Gastro-intestinal fluid chemistry of flounder acclimated to (a) seawater at 6 (n = 3) and 12 (n = 4) h after feeding, and (b) freshwater at 6 (n = 3) and 12 (n = 3) h after feeding. Statistically significant differences between plasma and intestinal fluid HCO_3^- concentrations within either salinity group are denoted by an asterisk; no statistically significant differences were found between seawater and freshwater measurements at any timepoint.

a.

Seawater	pH	Total CO_2 (mM)	Osmolality (mOsm)	Cl^- (mM)	Na^+ (mM)	K^+ (mM)	Ca^{2+} (mM)	Mg^{2+} (mM)	SO_4^{2-} (mM)
6 h									
Stom	4.78 (0.12)	0.3 (0.33)	584 (12)	105.6 (30.6)	80.9 (9.9)	49.1 (1.4)	1.4 (0.3)	20.5 (0.5)	4.2 (0.3)
Ant	7.81 (0.27)	19.0 (4.53)	434 (22)	31.9 (3.9)	100.5 (20.5)	11.8 (2.0)	0.4 (0.1)	20.3 (6.1)	8.5 (1.5)
Mid	8.30 (0.07)	30.5 (2.22)	389 (10)	27.7 (3.3)	93.6 (21.9)	7.4 (0.2)	0.4 (0.1)	31.4 (10.8)	13.2 (5.1)
Post	8.63 (0.08)	55.3 (10.24)*	352 (11)	28.1 (5.2)	60.0 (17.9)	3.9 (1.0)	1.9 (0.3)	74.4 (20.2)	30.9 (9.7)
Rec	8.74 [b]	[a]	378 (35)	83.2 (9.3)	34.2 (16.0)	12.0 (7.5)	1.2 (0.3)	133.7 (26.2)	62.4 (11.9)
12 h									
Stom	4.06 (0.23)	0.2 (0.23)	466 (21)	146.7 (19.5)	83.1 (8.9)	24.0 (4.3)	4.9 (1.3)	24.1 (4.2)	9.0 (1.4)
Ant	8.01 (0.18)	10.6 (6.94)	432 (27)	24.0 (2.3)	86.7 (11.6)	13.8 (1.9)	4.5 (2.4)	42.6 (11.6)	20.8 (4.6)
Mid	8.39 (0.08)	19.6 (9.17)	382 (9)	19.7 (2.7)	77.7 (13.5)	8.7 (0.8)	2.8 (2.1)	47.5 (14.1)	21.9 (6.6)
Post	8.64 (0.08)	45.4 (15.24)	360 (14)	16.6 (2.0)	51.1 (16.4)	5.2 (1.6)	5.4 (4.0)	77.6 (20.2)	35.9 (8.9)
Rec	8.67 (0.11)	34.8 (10.33)	338 (8)	18.7 (7.3)	37.5 (3.2)	4.7 (1.2)	4.7 (3.2)	86.8 (15.3)	40.2 (8.1)

b.

Freshwater	pH	Total CO_2 (mM)	Osmolality (mOsm)	Cl^- (mM)	Na^+ (mM)	K^+ (mM)	Ca^{2+} (mM)	Mg^{2+} (mM)	SO_4^{2-} (mM)
6 h									
Stom	4.83 (0.15)	1.2 (0.4)	504 (14)	113.6 (2.1)	70.7 (5.2)	45.1 (2.8)	0.6 (0.1)	17.2 (0.8)	[a]
Ant	8.07 (0.10)	28.2 (2.4)	406 (35)	38.5 (12.8)	111.0 (3.9)	16.2 (5.3)	0.6 (0.2)	13.9 (2.0)	2.8 (0.2)
Mid	8.38 (0.02)	44.2 (8.4)*	359 (4)	39.7 (6.9)	121.9 (2.8)	9.0 (0.8)	0.6 (0.3)	16.0 (3.9)	3.4 (0.1)
Post	8.65 (0.09)	53.7 (8.4)*	341 (2)	33.3 (5.7)	109.5 (6.8)	7.4 (0.7)	1.2 (0.6)	23.6 (3.6)	8.9 (3.8)
Rec	8.58 [b]	[a]	317 [b]	77.3 (32.8)	86.0 (9.6)	23.4 (14.7)	1.4 (0.2)	16.0 (1.8)	5.6 (0.2)
12 h									
Stom	3.34 (0.09)	[a]	[a]	104.3 (9.7)	24.4 (4.9)	31.0 (2.6)	1.4 (0.7)	7.7 (0.3)	[a]
Ant	7.75 (0.14)	0.0 (0.0)	395 (5)	19.9 (1.0)	125.6 (6.2)	14.5 (0.5)	7.2 (5.1)	15.2 (2.6)	4.0 (0.8)
Mid	8.10 (0.11)	0.7 (0.7)	391 (14)	17.5 (1.5)	97.1 (0.6)	15.0 (1.7)	5.9 (5.2)	15.7 (6.8)	4.9 (0.9)
Post	8.66 [b]	[a]	339 [b]	18.7 (5.8)	83.9 (16.2)	8.2 (0.7)	9.7 (5.4)	34.8 (8.3)	9.8 (1.8)
Rec	8.79 [b]	76.0 (9.0)	296 (12)	24.2 (1.0)	26.3 (5.4)	2.2 (0.3)	2.1 (1.6)	118.9 (44.1)	63.5 (27.0)

[a] n = 0 and [b] n = 1, due to small sample volumes

between freshwater and seawater fish. While Mg^{2+} and SO_4^{2-} are ingested in both seawater and the ragworm meal in seawater-acclimated fish, any significant Mg^{2+} and SO_4^{2-} concentrations along the gastro-intestinal tract of freshwater fish can be attributed almost exclusively to dietary intake and further amplification by subsequent water absorption.

Titration of ragworm diet

Titration of homogenized ragworms allowed us to calculate the amount of H^+ necessary to acidify stomach contents to the lowest mean postprandial pH, which occurred 12 h after feeding in both seawater and freshwater-acclimated fish (Table 4.2). Calculations were made based on a linear regression of log H^+ required vs. gastric pH (Fig. 4.4), the equation for which is given below:

$$\text{Log } H^+ = -0.2933*(\text{pH}) + 0.1196$$

Based on the lowest mean gastric pH of 4.1 ± 0.2 in seawater and 3.3 ± 0.1 in freshwater (both recorded 12 h post-feeding), seawater-acclimated flounder secreted approximately 354 μmol kg^{-1} h^{-1} H^+ into the stomach, while freshwater-acclimated flounder secreted approximately 575 μmol kg^{-1} h^{-1} H^+ into the stomach, between 0 and 12 h following feeding. This indicates a total gastric acid secretion and resulting systemic base gain of 6.9 mmol kg^{-1} in freshwater and 4.2 mmol kg^{-1} in seawater during this 12-hour period, assuming no considerable temporal lag between gastric acid and metabolic base secretions. By accounting for the base excreted at the gill, net theoretical postprandial internal base gain was calculated. Based on the implications of the total

ammonia and apparent titratable alkalinity flux measurements, changes in net branchial base efflux were calculated by subtracting the changes in integrated total ammonia efflux from integrated titratable alkalinity efflux changes (control efflux was normalized to zero in these calculations to isolate the effects of feeding) between 0-12 h in seawater and freshwater. Notably in freshwater fish, titratable alkalinity and total ammonia efflux were also significantly elevated over control measurements at the 24 h post-feeding timepoint (Fig. 4.1). The calculated value for feeding-induced branchial base excretion between 0 and 12 h was subtracted from the total postprandial metabolic base gain determined by ragworm titration (under the presumably conservative assumption that gastric acid secretion was largely completed by 12 h post-feeding). This yielded an estimated net internal base gain of 9.1 mmol kg^{-1} in freshwater fish (which in fact had a postprandial net acid excretion at the gill) and 3.4 mmol kg^{-1} in seawater.

Fig. 4.4. Gastric H^+ secretion required to acidify ragworms *N. diversicolor* (n = 4) to a series of pH values, mean ± SEM.

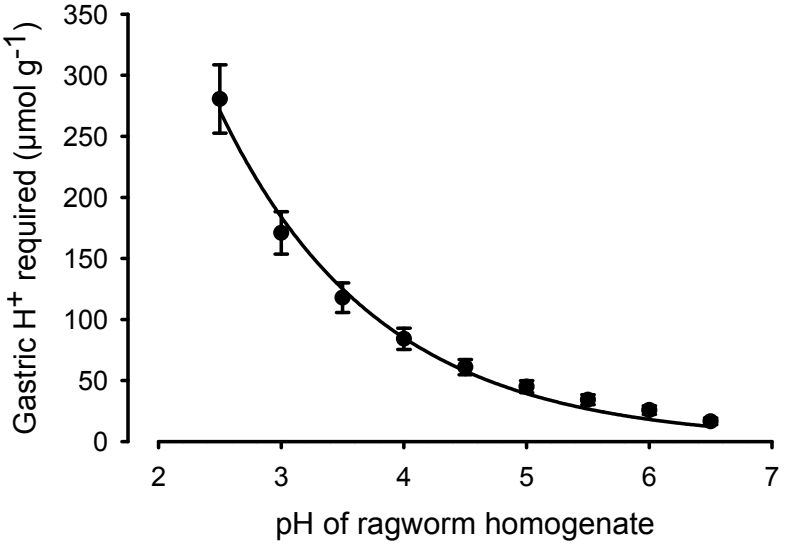

Conclusions

Acid-base exchange with the environment

Branchial NH_3 diffusion in freshwater and seawater-acclimated flounder

The great majority of nitrogen excretion in freshwater and seawater teleosts, under both fasting and fed conditions, has been shown to occur via the gills, with urinary nitrogen excretion comprising less than 4% of the total (Hickman and Trump 1969; Beamish and Thomas 1984; Wood 2001). The measurement of titratable alkalinity efflux in freshwater and seawater-acclimated flounder was intended to measure HCO_3^- efflux resulting from branchial Cl^-/HCO_3^- exchange; however, the present results show that total ammonia efflux accounts for most of the apparent base efflux measured. A regression of total ammonia efflux on titratable alkalinity efflux reveals R values of 0.90 and 0.95 in seawater and freshwater-acclimated flounder, respectively, which may suggest that at least 90% of the titratable alkalinity efflux can be accounted for by total ammonia efflux. Apparent base efflux in freshwater-acclimated flounder also notably exceeds (by nearly 4-fold) maximal Cl^- uptake rates. While the possibility of additional mechanisms of branchial base efflux is acknowledged, it is suggested that a more likely explanation is that measured "base efflux" is in fact mostly attributed to branchial ammonia excretion via NH_3 diffusion trapping (Wilkie 2002; Evans *et al.* 2005). Briefly, in this well-described mechanism, NH_4^+ in the extracellular fluid is deprotonated and diffuses across the gill epithelium as non-ionic NH_3. The gradient for NH_3 diffusion is maintained by protonation of NH_3 to NH_4^+ in the gill external boundary layer. This proton consumption in the

boundary layer would appear as an apparent base excretion, confounding the attempts to measure the HCO_3^- excreted via Cl^-/HCO_3^- exchange. In theory a simple subtraction of total ammonia efflux from apparent base efflux would provide a calculation of HCO_3^- excreted via anion exchange; however, in both seawater and freshwater trials, total ammonia efflux at all timepoints matched or exceeded apparent base efflux. These results indicate that branchial Cl^-/HCO_3^- exchange played a minimal role in alleviating postprandial metabolic alkalosis during these experiments. Notably, in seawater-acclimated fish rectal base excretion could have also contributed to apparent titratable alkalinity flux measurements (and may be a factor in the higher baseline efflux in this group); however, any HCO_3^- secreted into the intestinal lumen as a response to feeding was likely largely consumed in chyme titration and would thus result in minimal changes to rectal base excretion rates.

Branchial Na^+/H^+ and Cl^-/HCO_3^- exchange

Under fasting conditions, branchial exchange of strong ions and acid-base equivalents generally accounts for more than 90% of compensatory acid-base transfers in seawater and freshwater fishes (Goss *et al.* 1992; Evans *et al.* 2005). However, in addition to the aforementioned total ammonia and apparent base efflux data, measurements of branchial Cl^- and Na^+ uptake in freshwater suggest that the role of the gill in compensating for postprandial metabolic alkalosis was minimal in these fish. Unchanged postprandial Cl^- uptake in freshwater-acclimated fish supports the notion that apparent branchial base efflux was

indeed ammonia excretion via NH_3 diffusion trapping, and not a result of increased Cl^-/HCO_3^- exchange. Interestingly, the only change in Na^+ uptake (though not significantly different from control influx) was a drop 12 h after feeding which corresponds to the prediction of reduced Na^+ uptake to retain H^+ and combat a calculated metabolic base load within the blood.

Internal acid- base balance

Alkaline tide

While calculated net postprandial internal base gains of 3.4 mmol kg^{-1} in seawater and 9.1 mmol kg^{-1} in freshwater suggest the potential for alkaline tide in both groups of fish, the absence of changes in postprandial plasma chemistry led us to question how this estimated metabolic base load is handled. Additionally, the substantial difference (nearly 3-fold) in magnitude of calculated net internal base gain between freshwater and seawater-acclimated fish is a source of interest. One point of note is that gastric acid secretion in seawater-acclimated flounder may have been underestimated due to the buffering of secreted H^+ by the bicarbonate/carbonate present in seawater ingested during feeding. However, such an underestimation is likely to be only a few percent, given that the bicarbonate content in sea water is low (~2.0 mM) compared to the high protein content and buffer capacity of the meal. Even if fish ingested a volume of seawater equal to that of the meal (e.g. 5 ml of seawater plus 5 g of ragworm for a 100 g fish), which seems unlikely, it would only require 10 µmoles of H^+ to titrate the imbibed sea water to pH 4.1, whereas it would require ~400 µmoles of

H^+ to titrate the 5 g ragworm meal to the same pH (interpolated from Fig. 4.4). Conversely, calculations of gastric acid secretion based on the fluid phase pH of chyme may overestimate acid secretion if the chyme was non-homogenous (e.g. a neutral or alkaline bolus within an acidic fluid phase). Furthermore, the possibility cannot be eliminated that changes in gastric buffering capacity resulting from 12 h of peptic digestion (in addition to the HCl digestion simulated by the experimental design) occurred *in vivo*. However, the change in buffer capacity by peptic digestion has to current knowledge only been quantified by a single study (Fordtran and Walsh 1973) which measured a 33% increase in buffer capacity during the first two hours of digestion in human subjects. Such an increase in buffer capacity in the stomach content of the flounder used in the present investigation would render the present estimations of gastric acid secretion, and thus systemic base gain, conservative.

Our initial hypothesis of reduced capacity for branchial Cl^-/HCO_3^- exchange leading to an increased incidence of alkaline tide in freshwater was disputed by both the absence of changes in plasma chemistry, and by the results of the Cl^- uptake kinetics experiment. The J_{max} for Cl^- uptake in flounder is already rather low for freshwater fish generally (Tomasso and Grosell 2004), and at the experimental concentration Cl^- uptake would be operating at only 60% of J_{max}. This indicates that Cl^- limitation may to some degree account for the lack of branchial base excretion in freshwater. However, net branchial base efflux (calculated as titratable alkalinity minus total ammonia efflux) was minimal in both freshwater and seawater (where ambient $[Cl^-]$ is almost 1000-fold higher),

indicating that Cl^- limitation is not a likely source of the presumably higher internal base gain incurred in freshwater conditions.

Intestinal fluid chemistry

It is well-documented that Cl^-/HCO_3^- exchange plays a considerable role in acid-base balance both at the gill (Evans *et al.* 2005) and on the basolateral membrane of gastric epithelial cells (Niv and Fraser 2002), both of which have been discussed here with regard to their importance throughout a feeding event. While the present data indicate no significant role of branchial Cl^-/HCO_3^- exchange in alleviating a postprandial metabolic base load, they do, along with another recent study (Taylor and Grosell 2006b), indicate that intestinal HCO_3^- secretion is elevated postprandially in seawater and freshwater-acclimated teleosts. In addition to counteracting intestinal lumen acidification caused by entry of chyme from the stomach, contributing to Cl^- and water absorption, and facilitating $CaCO_3$ precipitation (Taylor and Grosell 2006b), intestinal Cl^-/HCO_3^- exchange may provide an outlet for the systemic base load incurred postprandially. The currently accepted model for intestinal Cl^-/HCO_3^- exchange suggests the primary source of HCO_3^- to be endogenous CO_2 (Grosell *et al.* 2005; Grosell 2006); however, experiments on isolated epithelia employing elevated and reduced serosal HCO_3^- concentrations suggest that serosal HCO_3^- may also provide substrate for apical Cl^-/HCO_3^- exchange (Grosell *et al.* 2005; Grosell 2006; Grosell and Genz 2006). A rapid or even anticipatory response could prevent the accumulation of an alkaline tide in the extracellular fluid, and is

supported by the high intestinal HCO_3^- concentrations immediately (6 h) following feeding. Potential mechanisms for HCO_3^- entry across the basolateral membrane of the enterocyte include basolateral Na^+/HCO_3^- cotransport (NBC), basolateral Cl^-/HCO_3^- exchange, and Na^+-driven Cl^-/HCO_3^- exchange (Grosell *et al.* 2005). If intestinal HCO_3^- secretion does in fact alleviate postprandial metabolic base gain resulting from gastric acid secretion, basolateral NBC or a similar mechanism would be necessary to transport HCO_3^- from the extracellular fluid into the enterocyte where it could be secreted into the intestinal lumen via apical Cl^-/HCO_3^- exchange. An alternate explanation may lie in the increased metabolic rate associated with feeding. The processing costs associated with food digestion are termed specific dynamic action (SDA), and can cause oxygen consumption to increase up to 44 times fasting levels in Burmese python, *Python molurus*, fed a meal equal to their body mass (Secor and Diamond 1998). While the scope of SDA is more modest in fish and other vertebrates ingesting a much smaller fraction of their body mass in a single meal, SDA is nonetheless generally accepted to account for an approximate doubling in oxygen consumption rates (Jobling 1981). As oxygen consumption increases, so do all cellular processes including tissue CO_2 production, and the post-prandial elevation will be even more dramatic in the intestine due to its central role in digestive and absorptive processes (e.g. 3- to 6-fold increase in protein synthesis in trout gastro-intestinal tract after a meal (McMillan and Houlihan 1998)). An increase in endogenous CO_2 production, perhaps combined with an increased carbonic anhydrase activity will likewise increase the intracellular substrate for

intestinal HCO_3^- secretion, thereby increasing the scope for basolateral H^+ extrusion (Grosell and Genz 2006; Grosell 2006), a consequence that could also prevent the accumulation of an alkaline tide. These novel possibilities have led us to question the mechanisms regulating intestinal HCO_3^- secretion. Apical Cl^-/HCO_3^- exchange and the associated mechanism(s) supplying the enterocyte with HCO_3^- could be regulated locally at the cellular level, based on osmoregulatory and acid-base balance regulation requirements across the intestinal epithelium, and/or could be regulated systemically, either by energetic/metabolic shifts as discussed above, or by such signals as digestive peptides, which may confer an anticipatory response. Preliminary data collected by WG Anderson, JR Taylor and M Grosell (unpubl.) suggest that HCO_3^- secretion across the isolated intestinal epithelia of fasting White-spotted bamboo shark (*Chiloscyllium plagiosum*) may be stimulated by both secretin and cholecystokinin (CCK), peptides which facilitate digestion of ingested food (Nelson and Sheridan 2006). In addition to teleost and non-teleostean fish species, these elasmobranchs have also been shown to utilize intestinal Cl^-/HCO_3^- exchange during osmotic challenge (Taylor and Grosell 2006a). While intestinal anion exchange has become a commonly accepted mechanism for osmoregulation in seawater fish (Grosell 2006), it is proposed that apical Cl^-/HCO_3^- exchange may also be important in freshwater fish following a feeding event that will inevitably induce both osmoregulatory and acid-base balance disturbances to the gastro-intestinal tract and extracellular fluid. In fact, fluid from the spiral valve (posterior intestine) analyzed 24 h after feeding in freshwater-

acclimated Siberian sturgeon, *Acipenser baerii*, was found to contain HCO_3^- concentrations over 7-fold those measured in the plasma, with concomitantly reduced intestinal fluid Cl^- concentrations (Taylor and Grosell unpubl.). While the potential for pancreatic islet cells to contribute to high postprandial intestinal HCO_3^- concentrations is recognized, low intestinal fluid Cl^- concentrations (despite a presumed influx of Cl^- with gastric HCl secretions) strongly suggest a considerable role of anion exchange in postprandial intestinal HCO_3^- secretion. These freshwater sturgeon data, along with the euryhaline flounder data, indicate the potential for postprandial intestinal anion exchange in freshwater fish, similar to that documented in a seawater-acclimated teleost (Taylor and Grosell 2006b), but used for a different purpose (i.e. acid-base regulation). This raises an interesting question of whether this ability would be absent in stenohaline freshwater species that may not transcribe/possess the genes/cellular apparatus for intestinal bicarbonate secretion in marine environments that are likely present in more euryhaline species such as sturgeon and flounder.

Conclusions

Our experiments suggest the potential for a direct link between postprandial acid-base balance regulation and osmoregulation in two osmotically distinct media. Despite the initial prediction that branchial base efflux may be compromised in a Cl^--limited freshwater environment resulting in a more prominent alkaline tide in freshwater-acclimated fish, the present results indicate minimal roles of both Cl^-/HCO_3^- and Na^+/H^+ exchange in alleviating the calculated

postprandial metabolic base load to the extracellular fluid. With no manifestation of postprandial metabolic base load (alkaline tide) in blood plasma chemistry, it is important to look to the intestine as a potential site of rapid, or even anticipatory, systemic acid-base balance regulation. Several studies (Wilson *et al.* 1996; Wilson 1999; Wilson and Grosell 2003) have indicated that intestinal base secretion does indeed represent a significant element of whole-animal acid-base balance. However, subsequent experiments indicated that the ability of intestinal HCO_3^- secretion to compensate for systemic acid-base balance disturbances may be limited. Experiments addressed by Wilson et al. (2002) suggest that in euryhaline rainbow trout (*Oncorhynchus mykiss*) and stenohaline flathead sole (*Hippoglossoides elassodon*), induction of a metabolic alkalosis by $NaHCO_3$ loading has no significant effect on intestinal HCO_3^- secretion rates (Wilson RW, Tierney ML and Wood CM, unpubl.). As physiological transformations associated with feeding in animals can be dramatic, there is a need for further work relating intestinal base secretion and systemic acid-base balance regulation under both fasting and fed conditions.

Acknowledgments

R.W. Wilson, J.M. Whittamore (Univ. of Exeter, UK) and M. Grosell (Univ. of Miami, FL, US) contributed to this work and are co-authors on the associated peer-reviewed manuscript. This work was supported by Journal of Experimental Biology/ Company of Biologists and Society for Experimental Biology travel

fellowships and a University of Miami fellowship to J.R. Taylor and by a National Science Foundation Grant to M. Grosell (NSF-IBN 0416440).

Chapter 5:

Basolateral NBCe1 plays a rate-limiting role in transepithelial intestinal HCO_3^- secretion serving marine fish osmoregulation

Summary

While endogenous CO_2 hydration and serosal HCO_3^- are both known to contribute to the high rates of intestinal HCO_3^- secretion important to marine fish osmoregulation, the basolateral step by which transepithelial HCO_3^- secretion is accomplished has received little attention. Isolated intestine HCO_3^- secretion rates, transepithelial potential (TEP) and conductance were found to be dependent on serosal [HCO_3^-] and sensitive to serosal DIDS, but elevated mucosal [Cl^-] did not increase HCO_3^- secretion rates nor affect electrophysiology. These characteristics indicate basolateral limitation of intestinal HCO_3^- secretion in seawater gulf toadfish, *Opsanus beta*. The isolated intestine has a high affinity for serosal HCO_3^- in the physiological range (K_m = 10.2 mM), indicating a potential to efficiently fine-tune systemic acid-base balance. High levels of intestinal tract expression have been confirmed for a basolateral Na^+/HCO_3^- cotransporter of the electrogenic NBCe1 isoform in toadfish (tfNBCe1), which shows elevated expression following salinity challenge, indicating its importance in marine fish osmoregulation. When expressed in *Xenopus* oocytes isolated tfNBCe1 displays transport characteristics corresponding to those of the isolated tissue, including a similar affinity for HCO_3^- (K_m = 8.5 mM). The affinity constant of tfNBCe1 for Na^+ (K_m = 68.2 mM) is much lower than physiological concentrations, suggesting that cotransporter activity is more likely to be

modulated by HCO_3^- rather than Na^+ availability *in vivo*. These similar functional characteristics of isolated tfNBCe1 and the intact tissue suggest a role of this cotransporter in the high HCO_3^- secretion rates of the marine fish intestine.

Background

During the last decade, intestinal HCO_3^- secretion via apical Cl^-/HCO_3^- exchange has become recognized as an important component in the processing of seawater ingested to meet the osmoregulatory needs of marine fish (Wilson *et al.* 2002; Marshall and Grosell 2005; Grosell 2006). This anion exchange has been shown to contribute up to 70% of net Cl^- uptake and thereby water absorption by the marine teleost intestine (Grosell *et al.* 2005), counteracting diffusive water loss to the dehydrating seawater environment. While both endogenous and serosal sources are known to contribute HCO_3^- to apical anion exchange (Wilson *et al.* 2002; Marshall and Grosell 2005; Grosell 2006), the basolateral step of transepithelial HCO_3^- secretion in the marine fish intestine has received relatively little attention. In most species examined, the contribution of serosal HCO_3^- is likely to match or exceed that of endogenous CO_2 hydration (Grosell 2006; Grosell and Genz 2006) under *in vivo* conditions where serosal HCO_3^- concentrations range from 4-10 mM (Wilson 1999). This significant contribution makes the characterization of basolateral HCO_3^- transport essential to the understanding of marine fish osmoregulation.

Intestinal HCO_3^- secretion in marine fish occurs by a similar transport mechanism to that known in mammals. The function of HCO_3^- secretion as part

of duodenal protection from gastric acid passing through the pyloric sphincter with chyme during the postprandial period is presumably shared among those vertebrates relying on gastric acid secretion for digestion. However, intestinal HCO_3^- secretion in fish serves an additional role in contributing to osmoregulation. This difference between mammals and marine fish likely explains why intestinal HCO_3^- secretion in mammals occurs at highly varied rates (Hogan 1994) and results in much lower intestinal fluid concentrations than seen in marine teleost fish. Dating back to the earliest studies of mammalian intestinal transport, intestinal fluid HCO_3^- concentration was found to range from 6.4 to 18.2 mM and was always less than that of the serum (Herrin 1935). Conversely, the osmoregulatory demands of marine fish lead to intestinal fluid HCO_3^- concentrations often approaching or even exceeding 100 mM (Wilson *et al.* 2002), indicating high secretion rates against a HCO_3^- gradient. In addition to apical Cl^-/HCO_3^- exchange facilitating water absorption by contributing to Cl^- uptake (Grosell *et al.* 2005), these high concentrations of HCO_3^- lead to precipitation of $CaCO_3$ from the intestinal fluids (Smith 1930; Walsh *et al.* 1991; Grosell 2006). This carbonate precipitation is a phenomenon unique to osmoregulating marine fish and provides osmotic pressure depression in intestinal fluids (by as much as 70 mOsm), thereby enhancing the osmotic gradient for fluid absorption along the intestinal tract (Wilson *et al.* 2002; Wilson and Grosell 2003; Marshall and Grosell 2005).

Action by three distinct acid/base transporters has been proposed in both mammalian and piscine intestinal HCO_3^- secretion. In addition to apical anion

exchange by a member of the SLC26 family (McMurtrie *et al.* 2004; Dorwart *et al.* 2008; Kurita *et al.* 2008), basolateral extrusion of H^+ produced during endogenous CO_2 hydration occurs in exchange for Na^+ in mammals (via Na^+/H^+ exchange, NHE (Hogan 1994)), with this mechanism of Na^+-dependent H^+ extrusion characterized in one fish species (gulf toadfish; (Grosell and Genz 2006)). Finally, a basolateral Na^+/HCO_3^- cotransporter (NBC) of the electrogenic, NBCe1 isoform has been described for both mammals (Romero and Boron 1999; Romero *et al.* 2004) and also recently in fish (Kurita *et al.* 2008) intestinal transepithelial HCO_3^- secretion. A comprehensive diagram of salt transport by the marine teleost intestine can be found in Fig. 1 of a recent review (Grosell 2006).

The implications of this high magnitude of intestinal base secretion for fish acid-base balance regulation have been largely overlooked. Elevated intestinal HCO_3^- secretion rates are suggested to be induced during the postprandial period (Taylor and Grosell 2006b) when many animals, including a limited number of fish species (an elasmobranch (Wood *et al.* 2005), and freshwater trout (Bucking and Wood 2008; Cooper and Wilson 2008)), have been shown to experience a metabolic alkalosis commonly referred to as alkaline tide (Niv and Fraser 2002). Based on studies indicating the absence of an anticipated alkaline tide (Taylor *et al.* 2007) and an increase in intestinal HCO_3^- secretion (Taylor and Grosell 2006b) in postprandial euryhaline fish, the intestine is presented as a potential site of metabolic alkalosis compensation via transepithelial HCO_3^- secretion. It is hypothesized that NBC is present in the basolateral membrane of seawater-acclimated toadfish intestine and is important for transepithelial HCO_3^-

transport. It is also predicted that NBC will have altered expression in conditions requiring high intestinal HCO_3^- secretion rates, and thereby to possibly control the rate of HCO_3^- secretion by the marine fish intestine. Since a specific pharmacological NBC inhibitor is not available, comparisons are made between the functional characteristics of the toadfish NBC transporter expressed in *Xenopous* oocytes and those of the isolated marine fish intestine and provide evidence for an essential role of basolateral NBC in transepithelial HCO_3^- secretion by the marine fish intestine.

Materials and Methods

Gulf toadfish (*Opsanus beta*) were obtained by trawl from Biscayne Bay as by-catch by shrimp fishermen local to Miami, FL, USA, between March 2007 and October 2008. Within hours of capture fish were transported to the wetlab facility at the Rosenstiel School of Marine and Atmospheric Science at the University of Miami, FL, US and subjected to an ecto-parasite treatment (McDonald *et al.* 2003). Prior to experimentation, fish were maintained in the laboratory for a minimum of two weeks in aquaria with a constant flow of filtered, aerated seawater (32±1‰) at 24±2ºC from Bear Cut, FL, US. These aquaria were equipped with PVC shelters to reduce stress and aggression among fish. Toadfish were fed chopped squid to satiation twice weekly until 72 h prior to experimentation, after which time food was withheld to ensure complete clearing of the gastro-intestinal tract. All experimental procedures have been approved by the Institutional Animal Care and Use Committee under protocol 08-017.

In vitro HCO_3^- secretion by isolated intestinal tissue: electrophysiological measurements and pH-stat titration

To simultaneously investigate electrophysiological parameters and HCO_3^- secretion rates of isolated intestinal epithelia, Ussing chambers (Physiological Instruments, San Diego, CA, USA) were set up in combination with pH-stat titration. A segment of the anterior intestine was excised from each experimental animal (toadfish ranging from 20-100 g), cut open, and mounted onto a tissue holder (model P2413, Physiological Instruments) exposing 0.71 cm^2 of the isolated tissue and positioned between two half-chambers (model P2400; Physiological Instruments) containing 1.6 ml of the appropriate, pre-gassed, mucosal or serosal saline (Table 5.1). The saline in each half-chamber was continually mixed by airlift gassing with either O_2 or 0.3% CO_2 in O_2 (Table 5.1), and a constant temperature of 25ºC was maintained by a thermostatic water bath. Current and voltage electrodes connected to amplifiers (model VCC600; Physiological Instruments) recorded the transepithelial potential (TEP) differences under current-clamp conditions at 0 µA, with 3-sec, 50 µA pulses from the mucosal to the serosal side at 60-sec intervals. These current-clamped conditions were maintained across all treatments. TEP measurements were logged on a personal computer using BIOPAC systems interface hardware and Acqknowledge software (version 3.8.1). TEP values are reported with a luminal reference of 0 mV. A pH electrode (model PHC4000.8, Radiometer) and microburette tip were submersed in the luminal half-chamber and were connected to a pH-stat titration system (model TIM 854 or 856, Radiometer)

grounded to the amplifier to allow for pH readings during current pulsing. The pH-stat titrations were performed on luminal salines at a physiological pH of 7.800 throughout all experiments (creating symmetrical pH conditions on either side of the epithelium), with pH values and rate of acid titrant (0.005 N HCl) addition logged on personal computers using Titramaster software (versions 1.3 and 2.1). Titratable alkalinity, representing HCO_3^- secretion (Grosell and Genz 2006), was calculated from the rate of titrant addition and its concentration. All experiments entailed an initial control period of 60 min with stable TEP and base secretion rates before manipulations were carried out as described below. The intestinal preparations from gulf toadfish are viable and stable for at least 5 hours under these conditions (Grosell and Genz 2006). The titration curves of each preparation were allowed to stabilize approximately 30 min after application of each experimental saline before HCO_3^- secretion rates and electrophysiological parameters were averaged and reported for the remaining 30 min of exposure.

Affinity for serosal HCO_3^-. Affinity of the isolated gulf toadfish anterior intestine for serosal HCO_3^- was investigated using serosal salines varying in HCO_3^- concentration from 0 to 20 mM (Table 5.1). Following a 60 min period during which HCO_3^- secretion rates were quantified under control mucosal and 20 mM HCO_3^- serosal salines, the serosal saline was carefully removed from the half-chamber via PE60 tubing connected to a 5 ml syringe. The serosal half-chamber (including the serosal membrane of the epithelium) was rinsed twice and refilled with an equal volume of serosal saline containing 10 mM HCO_3^-. An additional 60 min period was allowed for quantification of HCO_3^- secretion rates

with 10 mM serosal HCO_3^-, followed by identical treatments with serosal salines containing 5 and then 0 mM HCO_3^-.

Limitation by mucosal [Cl^-]. Upon finding evidence for saturation of intestinal HCO_3^- secretion rates at elevated serosal HCO_3^- concentrations, the possibility was investigated that apical anion exchange may be limited by mucosal Cl^- concentrations when serosal [HCO_3^-] is above *in vivo* concentrations. Following a 60 min period during which HCO_3^- secretion rates were quantified during exposure of the epithelium to control mucosal and 20 mM HCO_3^- serosal salines, the control mucosal saline was removed as above and replaced with high-Cl^- mucosal saline (Table 5.1). Once the physiological pH of 7.800 was reached in the experimental mucosal saline, pH-stat titration data were recorded for 60 min after which control conditions were resumed for an additional 60 min by replacing the mucosal saline as described above.

Inhibition of HCO_3^- secretion by serosal DIDS application. Bicarbonate secretion rates by the isolated intestine were quantified before and after serosal application of 4,4'-Diisothiocyanatostilbene-2,2'-disulfonic acid (DIDS, Sigma), which has been shown to inhibit both anion exchange and NBC (Romero *et al.* 1997). Prior to application, DIDS was dissolved in DMSO (Sigma) at a final concentration of less than < 0.01% DMSO. DIDS was applied at a final concentration of 1 mM in the serosal saline which in preliminary experiments was found to induce maximal inhibition (data not shown). Control experiments were carried out in presence of DMSO alone.

Table 5.1. Composition of serosal and mucosal salines used in isolated tissue experiments

	Serosal				Mucosal	
	0mM HCO_3^-	5mM HCO_3^-	10mM HCO_3^-	20mM HCO_3^-	Mucosal	High Cl^- mucosal
NaCl, mM	151	151	151	151	69	69
Choline-Cl, mM						32
KCl, mM	3	3	3	3	5	5
$MgCl_2$, mM					22.5	22.5
$MgSO_4$, mM	0.88	0.88	0.88	0.88	77.5	77.5
Na_2HPO_4, mM	0.5	0.5	0.5	0.5		
KH_2PO_4, mM	0.5	0.5	0.5	0.5		
$CaCl_2$, mM	1	1	1	1	5	5
$NaHCO_3$, mM	0	5	10	20		
HEPES						
Free acid, mM	11	11	11	11		
Sodium salt, mM	11	11	11	11		
Urea, mM	4.5	4.5	4.5	4.5		
Glucose, mM	5	5	5	5		
Osmolality, mosmol l^{-1}	355*	355*	355*	355*	355*	355**
pH	7.800‡	7.800‡	7.800‡	7.800‡	7.800†	7.800†
Gas	O_2	0.3% CO_2 in O_2	0.3% CO_2 in O_2	0.3% CO_2 in O_2	O_2	O_2

*Adjusted with mannitol to ensure transepithelial isosmotic conditions in all experiments
**Adjusted with choline-Cl rather than mannitol to ensure transepithelial isosmotic conditions in all experiments.
†pH 7.800 was maintained by pH-stat titration
‡pH was adjusted with HCl under continuous gassing prior to experimentation to ensure isionic H^+ conditions during measurements

Molecular characterization of NBC

RNA isolation. For the initial identification and characterization of NBC in gulf toadfish, total RNA was extracted from anterior intestine tissue using RNA STAT-60 (Tel-Test, Friendswood, TX, USA). Briefly, tissue was homogenized in RNA STAT-60 (approx. 50-100 mg tissue per ml RNA STAT-60) using an IKA-Werke (Wilmington, NC, USA) Ultra-turrax T8 tissue homogenizer, and subjected to chloroform extraction and isopropanol precipitation. Precipitated RNA was washed with chilled 75% (v/v) ethanol and dissolved in nuclease-free water, and its concentration was measured spectrophotometrically at 260nm. To remove any traces of genomic DNA, 10 µg from each sample was treated with DNase (Turbo DNA-free kit, Applied Biosystems/Ambion, Austin, TX, USA) followed by gel electrophoresis to confirm that RNA integrity was maintained.

Molecular cloning. cDNA was reverse transcribed from 1 µg Poly(A) RNA using random hexamers and the SuperScript First-Strand Synthesis System (Invitrogen, Carlsbad, CA, USA) according to the manufacturer's instruction. Conserved regions of rainbow trout, zebrafish, salamander, rat and human NBC1 (NM 001124325.1, NM 001034984, AF001958, AF004017 and AF069510, respectively) were used to design three sets of primers (NBC1 1-3, Table 5.2) to amplify overlapping fragments of toadfish NBC from the cDNA template described above using AmpliTaq Gold polymerase (Applied Biosystems/Ambion). Assemblage of the resulting 2406 bp contig was later confirmed by alignment with the entire open reading frame (ORF) subsequently cloned by PCR for expression in *Xenopus* oocytes (see below). This contig was then used to design

gene-specific and nested gene-specific primers (GSP and NGSP, respectively, Table 5.2) for rapid amplification of cDNA ends (RACE) to obtain full length NBC sequence. Briefly, the SmartRACE cDNA synthesis kit (Clontech, Mountain View, CA, USA) was used to reverse transcribe 1 µg poly(A) RNA and amplify RACE-ready cDNA, which was subjected to touchdown PCR cycling conditions per the manufacturer's recommendations. A second round of amplification was carried out on diluted aliquots (1:100) of the initial amplifications using nested gene-specific primers (Table 5.2). Products were gel-purified, TA-cloned into the pCR 2.1 vector (Invitrogen) and sequenced. The full-length NBC sequence was confirmed by BLAST (National Center for Biotechnology Information, Bethesda, MD, USA) query as the electrogenic NBCe1 isoform, hereafter referred to as tfNBCe1 (accession no. FJ463158). Subsequently, the entire coding region of tfNBCe1 was cloned by PCR (Table 5.2) using the Advantage 2 (Clontech) high-fidelity enzyme mix and 5' RACE-ready cDNA as template. Following TA cloning and sequence verification, the full-length ORF was subcloned into the EcoRI site of the pGH19 *Xenopus laevis* expression vector (graciously provided by Dr. Gerhard Dahl, University of Miami Miller School of Medicine, Miami, FL, USA) using the LigaFast Rapid DNA Ligation System (Promega, Madison, WI, USA).

Real-time PCR. Tissue distribution of tfNBCe1 in gulf toadfish was initially quantified by real-time PCR under SW control conditions. An acute salinity increase was then used to increase drinking rates (Marshall and Grosell 2005) and thereby exploit mechanisms associated with this increased need for intestinal water absorption. tfNBCe1 expression was accordingly quantified in

appropriate osmoregulatory tissues at 0, 6, 12, 24, and 96 h following acute salinity increase. Initially, eight fish (20-30 g) held in seawater aquaria as described above were given a lethal dose of MS-222 anaesthetic prior to severing the spinal cord. Esophagus, stomach, anterior intestine, mid intestine, posterior intestine, rectum, gill, kidney, muscle, liver, brain and spleen were obtained by dissection and immediately flash frozen in liquid nitrogen prior to transfer to a -80ºC freezer.

From a batch of 40 additional toadfish (20-30 g) split between four 75 L aquaria receiving biofiltered, recirculated seawater, 8 were sampled immediately (2 individuals from each tank) for gill, anterior, mid, posterior intestine and rectum by dissection. The remaining 32 fish were maintained in their respective aquaria as the salinity was raised to 60 ppt within a 5 min timeframe by the addition of a concentrated solution of Instant Ocean (Spectrum Brands, Inc). At 6, 12, 24 and 96 hours post transfer to 60 ppt, 8 fish per time point were sampled as above. From all tissues collected, RNA was extracted, purified and reverse transcribed as above. Quantitative PCR (Mx4000, Stratagene, La Jolla, CA, USA) was used to measure tfNBCe1 mRNA expression using primers listed in Table 5.2 with SYBR green (Sigma, St. Louis, MO) as the reporter dye. Cycling parameters were as follows: 95°C for 30 sec, 55°C for 30 sec and 72°C for 1 min. Calculations were performed based on the delta-delta-C_T approach (Livak and Schmittgen, 2001) using elongation factor 1α (EF1α) for normalization of template concentration. Due to the absence of available toadfish-specific sequence for EF1α, primers were designed from highly conserved regions across

multiple teleost species. All PCR product specificities were confirmed by sequencing and the production of single, distinct melting peaks following amplification. Relative tfNBCe1 expression was calculated for each exposure group such that the tissue expressing the lowest quantity of tfNBCe1 (i.e., kidney in SW control conditions, and gill under increased salinity conditions) was assigned an expression value of one.

Table 5.2. Primer pairs used to amplify an initial (2406 bp) fragment of tfNBCe1 (NBC1 1-3), RACE gene-specific (GSP) and nested gene-specific (NGSP) primers, those used to clone the entire open reading frame (NBC1 ORF), and qPCR primer pairs for tfNBCe1 and EF1α.

	Forward primer sequence (5'→3')	Reverse primer sequence (5'→3')
NBC1 1	CACCAGACCAAGAAGTCCAAC	GRATGAAKGACATSAGHGTGA
NBC1 2	CATGCAGGGYGTGTTGGAGAG	ATGTGDGCRATGGAGATGAC
NBC1 3	CTTCATCTTCATYTAYGAYGC	CATCCAGGTARCTGAGATCDTGCTG
NBC1 5' RACE GSP		GGGTGGTAAACAGCCTACTTGCACTGG
NBC1 3'RACE GSP	ATGCTCTGGATCCTCAAATCCACCGTGG	
NBC1 5' RACE NGSP		AGCGCAGGTTGGACTTCTTGGTCTGGTG
NBC1 3'RACE NGSP	TTCTCCCAGCACGATCTCAGCTACCTGG	
NBC1 ORF	GATGGAAGATGAGGCGGTGTTGGAC	CCTTGTAGTAGCGGAGCTTCTCAGCACG
NBC1 qPCR	ACCAAAGTTTCTGGGTGTCAGAGAGCA	ACAGCACAGGCATAGGGATGAACTTTA
EF1α	AGGTCATCATCCTGAACCAC	GTTGTCCTCAAGCTTCTTGC

Table 5.3. Composition of solutions used in oocyte ^{22}Na flux and electrophysiology experiments

	OR2	ND96								
		0mM HCO_3^-	5mM HCO_3^-	10mM HCO_3^-	20mM HCO_3^-	0mM Na^+	5mM Na^+	15mM Na^+	50mM Na^+	100mM Na^+
NaCl, mM	82.5	99	99	99	99	0	5	15	50	100
Choline-Cl, mM						100	95	85	50	0
KCl, mM	2.5	2	2	2	2	2	2	2	2	2
$MgCl_2$, mM	1	1	1	1	1	1	1	1	1	1
$CaCl_2$, mM	1	1.8	1.8	1.8	1.8	1.8	1.8	1.8	1.8	1.8
$NaHCO_3$, mM		0	5	10	20	10	10	10	10	10
$NaHPO_4$, mM	5									
HEPES (Free acid), mM	5	1	1	1	1	1	1	1	1	1
Osmolality, mosmol l^{-1}		240*	240*	240*	240	230	230	230	230	230
pH†	7.40	7.40	7.40	7.40	7.40	7.40	7.40	7.40	7.40	7.40

*Adjusted with mannitol to ensure equal osmotic gradients in all experiments

†pH adjusted with appropriate amounts of HCl or NaOH to pH 7.40 prior to experimentation

Expression of tfNBCe1 in Xenopus oocytes

Oocyte preparation. Oocytes were prepared for RNA injections as described previously (Dahl 1992). After being washed thoroughly with regular oocyte ringer (OR2, Table 5.3), oocytes devoid of follicle cells and having uniform pigmentation were selected and stored in OR2 at 17ºC. mRNA was transcribed *in vitro* by T7 RNA polymerase from 1µg of XhoI-linearized plasmid DNA using the mMessage mMachine kit (Applied Biosystems/Ambion). Oocytes were injected with 50 nl of water or 1µg/µl cRNA using a Nanoliter 2000 injector (World Precision Instruments, Sarasota, FL, USA). Oocytes were incubated at 17ºC in regular (pyruvate-free) ND96 medium (Table 5.3) containing antibiotics (Penicillin, 10,000 U ml^{-1}; Streptomycin, 10 mg ml^{-1}) until Na^+ flux and electrophysiology experiments commenced 3 and 4 days after injection, respectively, as described below.

^{22}Na Flux. On the 3rd day following injection, control (H_2O-) and tfNBCe1 RNA-injected oocytes were selected in groups of 10, rinsed briefly in the appropriate antibiotic-free experimental ND96 saline (Table 5.3) containing the NHE and NKCC inhibitors amiloride (100 µM, Sigma) and bumetanide (10 µM, Sigma), respectively. Amiloride and bumetanide were added to all experimental salines to inhibit any intrinsic NHE and NKCC activity by oocytes (Dascal 1987). Groups of 10 oocytes were then placed in conical-bottomed wells of a 96-well plate, each containing 150 µl of the experimental saline (Table 5.3) to which 7.5 µCi ^{22}Na (Amersham Biosciences, Sweden) per well had been added. Initial flux samples (10 µl) were aliquoted for gamma counting so that any dilution of the

experimental media during oocyte addition could be accounted for. Following preliminary experiments revealing possible saturation of ^{22}Na uptake by oocytes after 90 to 120-minutes (data not shown), 75 min was identified as the most appropriate flux time and was used for all subsequent experiments. At the end of the flux period, all 10 oocytes were carefully removed from the well using a Pasteur pipette and subjected to three serial rinses in regular antibiotic-, drug- and HCO_3^--free ND96 saline. Following the final rinse, oocytes were examined under a dissection scope for damage to the plasma membrane. Undamaged oocytes (generally 80-90%) were selected for gamma counting. A final flux sample (10 µl) was also taken from each well for gamma counting. Samples were analyzed for ^{22}Na activity (Packard Cobra II Auto-Gamma, Meriden, Connecticut, USA), $[Na^+]$ was measured by flame atomic absorption spectrophotometry (Varian SpectrAA220, Mulgrave, Victoria, Australia), and Na uptake was calculated from the ^{22}Na radioactivity and specific activity measurements. These experiments were designed to complement isolated tissue measurements by allowing us to quantify affinity of the isolated tfNBCe1 for HCO_3^- during exposure to 0, 5, 10 and 20 mM HCO_3^-.

Electrophysiology. On the 4th day following injection, control and tfNBCe1-injected oocytes were individually selected and placed in a recording chamber continuously perfused with experimental saline (Table 5.3). Individual oocytes were probed with two electrodes, one recording membrane potential and the other for current injection. Voltage-measuring and current-passing microelectrodes were pulled with a vertical Puller (David Kopf Instruments,

Tujunga, CA) and filled with 3M KCl. As detailed by Wang et al. (2007), electrodes were connected to a voltage clamp circuit, which allowed the potential to be clamped and also for measurement of clamp current. Whole cell membrane current was used as a measure of Na^+ transport (Ussing and Zerahn 1951) by the electrogenic tfNBCe1 transporter and was quantified during voltage clamp to *in vivo*-like conditions of -20 mV (Geneclamp 500B; Axon Instruments, Sunnyvale, CA), with pulses of 10 mV for determination of membrane conductance. Measurements were recorded with a chart recorder (Soltec, San Fernando, CA). Oocytes were exposed to bathing solutions of ND96 containing 10 mM HCO_3^- and [Na^+] increasing from 0 to 5, 15, 50, and 100 mM Na^+, with the [Cl^-] of the media held constant by addition of choline-Cl to the experimental salines as described in Table 5.3.

tfNBCe1 transmembrane topology prediction. The amino acid sequence of tfNBCe1 was used to predict the transmembrane topology of this protein using hydropathy plots based on Kyte and Doolittle (1982; Brown *et al.* 1996), and models generated by TMPred (hosted by the Swiss Institute of Bioinformatics) and ConPredII (Japan).

Localization of intestinal tfNBCe1

Immunostaining was used to localize tfNBCe1 in seawater-acclimated toadfish anterior intestine. Tissue was cut to approx. 2 mM thick sections and fixed overnight at 4ºC in 5 volumes 4% paraformaldehyde (PFA) in 0.1 M phosphate buffered saline (PBS), which was replaced by ice cold 15% (w/v)

sucrose and incubated 2-4 h at 4ºC, then replaced by 30% (w/v) sucrose for storage at 4ºC. Fixed tissues were sectioned to 6µM using a cryostat (Leica CM1850) at -20ºC, with 10 sections mounted on each pre-cleaned glass micro slide. Slides were heated on a warming block at 42ºC for 30 min, and sections were circled with a mini pap pen to create a hydrophobic barrier. Sections were immediately incubated with 1% sodium dodecyl sulfate (SDS) in 0.1 M PBS, 5 min at room temperature (RT) for antigen retrieval (Brown et al., 1996) and then rinsed quickly by Pasteur pipette and washed thoroughly in Coplin jars (15 min with renewal of wash media every 5 min) containing a solution of 1% bovine serum albumin (BSA, Sigma) and 0.05% Tween (Tween 20, Sigma) in 0.1 M PBS (BTPBS). Excess wash solution was aspirated and a blocking step commenced, entailing a 60 min incubation at RT with 5% normal goat serum (NGS, Invitrogen) in BTPBS, after which slides were rinsed, washed and aspirated as above. Primary mefugu NBCe1 antiserum and preimmune (negative control) serum were generously provided by Dr. Hirose and co-workers (Kurita et al., 2008) and were applied to sections in a 1:1000 dilution in BTPBS. Sections were incubated in the dark with respective primary antibody for 2 h at RT. Primary antibody were rinsed from the sections and slides were washed and aspirated as above. Secondary antibody solutions containing Alexa Fluor 488-conjugated anti-rabbit IgG (1:500 dilution, Invitrogen) in BTPBS, were applied to all sections for a 1 h dark incubation at RT. Following rinsing, washing, and aspiration of slides as above, sections were mounted with Vectashield mounting medium for fluorescence with DAPI (Vector Laboratories, Inc, Burlingame, CA,

USA). Fluorescence was detected using an Olympus BX61 fluorescent microscope with micropublisher 3 MP color CCD camera. Images were captured using a QCapture imaging system (QImaging, Surrey, BC, Canada) and processed using IPLab imaging software (BD Biosciences, Rockville, MD, USA).

Statistics

Data are presented as mean ± SEM. For all isolated tissue measurements, repeated measures ANOVA or paired t-tests were used to determine statistically significant differences from control conditions. Significant expression of tfNBCe1 in tissues from SW-acclimated toadfish was determined by ANOVA comparison of normalized tfNBCe1 expression in each tissue to that of the lowest-expressing tissue, the kidney (normalized tfNBCe1 expression = 1). In measurements of tfNBCe1 expression following salinity transfer, expression in each tissue sample was quantified by comparison with the lowest-expressing sample, gill 0 h post-transfer (normalized tfNBCe1 expression = 1). Between-timepoint comparisons were made within each tissue group using one-way ANOVA. Significant changes in oocyte Na^+ uptake from that of controls were also determined by one-way ANOVA, while oocyte electrophysiological measurements were analyzed using repeated-measures ANOVA. The Student-Newman-Keuls test was used for all multiple comparisons as appropriate, and statistical significance was given at $P < 0.05$ in all cases. Hyperbolic curves of equation $f = ax/(b+x)$ or $f = y_0 + ax/(b+x)$ were fit to relevant data sets using SigmaPlot 8.0, with $a = V_{max}$ and $b = K_m$.

Results

Isolated intestinal tissue transport characteristics

Affinity for serosal HCO_3^-. A plot of HCO_3^- secretion rate by the isolated toadfish anterior intestine as a function of serosal HCO_3^- concentration is shown in Fig. 5.1. A hyperbolic curve was fit (R = 0.70) to these data and maximal HCO_3^- secretion rates (V_{max}) of 1.26 μmol cm^{-2} h^{-1} were calculated. Subtraction of HCO_3^- secretion rates under HCO_3^--free conditions (Table 5.4) suggests 0.92 μmol cm^{-2} h^{-1} (>70%) of this V_{max} is conferred by transepithelial rather than endogenous HCO_3^- secretion, during the constant metabolic conditions expected under these experimental conditions. For calculation of the basolateral HCO_3^- affinity constant K_m, secretion rates during exposure to 0 mM serosal HCO_3^- were subtracted from all measurements such that the calculated K_m of 10.2 mM HCO_3^- is exclusively a measure of affinity for serosal HCO_3^- without interference by endogenous CO_2-mediated HCO_3^- secretion. Depressed HCO_3^- secretion rates under decreasing serosal [HCO_3^-] were accompanied by significant reductions in both TEP and conductance (Table 5.4). Changes in conductance were notably modest compared to those seen to TEP and reflect the substantial contribution of electroneutral ion absorption such as that by NaCl and NKCC cotransport, to conductance of the highly absorptive marine teleost intestinal epithelia.

Fig. 5.1. The isolated toadfish anterior intestine (n = 8) shows saturation of luminal HCO_3^- secretion rates with increasing serosal [HCO_3^-]. Asterisks denote a significant increase in HCO_3^- secretion rate from that at 0mM serosal HCO_3^- (0.34 µmol cm^{-2} h^{-1}; lower dashed line). Maximal HCO_3^- secretion rate (V_{max}) by the entire system (both serosal and endogenous sources of HCO_3^-) was calculated to be 0.92 µmol cm^{-2} h^{-1}.

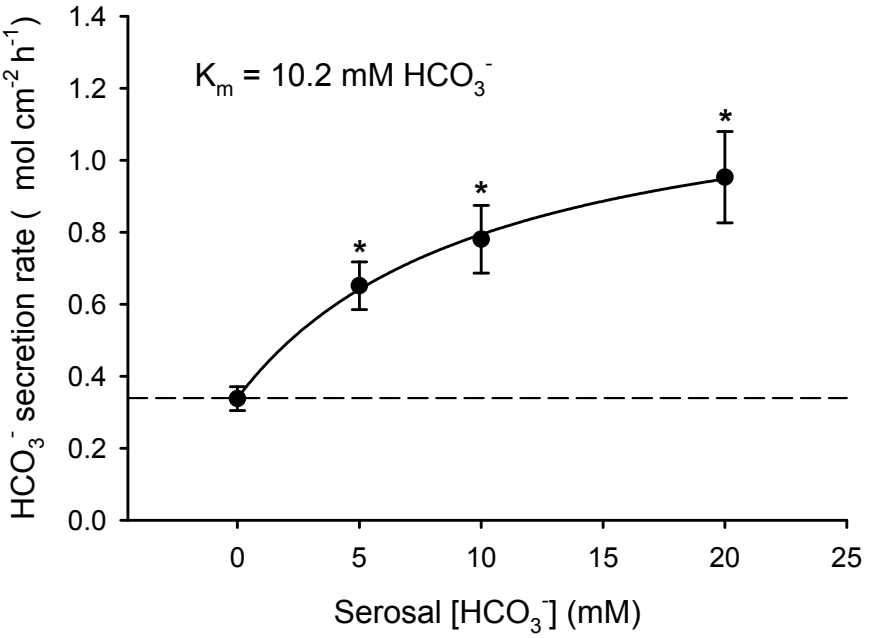

Limitation by mucosal [Cl^-]. To further investigate the saturation of HCO_3^- secretion rates with increasing serosal [HCO_3^-], experiments using a range of serosal [Na^+] were attempted; however, saline chemistry limitations unfortunately prevent the use of low serosal [Na^+] without simultaneously altering [Cl^-]. Thus experiments alternating normal and high [Cl^-] mucosal salines were undertaken to ensure that the saturation of HCO_3^- secretion induced by increased serosal [HCO_3^-] was in fact due to basolateral limitation rather than limitation of apical Cl^- /HCO_3^- exchange by mucosal Cl^- substrate. In the case of apical anion exchange limitation by mucosal Cl^- substrate, increasing the mucosal [Cl^-] would be expected to increase the HCO_3^- secretion rates of the isolated tissue. However,

the present data show a significant and irreversible *decrease* in HCO_3^- secretion under high mucosal [Cl^-] as compared to normal mucosal [Cl^-] rates (Table 5.4). Electrophysiological data show no significant changes in either TEP or conductance under high mucosal [Cl^-] (Table 5.4).

Serosal DIDS application. Serosal application of the NBC and anion exchange inhibitor DIDS significantly decreased HCO_3^- secretion by the isolated tissue under 20 mM serosal HCO_3^- from 1.25 ± 0.11 μmol cm^{-2} h^{-1} to 0.78 ± 0.07 μmol cm^{-2} h^{-1}. This incomplete inhibition by DIDs resulted at least in part from the continuation of endogenous CO_2 production during serosal DIDs application. Likewise, TEP and conductance are both significantly inhibited in the presence of serosal DIDS (Table 5.4), albeit to a relatively smaller degree than HCO_3^- secretion rates due to their dependence on processes other than HCO_3^- secretion (i.e., Na^+/K^+-ATPase).

Table 5.4. Measurements of the toadfish isolated anterior intestine, presented as mean ± SEM.

	HCO_3^- secretion ($\mu mol\ cm^{-2}\ h^{-1}$)	TEP (mV)	Conductance (μSi)
Affinity for serosal HCO_3^- (n = 8)			
0mM serosal HCO_3^-	0.34 ± 0.03	-14.23 ± 1.90	11.01 ± 0.44
5mM serosal HCO_3^-	0.65 ± 0.07*	-16.86 ± 1.75*	11.55 ± 0.40*
10mM serosal HCO_3^-	0.78 ± 0.09*	-19.18 ± 1.54*	11.57 ± 0.33*
20mM serosal HCO_3^-	0.95 ± 0.13*	-22.66 ± 0.77*	11.63 ± 0.40*
Effects of mucosal [Cl⁻] (n = 6)			
Control mucosal [Cl^-] (treatment 1)	1.19 ± 0.06	-24.49 ± 1.56	12.25 ± 0.29
High mucosal [Cl^-] (treatment 2)	0.81 ± 0.05*	-24.50 ± 1.31	12.50 ± 0.30
Control mucosal [Cl^-] (treatment 3)	0.86 ± 0.10*	-24.70 ± 2.40	12.71 ± 0.77
Serosal DIDS application (n = 6)			
Control	1.25 ± 0.11	-23.65 ± 1.65	11.76 ± 0.35
DIDS	0.78 ± 0.07*	-19.41 ± 2.64*	10.11 ± 0.64*
Serosal DMSO sham application (n = 6)			
Control	1.29 ± 0.09	-23.72 ± 3.36	12.37 ± 0.23
DMSO	1.08 ± 0.08	-21.33 ± 4.46	12.64 ± 0.22

"*" denotes statistically significant difference from control

tfNBCe1 mRNA expression

The tfNBCe1 is most highly expressed along the intestinal tract of SW-acclimated gulf toadfish, with the highest prevalence in the anterior intestinal tissue and decreasing sequentially in posterior segments. Significant tfNBCe1 expression was also measured in the brain (Fig. 5.2). Acute salinity increase allowed us to further investigate the role of tfNBCe1 in salt and water balance of toadfish. Based on their osmoregulatory importance, the intestinal tract and gill were the focus of tissue sampling following acute salinity challenge. A trend towards increased tfNBCe1 expression was seen in all tissues except for the gill, and appeared to peak between the 6 to 24 h post-transfer periods with increases

ranging from 20 to nearly 300%. These increases in expression reached statistical significance only for the middle intestine (Fig. 5.3).

Fig. 5.2. Tissue distribution of tfNBCe1 mRNA expression in toadfish acclimated to seawater (n = 6-8 for each tissue), normalized using the EF1α housekeeping gene and scaled relative to the tissue of lowest tfNBCe1 expression (kidney) which was assigned an expression value of one. Asterisks indicate tissues expressing tfNBCe1 to a significantly greater level than that of the kidney.

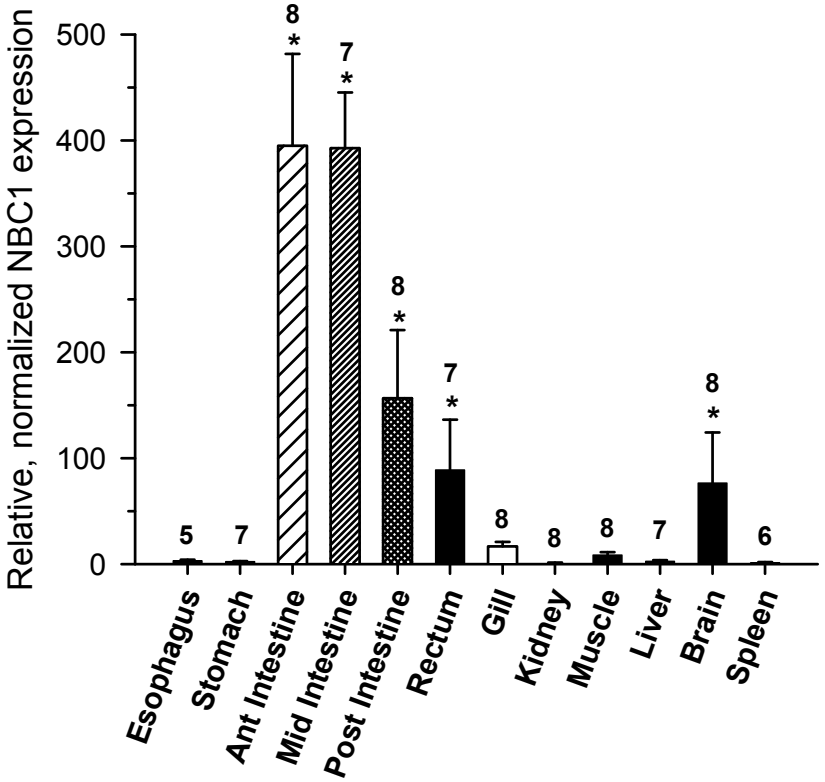

Fig. 5.3. tfNBCe1 mRNA expression in toadfish intestine, rectum, and gill following acute transfer from seawater (35ppt) to 60ppt seawater, normalized using the EF1α housekeeping gene and scaled relative to the tissue of lowest NBC1 expression (gill 0h post-transfer) which was assigned an expression value of one. Asterisks indicate significant increases in tfNBCe1 expression from 0h levels. N = 6-8 for each tissue. N = 8 for each tissue at each timepoint, with the exception of 96h rectum samples (N = 7).

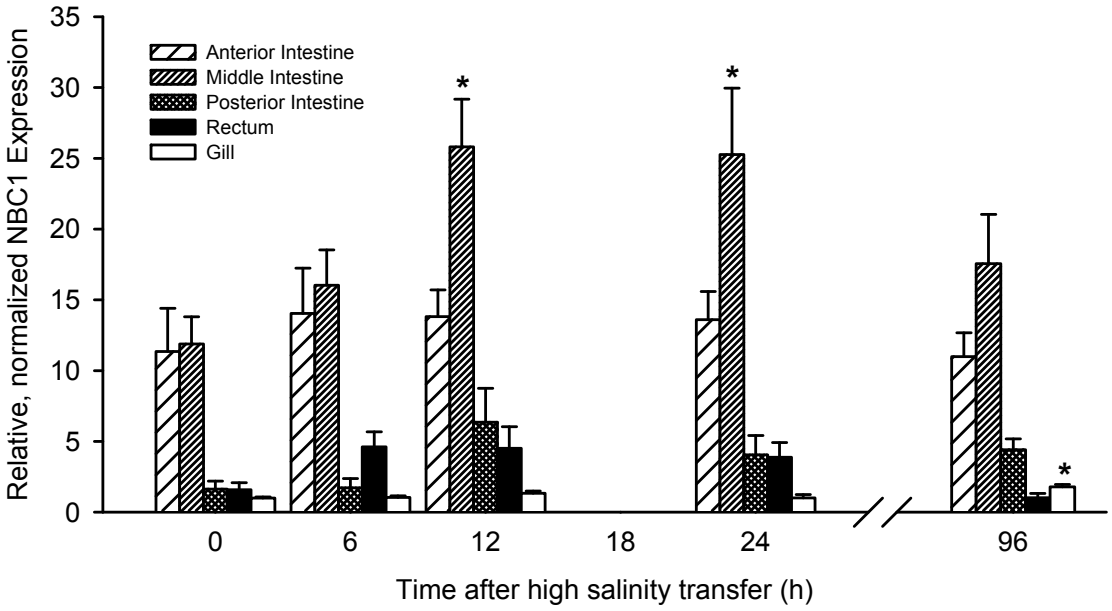

Isolated tfNBCe1 transport characteristics

tfNBCe1 was expressed in *Xenopus* oocytes as indicated by significantly higher ^{22}Na uptake (Fig. 5.4a) and conductivity (Fig 5.5a) than water-injected controls. In addition to the results described below, pharmacological inhibition of NBC in oocytes was attempted but unfortunately the DMSO vector required to dissolve DIDS proved too caustic to the oocyte membrane to yield reliable results (data not shown). While stoichiometry and I/V relationships exceed the scope of the present study, the secretory nature of HCO_3^- transport by the marine teleost

intestine suggests tfNBCe1 to likely confer a HCO_3^--to-Na^+ stoichiometry of 2:1 (Gross *et al.* 2002; Kurita *et al.* 2008), with reversal potentials for these cotransporters reported to be approx. -70 mV in *Xenopus* oocytes (Ducoudret et al. 2001). NBC1 as expressed in *Xenopus* oocytes is thought to require the presence of an accessory protein or modification factor to exceed a stoichiometry of 2:1 (Romero 2001).

Affinity for HCO_3^-. The tfNBCe1 as expressed in *Xenopus* oocytes displayed affinity for HCO_3^- at a similar level to that of the isolated toadfish intestinal tissue. Increasing the HCO_3^- concentration of the flux media from 0 to 5, 10 and 20 mM HCO_3^- resulted in saturation of Na^+ uptake by tfNBCe1-expressing oocytes (Fig. 5.4b). Once counts were normalized to zero ^{22}Na uptake by oocytes fluxed in media containing 0 mM HCO_3^-, a hyperbolic curve was fitted ($R = 0.70$) to these data with K_m = 8.5 mM HCO_3^-. These calculations were made assuming all Na^+/HCO_3^- cotransport occurred as uptake, with no interfering Na^+ efflux. This assumption was made based on the Na^+ reversal potential of approx. +55 mV under the experimental conditions.

Fig. 5.4. (a) Expression of tfNBCe1 in *Xenopus* oocytes is indicated by significantly higher Na^+ uptake in tfNBCe1 RNA vs H_2O-injected control oocytes during exposure to 10mM HCO_3^- media. (b) Affinity of tfNBCe1 for HCO_3^- was determined by measuring Na^+ uptake in tfNBCe1-expressing oocytes exposed to varying HCO_3^- concentrations (n = 18-20 oocytes at each [HCO_3^-]). Uptake has been adjusted for H_2O-injected controls and also such that background ^{22}Na uptake observed from HCO_3^--free saline has been subtracted from all values. A hyperbolic regression was used to calculate the affinity of tfNBCe1 for HCO_3^- as described in the text. Asterisks denote a significant increase in Na^+ uptake from oocytes exposed to HCO_3^--free saline (i.e., zero).

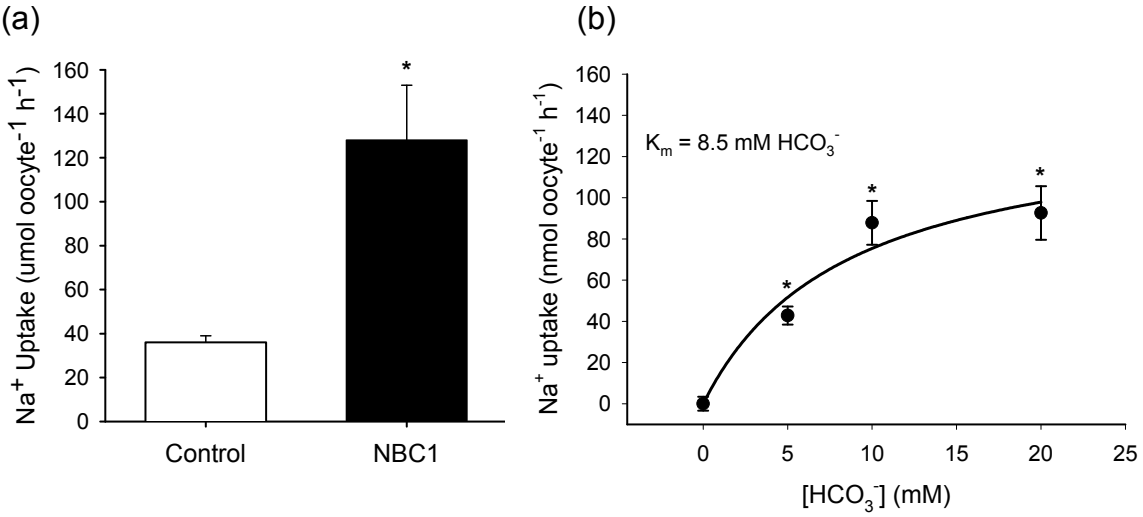

Fig. 5.5. Conductance measurements were made during voltage clamp at -20 mV with 10 mV pulses. (a) Expression of tfNBCe1 in *Xenopus* oocytes is indicated by significantly higher conductance in tfNBCe1 RNA vs H_2O-injected control oocytes (n = 6). (b) Affinity of tfNBCe1 for Na^+ was determined by measuring conductance across the membrane of tfNBCe1-expressing *Xenopus* oocytes (n = 6) exposed sequentially to increasing Na^+ concentrations. Conductance has been adjusted for H_2O-injected controls and also such that oocytes bathed in saline containing Na^+ at the reversal concentration of approx. 5 mM have zero conductance. A hyperbolic regression was used to calculate the affinity of tfNBCe1 for Na^+ as described in the text. Asterisks denote a significant increase ($P < 0.05$ by repeated measures ANOVA followed by multiple comparison by the Student-Newman-Keuls method) in membrane conductance from that measured in saline containing 5 mM Na^+ (i.e., zero).

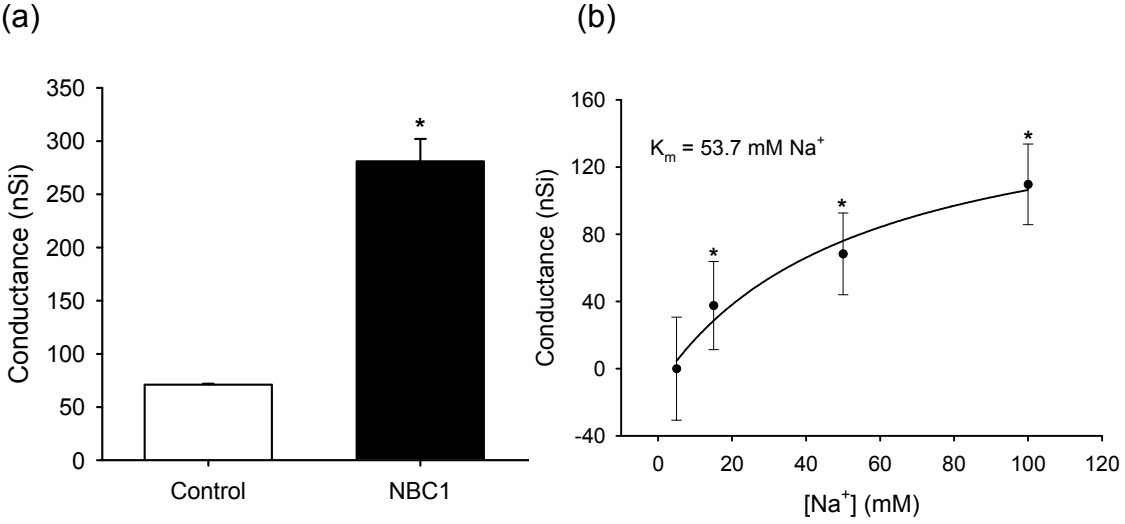

Affinity for Na^+. The tfNBCe1 as expressed in *Xenopus* oocytes is not likely to be limited by Na^+ *in vivo*. Conductance was used as a measure of ion flux across the oocyte membrane, and increased as oocytes were bathed in salines of increasing [Na^+] (Fig. 5.5). When measurements were normalized such that tfNBCe1-injected oocytes exposed to saline containing Na^+ at the reversal concentration of approx. 5 mM had zero conductance, a hyperbolic curve (R = 0.55) was fit to conductance measurements in salines at and above the reversal concentration, with K_m = 53.7 mM Na^+. Measurements of conductance at 0 mM Na^+ are not reported, as conductance during exposure to [Na^+] below the Na^+ reversal concentration of approx. 5 mM may be attributed to Na^+ efflux rather than influx and may thereby interfere with kinetics calculations.

Topology prediction. In order to draw more direct comparisons of the tfNBCe1 to other known NBCe1 proteins with respect to both structure and possible function, topology has been predicted for this protein. The structure of tfNBCe1 was predicted based on the 1,071 amino acid sequence including 12 transmembrane-spanning domains, with N and –COOH terminals predicted to be cytosolic (Fig. 5.6). This structure prediction closely resembles those of other known NBCe1 proteins which is not surprising considering the strong amino acid sequence similarity between vertebrate NBCe1 proteins. A number of putative binding domains have been identified (Fig. 5.6) based on those characterized in other NBCe1 proteins and are discussed below with respect to their possible implications for protein function.

Fig. 5.6. Putative membrane topology of tfNBCe1 (FJ463158) with amino acids color coded based on the scheme of ConPredII (Japan). Putative DIDS and CAII-binding and basolateral targeting motifs are indicated by red, black, and yellow shaded areas, respectively. The 4th extracellular loop (shaded gray) has been suggested to interact with CAIV (Alvarez et al. 2003). Putative transmembrane domains are indicated by vertical rectangles shaded light green

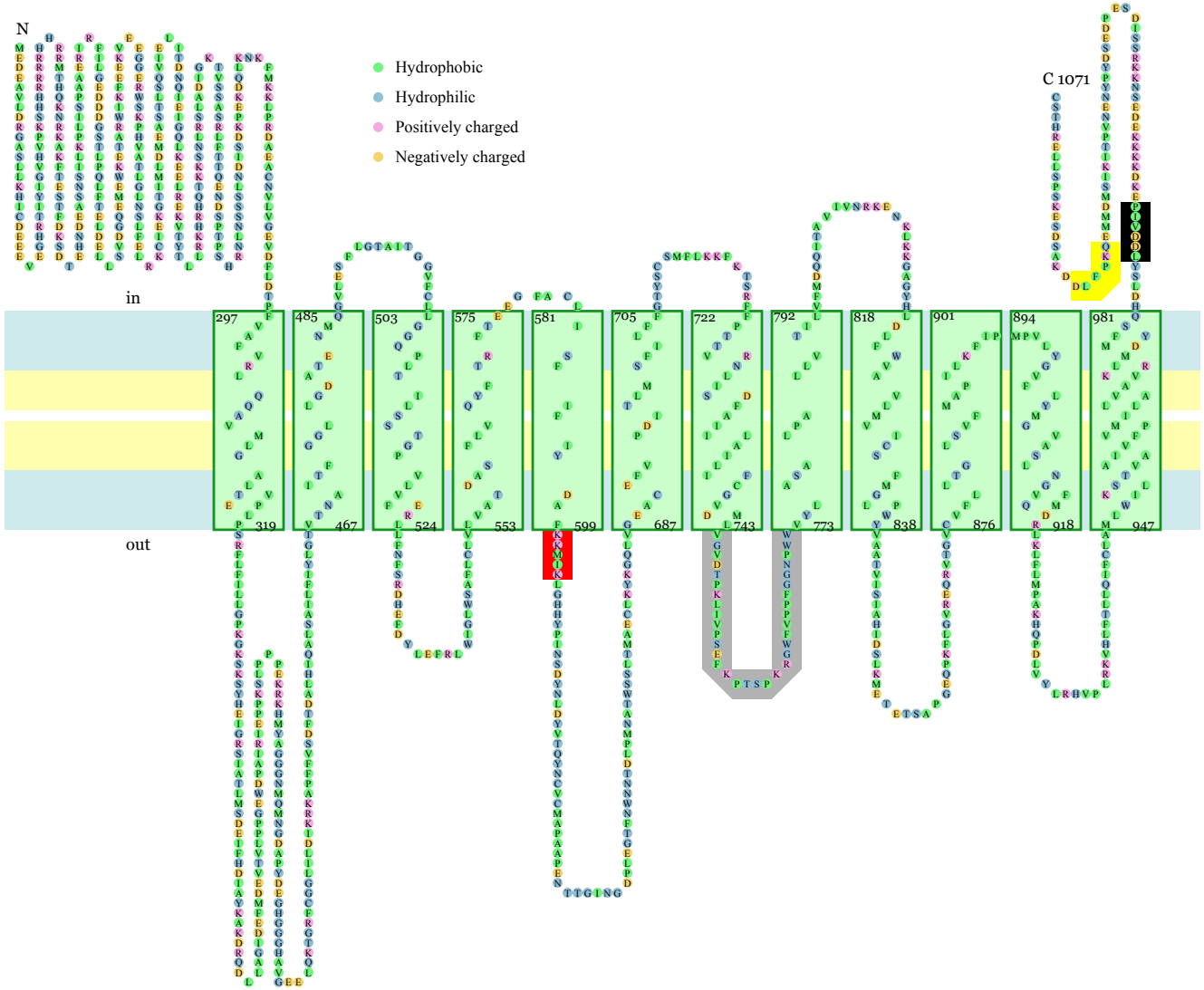

Localization of intestinal tfNBCe1

Basolateral localization of tfNBCe1 in seawater toadfish enterocytes was confirmed by immunohistochemistry (Fig. 5.7). The tfNBCe1shows strong basal presence in addition to lateral staining but is absent from the apical membrane. These results support the identification of a putative basolateral targeting motif in the tfNBCe1 amino acid sequence (Fig. 5.6).

Fig. 5.7. Immune (a) and pre-immune (b) fluorescence staining of tfNBCe1 (green) in the toadfish anterior intestine during control SW-acclimated conditions. Nuclei were stained (blue) with DAPI as detailed in the text. Scale bar = 10 μm.

a.

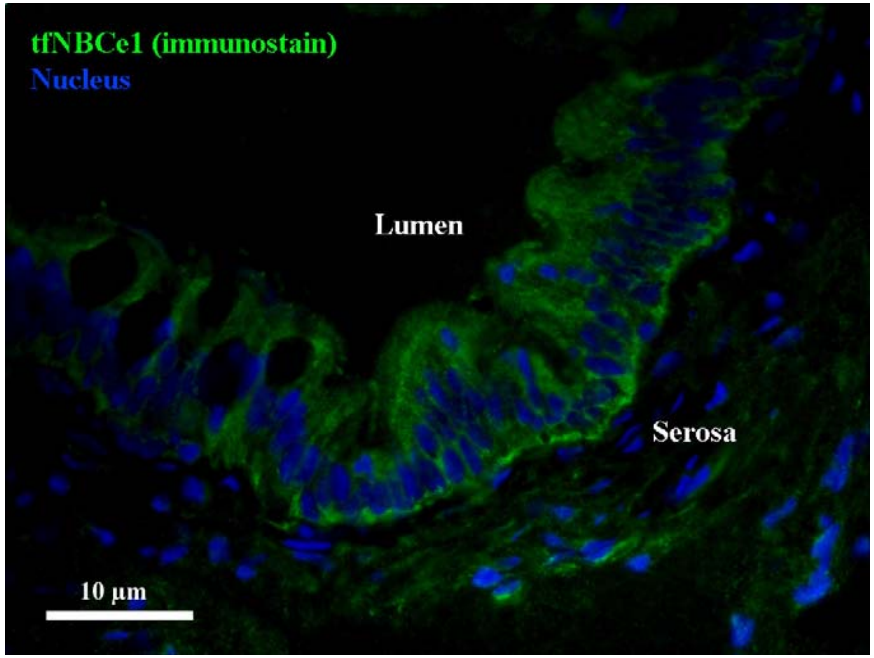

b.

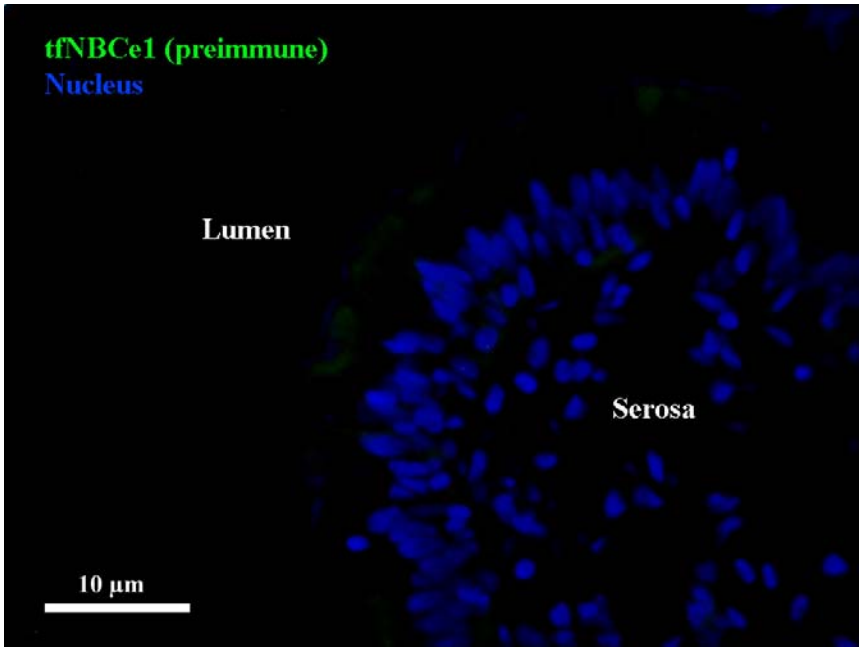

Conclusions

The comparison of isolated toadfish intestine characteristics to those of isolated tfNBCe1 provides strong support for the involvement of NBCe1 in intestinal base secretion for marine osmoregulation. This role is supported by elevated mRNA expression of NBCe1 in the marine toadfish (present study) and the euryhaline pufferfish (Kurita *et al.* 2008) in response to elevated salinity.

Serosal HCO_3^- has been shown to contribute significantly to HCO_3^- secretion by the isolated toadfish intestine under *in vivo*-like conditions of 4-10 mM plasma [HCO_3^-] (Wilson 1999). At plasma [HCO_3^-] of 7 mM, an estimated 48% of HCO_3^- secretion can be accounted for by endogenous CO_2, in agreement with findings by Grosell and Genz (2006) that 56% of isolated toadfish intestine HCO_3^- secretion could be explained by endogenous CO_2 at 5 mM serosal [HCO_3^-]. The high affinity of the basolaterally limited, isolated intestine for serosal HCO_3^- in the physiological range suggests its potential to efficiently fine-tune systemic acid-base balance by transepithelial intestinal HCO_3^- secretion and subsequent excretion in the rectal fluid. In addition to identifying this prospective role of transepithelial intestinal HCO_3^- secretion in plasma HCO_3^- regulation, the findings in toadfish are consistent with data from other species including trout (Grosell *et al.* 2007) and pufferfish (Kurita *et al.* 2008), suggesting that transepithelial HCO_3^- secretion is an important and universal feature of marine fish osmoregulation.

Expression of the Na^+/HCO_3^- cotransporter, tfNBCe1, has been verified along the intestinal tract of seawater toadfish as a means by which this transepithelial HCO_3^- secretion is accomplished. Transiently increased tfNBCe1

expression following acute salinity increase (Fig. 5.3) supports recent findings by Kurita et al. (2008) showing elevated intestinal NBCe1 expression in pufferfish in response to elevated salinity, and underscores the importance of transepithelial HCO_3^- secretion, facilitated by basolateral tfNBCe1, in marine fish osmoregulation. Additionally, the present results indicate that the scope for adjustment of intestinal HCO_3^- secretion rates by shifting serosal HCO_3^- availability is quite large. Despite the high levels of tfNBCe1 in both the anterior and middle intestine under control conditions, salinity challenge reveals a shift towards higher expression of tfNBCe1 in the middle intestinal tissue. The importance of anterior intestinal HCO_3^- secretion to chyme neutralization during digestion and the dominant role for this intestinal segment in salt and water absorption under normal SW conditions (Grosell and Taylor 2007) may be the basis for its more consistent high expression. However, more posterior segments of the intestinal tract appear to have a greater scope for increasing tfNBCe1 expression to maintain homeostasis during further osmoregulatory challenge.

Serosal HCO_3^- availability is altered by a number of physiological disturbances including postprandial metabolic alkalosis commonly referred to as the alkaline tide (Niv and Fraser 2002), during which fish can experience plasma [HCO_3^-] up to approximately 12 mM (Bucking and Wood 2008). At these high levels, serosal HCO_3^- has the potential to contribute nearly 60% to intestinal HCO_3^- secretion, assuming constant metabolic rate of the intestinal tissue. However, postprandial alkaline tide is accompanied by specific dynamic action (SDA) which in fishes accounts for an approximate 136% increase in whole-

animal metabolic rates (Secor 2009). Notably, organ-specific metabolic rate increases can be even more substantial (Secor 2009) and may account for some or all of the elevated intestinal HCO_3^- secretion noted by Taylor and Grosell (2006b) in postprandial toadfish. These postprandial changes in whole-animal, and more specifically, intestinal tissue CO_2 production rates must be quantified for a more accurate assessment of the contribution of serosal HCO_3^- to intestinal HCO_3^- secretion and resulting implications for postprandial acid-base balance regulation. However, secretion of HCO_3^- derived from endogenous CO_2 will also result in an equimolar H^+ extrusion from the cell (Grosell 2006; Grosell and Genz 2006; Grosell 2007; Grosell *et al.* 2007) which should be investigated in more detail to determine its polarity and implications for acid/base balance regulation.

Our isolated intestinal tissue experiments indicate basolateral limitation of intestinal HCO_3^- secretion by an electrogenic mechanism. The dependence of HCO_3^- secretion rate, TEP, and conductance on serosal [HCO_3^-] suggests both basolateral limitation and electrogenicity, while the lack of HCO_3^- secretion stimulation under elevated mucosal [Cl^-] provides additional evidence against apical limitation. A crucial role of the electrogenic tfNBCe1 in intestinal HCO_3^- secretion is supported by transporter characteristics that very closely match the basolaterally limited HCO_3^- -transporting ability of the isolated intestine. The affinity of isolated tfNBCe1 for HCO_3^- is analogous to that of the isolated intestine tissue, with K_m very closely approximating reported plasma [HCO_3^-] under normal (Wilson, 1999) and alkaline tide (Bucking and Wood 2008) circumstances. Meanwhile, the K_m of tfNBCe1 for Na^+ is less than half of normal teleost plasma

[Na^+], suggesting that cotransport is more likely to be limited by serosal HCO_3^- availability under physiological conditions. Also, the seemingly counterintuitive decrease in isolated intestinal tissue HCO_3^- secretion rates under elevated mucosal [Cl^-] supports previous suggestions that NaCl absorption is dominated by NaCl and NKCC cotransport mechanisms under relatively high luminal [NaCl], while Cl^-/HCO_3^- gains importance when luminal substrates are limited to concentrations found *in vivo* (Grosell and Taylor 2007).

A sizeable body of literature pertaining to structure-function relationships within the HCO_3^- transporting protein superfamily (McMurtrie *et al.* 2004; Romero *et al.* 2004; Dorwart *et al.* 2008) has allowed us to make several correlations between the characterization of transepithelial HCO_3^- secretion and structural features predicted for tfNBCe1. First, a basolateral targeting motif with amino acid sequence QQPFLS has been identified in the cytoplasmic tail of mammalian kidney NBC1 (Li *et al.* 2007). Following a series of mutations the authors proposed the FL motif to be essential for the targeting of NBC1 to the basolateral membrane. The cytoplasmic tail of tfNBCe1 contains a similar amino acid motif at positions 1047-1052 (QKPFLD, Fig. 5.6), which notably contains the crucial FL motif and agrees with the immunohistochemical results for basolateral localization of tfNBCe1 (Fig. 5.7). Second, as noted previously, the pharmacological inhibitor DIDS is not specific for NBC, but also inhibits anion exchange. This is due to a homologous positively charged motif with several conserved amino acids between the two protein families, with the sequence KKMIK playing an important role in both reversible and irreversible DIDS

blockade of NBCe1 (Lu and Boron 2007). This DIDS-binding motif is present and unaltered at positions 600-604 at the extracellular end of TM5 in tfNBCe1 (Fig. 5.6), as predicted in human NBCe1 (Lu and Boron 2007), and explains the inhibition of HCO_3^- secretion by the isolated tissue during serosal DIDS application (Table 5.4). Third and finally, the presence of putative carbonic anhydrase (CA) binding domains in tfNBCe1 support the proposal by McMurtrie et al. (2004) for a HCO_3^- transport metabolon comprising apical anion exchange and basolateral NBC, both forming physical associations with intracellular CAII and extracellular CAIV. Interactions with CAIV are thought to occur in the 4th extracellular loop of tfNBCe1 as suggested by Alvarez et al. (2003), and acidic CAII binding domains (Sterling *et al.* 2001) have been identified in the carboxy-terminus. In the case of marine fish intestinal HCO_3^- secretion, the cytoplasmic CAc (equivalent to CAII) isoform is also important in endogenous CO_2 hydration (McMurtrie *et al.* 2004; Grosell *et al.* 2007). Additionally, a mechanism involving CO_2 recirculation has been proposed via apical anion exchange and subsequent dehydration of luminal HCO_3^- by protons supplied by apical H^+-ATPase and/or NHE and facilitated by extracellular, apically bound CAIV (Grosell *et al.* 2007). A similar model by which serosal CO_2 is pulled to basolateral NBC1, hydrated to HCO_3^- by extracellularly bound CAIV and "drawn" through the cotransporter by intracellularly-bound CAII dehydration has been proposed by Alvarez et al. (2003). Together these proposed putative metabolon systems are likely to explain the noteworthy efficiency of marine fish transepithelial HCO_3^- secretion including the high affinity of both the isolated tissue and isolated tfNBCe1 for

serosal HCO_3^-. Modulation of the NBC1/CAII interaction has been suggested as a mode of NBC1 regulation (Gross *et al.* 2002), although this idea has been disputed by several recent studies (Lu *et al.* 2006; Piermarini *et al.* 2007). Given the efficiency of transepithelial HCO_3^- transport in the marine fish intestine, it is suggested that this model may be ideally suited for further evaluation of physical and functional interactions within the proposed metabolons.

Using a suite of complementary methods, evidence has been presented suggesting basolateral tfNBCe1 is a rate-limiting component of intestinal HCO_3^- secretion in SW-acclimated gulf toadfish with the potential to fine-tune plasma [HCO_3^-]. The affinities of the isolated tfNBCe1 and the basolaterally limited epithelium for HCO_3^- are high and similar. The amino acid sequence of tfNBCe1 contains motifs specific for basolateral targeting and DIDS binding which is in agreement with the observations of basolateral localization and DIDS sensitivity in intact tissue. These structure-function relationships combined with the high HCO_3^- secretion rates of marine teleost intestinal epithelia potentially arising from physical associations of tfNBCe1 with intracellular CAII and extracellular CAIV remain a fruitful model for study of tubular secretion of HCO_3^- in vertebrates. While assertions that tfNBCe1 comprises a significant route of base excretion during the postprandial period must be reserved to allow for quantification of intestinal tissue specific dynamic action, the transport characteristics of tfNBCe1 provided some support for this idea. The efficiency of tfNBCe1 in transepithelial intestinal HCO_3^- secretion most likely has implications for plasma HCO_3^- regulation, which require further investigation.

Acknowledgments

E.M. Mager and M. Grosell contributed to this work and are listed as co-authors on the peer-reviewed publication based on this dissertation chapter. Also, Jimbo's and Ray Hurley and Debbie Fretz, Miami, FL, USA, for supplying toadfish; Dr. Gerhard Dahl and his group at the University of Miami Miller Medical School, Miami, FL, USA, for providing *Xenopus* oocytes, expression vector, electrophysiological equipment and expertise; and Drs. S. Hirose, M.D. McDonald, M. Schmale, and J.M. Wilson for providing immunohistochemistry materials and guidance. The present study was supported by an NSF award (IOB 0718460) to M. Grosell.

Chapter 6:

The intestinal response to feeding in seawater gulf toadfish, *Opsanus beta*, includes elevated base secretion and increased oxygen consumption

Summary

Intestinal HCO_3^- secretion is essential to the osmoregulatory strategy of marine teleost fish and comprises a considerable source of base efflux attributable to both serosal HCO_3^- and endogenous CO_2 hydration. The role of intestinal HCO_3^- secretion in dynamic regulation of acid-base balance appears negligible in studies of unfed fish, but recent evidence of high intestinal fluid [HCO_3^-] in fed marine teleosts led us to investigate the source of this HCO_3^- and its potential role in offsetting the postprandial "alkaline tide" commonly associated with digestion. Elevated metabolic rate and thus endogenous CO_2 production by the intestinal tissue as well as increased transepithelial intestinal HCO_3^- secretion may both occur post feeding to offset a postprandial alkaline tide. To test these hypotheses, postprandial changes in HCO_3^- secretion and O_2 consumption by the gulf toadfish (*Opsanus beta*) isolated intestine were quantified at 0, 3, 6, 12, 24 and 48 h after feeding. The intestinal tissue in general showed high rates of both HCO_3^- secretion (15.5 μmol g^{-1} h^{-1}) and O_2 consumption (8.9 μmol g^{-1} h^{-1}). Furthermore, significant postprandial increases in both intestinal HCO_3^- secretion and O_2 consumption (1.6 and 1.9-fold peak increases, respectively) were observed. Elevated intestinal HCO_3^- secretion rates preceded and also outlasted those of O_2 consumption, and occurred at a magnitude and duration sufficient to offset an alkaline tide. Dependence of these high rates of postprandial intestinal

base secretion on serosal HCO_3^- indicates that transepithelial HCO_3^- transport increases disproportionately more than endogenous CO_2 production. Significantly elevated postprandial intestinal HCO_3^- secretion is of such magnitude that the intestine certainly is capable of postprandial regulation of acid-base balance.

Background

Intestinal HCO_3^- secretion has become widely recognized as an essential component of marine fish osmoregulation (Wilson *et al.* 2002; Grosell *et al.* 2005; Grosell 2007; Grosell *et al.* 2009b), and the excretion of resulting carbonates occurs at rates high enough to impact the inorganic oceanic carbon cycle (Wilson *et al.* 2009). Studies have shown intestinal base excretion to be countered by branchial acid efflux in unfed marine teleost fish (Wilson *et al.* 1996; Wilson and Grosell 2003; Genz *et al.* 2008), suggesting it is unlikely to play a role in dynamic regulation of acid-base balance. However, the possibility that intestinal HCO_3^- secretion plays a role in dynamic regulation of acid-base balance during digestion has been a topic of recent interest (Taylor and Grosell 2006b; Taylor *et al.* 2007; Wood *et al.* 2007b; Bucking and Wood 2008; Cooper and Wilson 2008). Stomach acidification in fish proceeds via a mechanism of HCl secretion parallel to that of mammals, resulting in an equimolar secretion of base, as HCO_3^-, to the systemic circulation by the gastric parietal cells (Hersey and Sachs 1995; Niv and Fraser 2002). The ensuing metabolic alkalosis is commonly referred to as “alkaline tide” and ranges from a modest response in most mammals (Rune

1965), to a more extreme alkalosis of 0.3 pH units with a 2.5-fold increase in plasma [HCO_3^-], lasting upwards of 6 days after meal consumption in opportunistically feeding reptiles (Secor and Diamond 1995; Wang *et al.* 2001). The occurrence of alkaline tide in fish has received increasing attention in recent years, but has thus far been ascertained in only a handful of fish species including a freshwater teleost (Bucking and Wood 2008; Cooper and Wilson 2008), and a marine elasmobranch (Wood *et al.* 2005; Wood *et al.* 2007a). These studies show increases in pH (0.15 to 0.25 units) with approx. 1.5-fold increases in plasma [HCO_3^-] between 3 to 9 hours after feeding (Wood *et al.* 2005; Bucking and Wood 2008; Cooper and Wilson 2008), with no evidence of the respiratory compensation often observed in the postprandial metabolic response in air-breathing animals (Wang *et al.* 2001; Andrade *et al.* 2004). Conversely, investigations of the postprandial metabolic response in seawater teleosts including gulf toadfish, *Opsanus beta* (Taylor and Grosell 2006b), and European flounder, *Platichthys flesus* (Taylor *et al.* 2007), have shown no evidence of either alkaline tide or respiratory compensation, and indicate that increases in base excretion are insufficient to compensate for the systemic base gain resulting from gastric acid secretion (Taylor *et al.* 2007). Furthermore, the composition of postprandial intestinal fluids in gulf toadfish (Taylor and Grosell 2006b) indicates a substantial increase in anion exchange during digestion, and led us to examine the intestine more closely as a potential site of dynamic postprandial acid-base balance regulation.

Intestinal anion exchange in marine teleosts occurs at the apical membrane and draws from both serosal HCO_3^- and endogenous CO_2, the latter undergoing hydration facilitated by carbonic anhydrase (CA), yielding HCO_3^- and H^+ (Wilson *et al.* 2002; Grosell 2006). As HCO_3^- arising from the CO_2 hydration reaction is exchanged across the apical membrane for Cl^-, equimolar extrusion of H^+ maintains cellular acid-base balance and has been shown to occur via several mechanisms in marine teleosts (Wilson *et al.* 2002; Grosell 2007; Grosell *et al.* 2009a). An additional source stems from serosal HCO_3^- taken up across the basolateral membrane via Na^+/HCO_3^- cotransport (NBC), driven by the electrochemical gradient for Na^+ created by basolateral Na^+/K^+-ATPase (NKA). Basolateral NBC has recently been characterized in seawater teleosts (Kurita *et al.* 2008) including toadfish (Taylor *et al.* 2009) and provides a route of transepithelial HCO_3^- secretion ideally suited for dynamic regulation of systemic acid-base balance. While the serosal source of HCO_3^- for intestinal HCO_3^- secretion by marine teleosts has direct implications for alkaline tide compensation, endogenous CO_2 production is also likely affected by feeding. Any changes in endogenous CO_2 production may result in proportional changes in basolateral H^+ extrusion to the serosa. In addition to alkaline tide, the postprandial metabolic response includes a well-characterized increase in metabolic rate referred to as specific dynamic action (SDA) (Jobling 1981; Mccue 2006; Secor 2009). SDA has been shown to comprise an average maximum metabolic rate increase of 25% in humans, with a duration of 4 to 6 h after feeding (Secor 2009). Animals with more opportunistic feeding strategies, such

as snakes, have been shown to experience postprandial metabolic rate increases lasting 6 d following feeding, with an average maximum increase of 687% (Secor 2009). The SDA response of most fishes falls between the modest response seen in humans and the extreme response of snakes to feeding. Postprandial maximum metabolic rate increases average 136% in fish, with elevated metabolic rates persisting 20 h after feeding (Jobling 1981; Secor 2009). The variability associated with feeding lends an exceptional complexity to these investigations; the SDA response in all animals is dependent on a suite of variables including meal mass and composition, body temperature, and body size (Jobling 1981; Mccue 2006; Secor 2009). One consequence of this variability both within and between species is that SDA has been well-characterized in a variety of animals, but the exact source of the metabolic rate increase associated with feeding are difficult to discern and remain relatively speculative.

In mammals, the gastrointestinal (GI) tract is a site of high O_2 uptake that amounts to 20-25% of the whole-body O_2 consumption, even in the post-absorptive or fasting state (Britton and Krehbiel 1993; Duee *et al.* 1995). This energy consumption is disproportionate for the size of the tissue (about 6% of body weight). Accordingly, the coupling of active transport to oxidative metabolism in epithelial tissues (Zerahn 1956; Mandel and Balaban 1981) suggests that the GI tract likely elicits an even greater SDA response, relative to its mass, than that of the whole animal, although investigations of postprandial oxygen consumption by isolated intestinal epithelia are scant. The importance of

the marine fish intestine in osmoregulation suggests the baseline (i.e. fasting) oxygen demand by this organ may be higher than that in other animals. The intestinal tissue oxygen demand is a particular point of interest due to the reliance of intestinal HCO_3^- secretion on endogenous CO_2 production.

The objectives of the present study are to quantify the postprandial changes in HCO_3^- secretion and oxygen consumption by the toadfish intestine. Monitoring these parameters in a parallel postprandial time course will enable more clear deduction of the source of high postprandial intestinal fluid [HCO_3^-] and thereby its possible contribution to dynamic regulation of acid-base balance.

Materials and Methods

Gulf toadfish (*Opsanus beta*), were obtained by trawl from Biscayne Bay as by-catch by shrimp fishermen local to Miami, FL, USA, during January and February 2008. Within hours of capture fish were transported to the wetlab facility at the Rosenstiel School of Marine and Atmospheric Science at the University of Miami, FL, US and subjected to an ecto-parasite treatment (McDonald *et al.* 2003). Prior to experimentation, fish were maintained in the laboratory for a minimum of two weeks in aquaria with a constant flow of filtered, aerated seawater (32±1‰) at 21±2ºC from Bear Cut, FL, US. These aquaria were equipped with PVC shelters to reduce stress and aggression among fish. Toadfish were fed chopped whole squid, *Loligo sp.*, to satiation twice weekly until 72 h prior to experimentation, after which time food was withheld to ensure complete clearing of the gastro-intestinal tract.

A natural feeding protocol was employed in which each 80 L tank of <10 toadfish (ranging from 15-30g unless otherwise noted) was presented chopped squid and allowed to feed to satiation for one hour before excess food was vigilantly removed from the tank. For all isolated tissue work described below toadfish intestinal tissue was collected before feeding and 3, 6, 12, 24, and 48 h after feeding as follows. Toadfish displaying gastric distention were selected for all postprandial timepoints, and all fish were euthanized by a lethal dose (5 g/L) of Tricaine methanesulfonate (MS-222) after which the spine was severed. Anterior intestinal tissue was excised from just posterior to the bile duct, cut open lengthwise, and mounted on the appropriate tissue holder for pH-stat and O_2 consumption measurements as described below. Stomach contents were recovered from fish sampled at 3, 6, 12 and 24h postprandially and used to estimate meal size with respect to body mass. All experimental procedures have been approved by the University of Miami Animal Care and Use Committee under protocol 08-017.

Quantification of gastro-intestinal tract contribution to whole animal mass

To more accurately quantify the contribution of intestinal tissue HCO_3^- secretion and O_2 consumption to whole animal acid-base balance and metabolism, percentage body mass accounted for by this base secreting, likely metabolically demanding tissue was determined under starved and postprandial conditions. Toadfish (mass = 46.7 ± 1.6 g) were sampled before feeding (n = 12), at which time these and all remaining experimental animals were weighed to

obtain pre-feeding mass. Postprandial sampling was done 3 days (n = 18) and 6 days (n = 6) after feeding. Fish were euthanized as described above, mass recorded, and the entire gastro-intestinal tract excised. The gastro-intestinal tract was separated into stomach and intestinal (including rectal) tissue at the pyloric sphincter. Wet mass of each tissue was measured in pre-weighed plastic weigh trays, and tissues were desiccated overnight to constant weight at 50°C. Dry mass was then recorded and compared to wet mass to estimate tissue water content in control and postprandial fish.

Isolated intestine HCO_3^- secretion and electrophysiology

To simultaneously investigate electrophysiological parameters and HCO_3^- secretion rates of isolated intestinal epithelia, Ussing chambers (Physiological Instruments, San Diego, CA, USA) were set up in combination with an automated pH-stat titration system (model TIM 854 or 856, Radiometer) as described previously (Grosell and Genz 2006). A segment of the anterior intestine was excised as described above and mounted onto a tissue holder (model P2413, Physiological Instruments) exposing 0.71 cm^2 of the isolated tissue and positioned between two half-chambers (model P2400; Physiological Instruments) containing 1.6 ml of the appropriate, pre-gassed, mucosal or serosal saline (Table 6.1). The saline in each half-chamber was continually mixed by airlift gassing with either O_2 or 0.3% CO_2 in O_2 (Table 6.1), and a constant temperature of 25ºC was maintained by a thermostatic water bath. Current and voltage electrodes connected to amplifiers (model VCC600; Physiological Instruments)

recorded the transepithelial potential (TEP) differences under current-clamp conditions at 0 μA, with 3-sec, 50 μA pulses from the mucosal to the serosal side at 60-sec intervals. These current-clamped conditions were maintained across all treatments. TEP measurements were logged on a personal computer using BIOPAC systems interface hardware and Acqknowledge software (version 3.8.1). TEP values are reported with a luminal reference of 0 mV. A pH electrode (model PHC4000.8, Radiometer) and microburette tip were submersed in the luminal half-chamber and were connected to the automated pH-stat titration system which was grounded to the amplifier to allow for pH readings during current pulsing. The pH-stat titrations were performed on luminal salines at a physiological pH of 7.800 throughout all experiments (creating symmetrical pH conditions on either side of the epithelium), with pH values and rate of acid titrant (0.005 N HCl) addition logged to a PC using Titramaster software (version 5.1). Titratable alkalinity, representing HCO_3^- secretion (Grosell and Genz 2006), was calculated from the rate of titrant addition and its concentration. Intestinal preparations from gulf toadfish are viable and stable for at least 5 hours under these experimental conditions (Grosell and Genz 2006). The titration curves and electrophysiological measurements of each preparation were allowed to stabilize 60 min after introduction to the chamber before HCO_3^- secretion rates and electrophysiological parameters were averaged and reported for the following 60 min of exposure.

Table 6.1. Composition of serosal and mucosal salines used in isolated intestinal tissue experiments

	Serosal		Mucosal
	0 mM HCO_3^-	10 mM HCO_3^-	
NaCl, mM	151	151	69
KCl, mM	3	3	5
$MgCl_2$, mM			22.5
$MgSO_4$, mM	0.88	0.88	77.5
Na_2HPO_4, mM	0.5	0.5	
KH_2PO_4, mM	0.5	0.5	
$CaCl_2$, mM	1	1	5
$NaHCO_3$, mM	0	10	
HEPES			
Free acid, mM	11	11	
Sodium salt, mM	11	11	
Urea, mM	4.5	4.5	
Glucose, mM	5	5	
Osmolality, mosmol l^{-1}	320*	320	320*
pH	7.800‡	7.800‡	7.800†
Gas	O_2	0.3% CO_2 in O_2	O_2

* Adjusted with mannitol to ensure transepithelial isosmotic conditions in all experiments
‡ pH adjusted to 7.800 by NaOH addition
† pH 7.800 was maintained by pH-stat titration

Postprandial HCO_3^- secretion and electrophysiology

The combined pH-stat titration/ electrophysiology approach described above was employed to quantify changes in HCO_3^- secretion rates and electrophysiology of the isolated intestine after feeding. For these experiments, tissue measurements were made from fish sampled in the postprandial time course (n = 8 at each time point) described above.

Dependence on serosal HCO_3^-

To quantify any changes in the contribution of endogenous CO_2 to intestinal HCO_3^- secretion under fed vs. control conditions, additional experiments were completed in unfed and 3h postprandial fish (n = 6). For each fish, whether control or fed, the intestine was dissected out as described above, and then split lengthwise into two halves which were mounted onto tissue holders (model P2404) exposing 0.25 cm^2 tissue to the chamber. The two tissue preparations taken from the same length of intestine were run simultaneously in two parallel systems. One of the preparations was exposed to HCO_3^--free serosal saline for 120 min (60 min stabilizing period and 60 min measurement period, as described above), while the other was exposed to serosal saline containing 10mM HCO_3^- (Table 6.1). These parallel measurements of HCO_3^- secretion in presence of serosal HCO_3^- and under HCO_3^--free conditions by epithelia taken from the same animal and same length of intestine allowed us to calculate the contribution of endogenous vs. serosal substrate to HCO_3^- secretion before and after feeding.

O_2 consumption by isolated intestinal tissue

Newly designed, custom made glass Ussing chambers (Loligo Systems, Denmark, model CH10500) were used to measure O_2 consumption (reported in µmol per hour relative to intestinal tissue surface area and/or mass) by the isolated toadfish anterior intestine, while simultaneously monitoring tissue electrophysiological parameters to ensure tissue viability. Glass-teflon connected

current and voltage electrode ports allowed for electrophysiology measurements to be collected by a hardware and software combination identical to that used during pH-stat measurements (described above). These glass Ussing chambers are designed to have a small volume (2.95 ml in each half-chamber) to epithelia surface area (0.87 cm^2) ratio, and the salines contained therein (Table 6.2) were continually mixed via micro magnetic stirrers rather than airlift gassing. Teflon tissue holders ensure gas-tight connection between the epithelium and glass chambers. Oxygen measurements were made using a fiber-optic oxygen sensor connected to Fibox 3 single-channel oxygen meters (Loligo), with data recorded by OxyView software allowing for parallel measurement of O_2 consumption in each (mucosal and serosal) half-chamber. The fiber-optic light source is secured on the outside of the glass chambers while O_2 sensors are glued to the inside of the chamber, reflecting light through the glass chamber wall. This approach minimizes the number of ports and thereby the source of error as compared to measurements made using traditional O_2 electrodes. Calibration of O_2 sensors was done daily by gassing mucosal and serosal salines (Table 6.1) with N_2 for their respective zero, and gassing with air for calibration to 100% air. In all experiments, O_2 consumption measurements are performed using intermittent-flow respirometry with flushing controlled manually using a gravity-fed saline replacement system. Initial experiments using this novel system quantified O_2 consumption during exposure of control epithelia sequentially to (1) mucosal salines at 100% air saturation and serosal salines at 0% air (gassed with N_2), and (2) mucosal salines at 0% air saturation and serosal salines at 100% air.

These experiments served to quantify any unidirectional or bidirectional diffusion of O_2 across the isolated toadfish intestine.

Intestinal tissue substrate utilization.

To determine the most appropriate saline composition for subsequent experiments (i.e. to ensure tissue O_2 consumption is not limited by substrate availability), a series of experiments was undertaken using varying combinations of mucosal and HCO_3^--free serosal salines (Table 6.1). While salines used in isolated teleost intestine experiments typically include approx. 5mM glucose in the serosal saline (Grosell *et al.* 2005; Grosell and Genz 2006; Grosell *et al.* 2009a), literature on substrate utilization in isolated mammalian intestinal epithelia (Duee *et al.* 1995) led us to investigate the effects of adding 5mM glutamate to the "standard" (Table 6.1) HCO_3^--free serosal saline and also the addition of these two substrates to the "standard" (Table 6.1) mucosal saline. Furthermore, the impact of a mucosal saline containing a more complete mixture of amino acids, intended to more closely mimic the composition of chyme, was investigated on control (unfed) tissue using L-15 media (Sigma). The O_2 consumption was quantified for isolated toadfish intestine exposed to the following four saline combinations: (1) mucosal + serosal (with glucose), (2) mucosal + serosal (with glucose and glutamate), and (3) mucosal (with glucose and glutamate) + serosal (with glucose and glutamate), applied sequentially in randomized order to single preparations (n = 8), and (4) mucosal (L-15) + serosal (with glucose), applied to separate preparations (n = 5). Oxygen depletion from

mucosal and serosal salines was measured in parallel and O_2 consumption was quantified between 90-95% air saturation in each half-chamber. These measurements from mucosal and serosal half-chambers were combined to give O_2 consumption of the isolated tissue.

Constancy of O_2 consumption.

To investigate the influence of PO_2 on O_2 consumption by isolated toadfish anterior intestine, a series of experiments was completed on tissue from starved toadfish (n = 8) in which oxygen tension was allowed to drop 50% from air saturation as a consequence of tissue O_2 consumption. Standard mucosal and HCO_3^--free serosal (with 5 mM glucose) salines (Table 6.1) were used in these experiments. O_2 consumption was calculated in parallel for mucosal and serosal half-chambers for every 5% drop in O_2 from air saturation and combined to give total tissue O_2 consumption.

Specific dynamic action (SDA).

The presence and magnitude of specific dynamic action by the isolated toadfish intestine was investigated by measuring O_2 consumption of tissues sampled in a time course following feeding as described above. Eight fish were sampled at each time point, with mean tissue O_2 consumption analyzed as an indicator of tissue metabolic rate. Standard mucosal and HCO_3^--free serosal (with 5 mM glucose) salines (Table 6.1) were used in these experiments. Furthermore, mucosal L-15 media (Sigma) was also applied to postprandial epithelia to

investigate the effects of a saline more closely resembling chyme. Standard serosal saline (Table 6.1) was used during mucosal L-15 treatment. In all control and postprandial intestinal preparations, O_2 consumption was calculated in parallel for mucosal and serosal half-chambers during 90-95% air saturation and combined to give total tissue O_2 consumption.

Statistics

Data are presented as mean ± SEM. Statistical comparisons were made using one-way ANOVA followed by the Student-Newman-Keuls test for multiple comparisons as appropriate. Paired t-tests were used to determine dependence of HCO_3^- secretion and electrophysiology on serosal HCO_3^- within each group (control vs. fed). Statistical significance was determined at $P < 0.05$ in all cases.

Results

Meal size in naturally feeding toadfish

Stomach contents were recovered from 3, 6, 12 and 24 h postprandial toadfish at 9.1 (± 0.7), 7.8 (± 1.0), 6.3 (± 0.9) and 5.2 (± 1.3) % body mass, respectively (Fig. 6.1). Reciprocal transformation (Jobling 1981) of these data yielded the best-fitting curve ($R = 0.55$), indicating non-linear rates of gastric emptying. The y-intercept of the linear equation fitted to these data indicates 9.5% body mass to be the maximal meal size, suggesting relatively little gastric emptying occurs in the first 3h after feeding.

Fig. 6.1. A time course of stomach contents relative to body mass allowed for estimation of meal size and gastric emptying time as described in the text. Data are best fitted (R = 0.55) to the equation 1/y = 0.0065x+0.1056. Stomach contents were collected 3 h (n = 21), 6 h (n = 8), 12 h (n = 8) and 24 h (n = 7) postprandially and are displayed as mean ± SEM, with asterisks indicative of statistically significant decline from 3 h values.

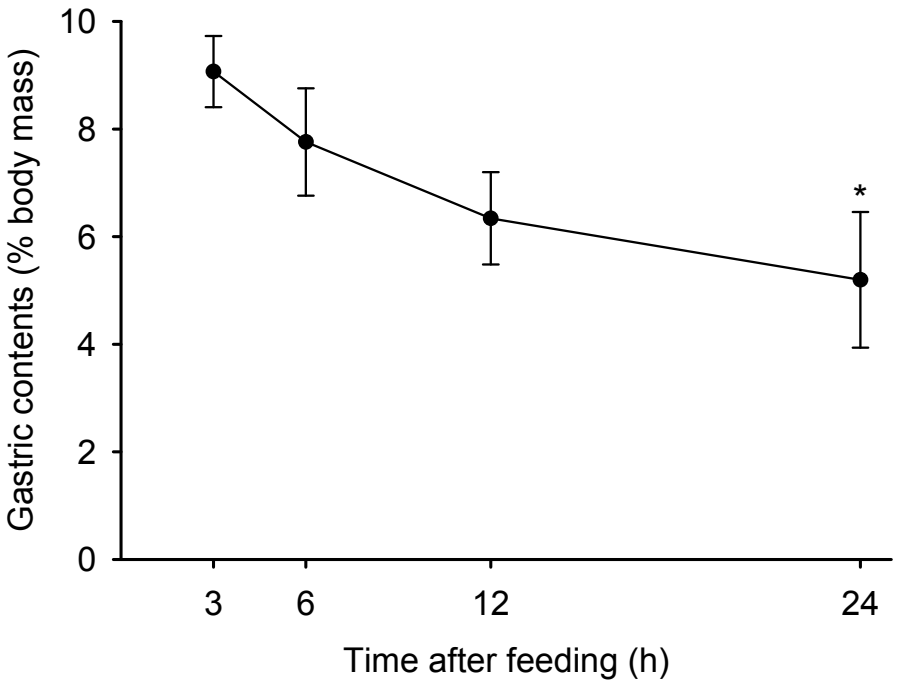

Fig. 6.2. (a) The contribution of the gastrointestinal (GI) tract to body mass was quantified under control (n = 12), 3 d (n = 18) and 6 d (n = 6) postprandial toadfish. Stomach and intestinal tissue samples were analyzed for wet vs. dry weight in order to estimate changes in (b) organ water content resulting from feeding. Data are displayed as mean ± SEM.

a.

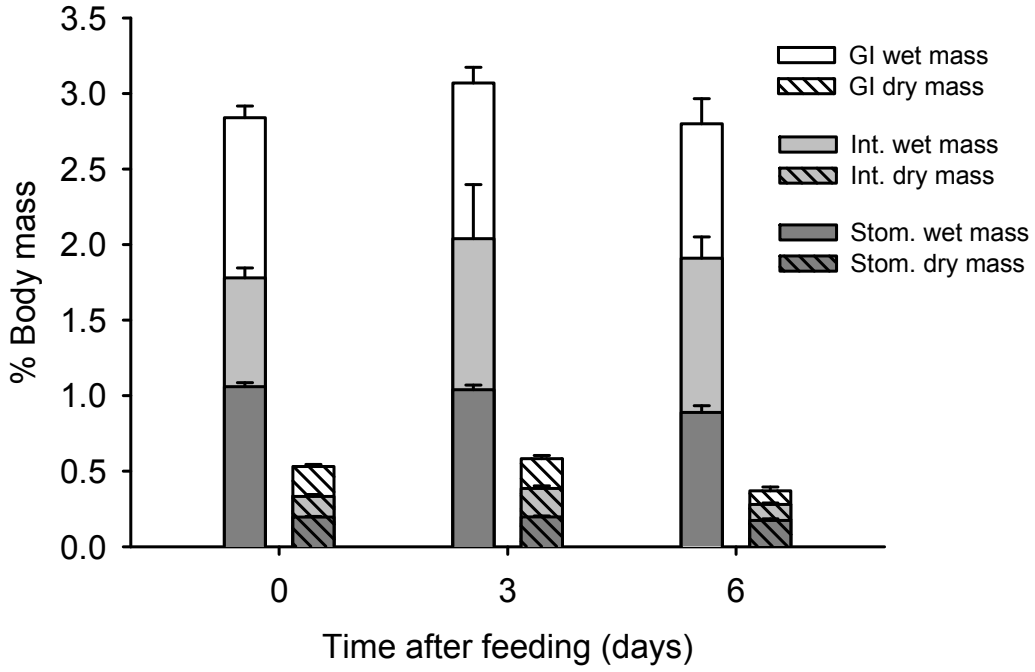

b.

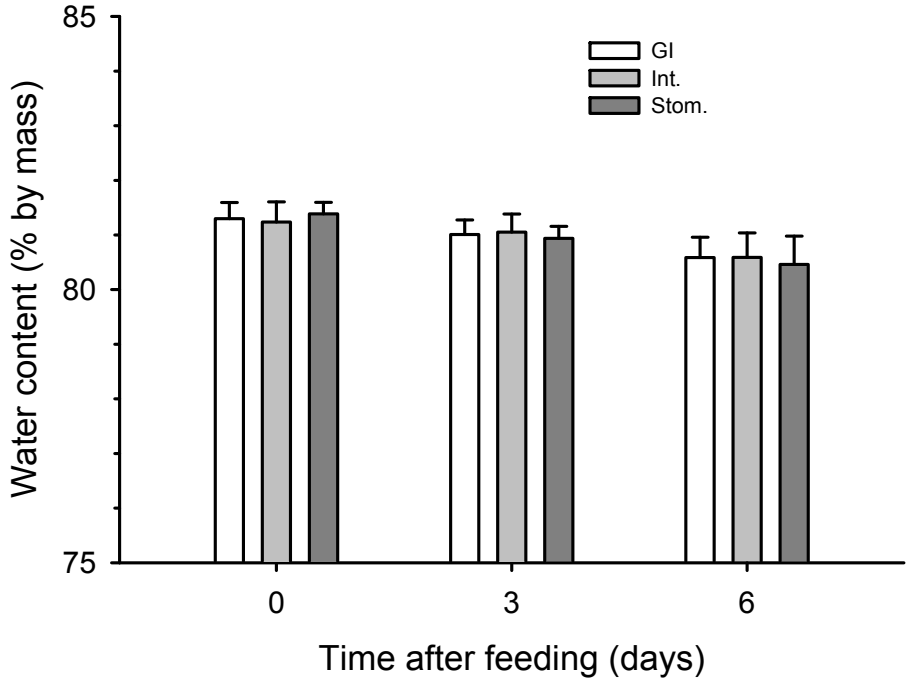

Quantification of gastro-intestinal tract contribution to whole animal mass

The gastro-intestinal tract of starved toadfish was found to contribute 2.84 ± 0.08% of body mass, with 81.3% water content (Fig. 6.2). The intestinal tissue was responsible for 64.0% of gastro-intestinal tract mass, and was 81.5% water by weight. Feeding gave no statistically significant changes to gastro-intestinal mass (Fig. 6.2), but a trend of increased wet and dry gastro-intestinal mass 3 d postprandial appears to be attributable to increases in intestinal, rather than stomach, mass. Indeed, the intestinal contribution to body mass was elevated 14.6% at this time, an increase that cannot be accounted for by its water content which was 81.1 ± 0.33% (Fig. 6.2).

Isolated intestine HCO_3^- secretion and electrophysiology

Postprandial HCO_3^- secretion and electrophysiology

Isolated toadfish intestine exhibits a significant postprandial increase in HCO_3^- secretion that persists 48 h after feeding, with an apparent peak at 3h (Fig. 6.3). Corresponding electrophysiological data (Fig. 6.3) show no statistically significant changes in either TEP or epithelial conductance at any point after feeding.

Fig. 6.3. Postprandial (a) HCO_3^- secretion, (b) TEP, and (c) conductance by isolated toadfish intestine. n = 8 for each time point, with statistically significant differences from control (0 h) indicated by asterisks. Data are displayed as mean ± SEM.

a.

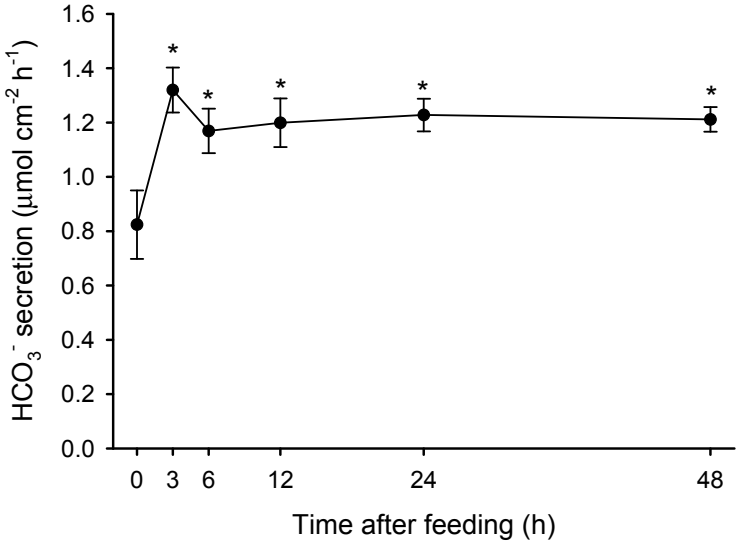

b.

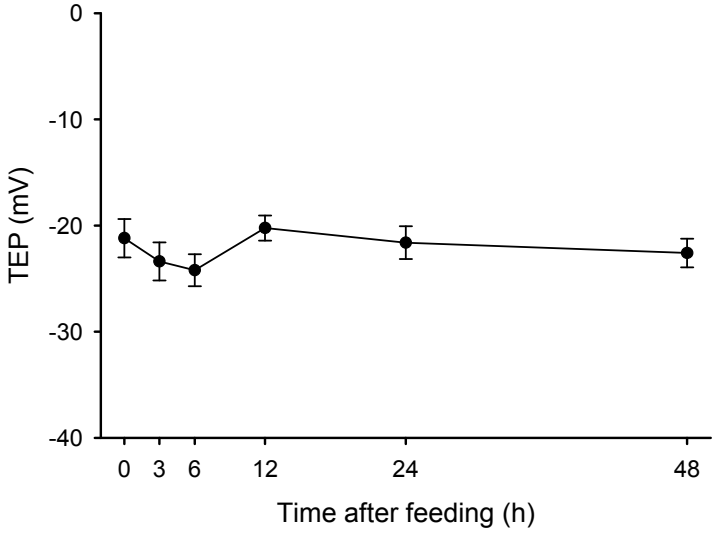

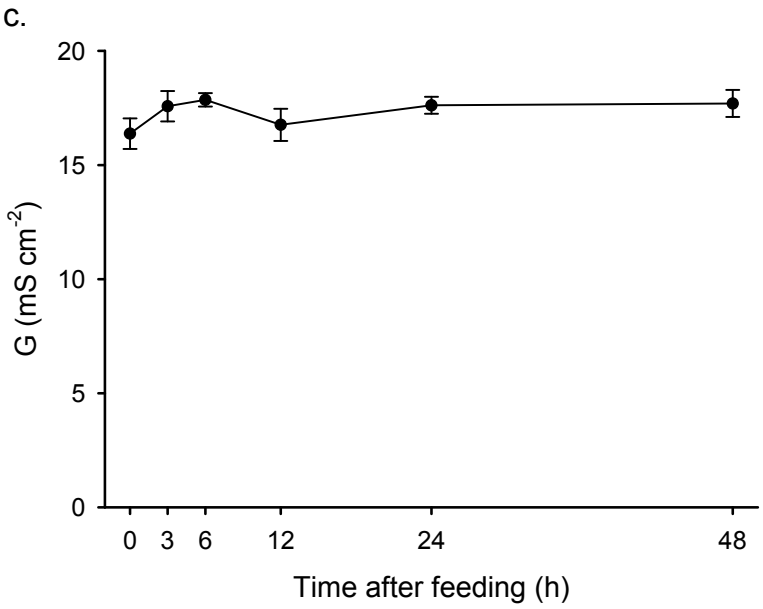

Dependence on serosal HCO_3^-

Bicarbonate secretion by the isolated toadfish intestine shows a strong dependence on serosal HCO_3^- availability, with the contribution of serosal HCO_3^- increasing following feeding (Fig. 6.4). Total postprandial HCO_3^- secretion rates were 39% greater than control rates (Fig. 6.4); however, the fraction attributable to serosal HCO_3^- was 49% higher in postprandial epithelia than unfed controls. Under HCO_3^--free conditions, rates of HCO_3^- secretion were not significantly different between control and postprandial intestinal epithelia (Fig. 6.4). While electrophysiological parameters showed no statistically significant dependence on serosal HCO_3^-, a trend was noted towards increased epithelial conductance in the presence of serosal HCO_3^- in 3 h postprandial epithelia, but not in control preparations (Table 6.2).

Fig. 6.4. Dependence of HCO_3^- secretion rates on serosal HCO_3^- in control and 3 h postprandial isolated epithelia. n = 6 for each set (control vs. 3 h postprandial) of paired (HCO_3^--free vs. 10mM serosal HCO_3^-) measurements, with statistically significant differences indicated by upper and lower case letters. Data are displayed as mean ± SEM.

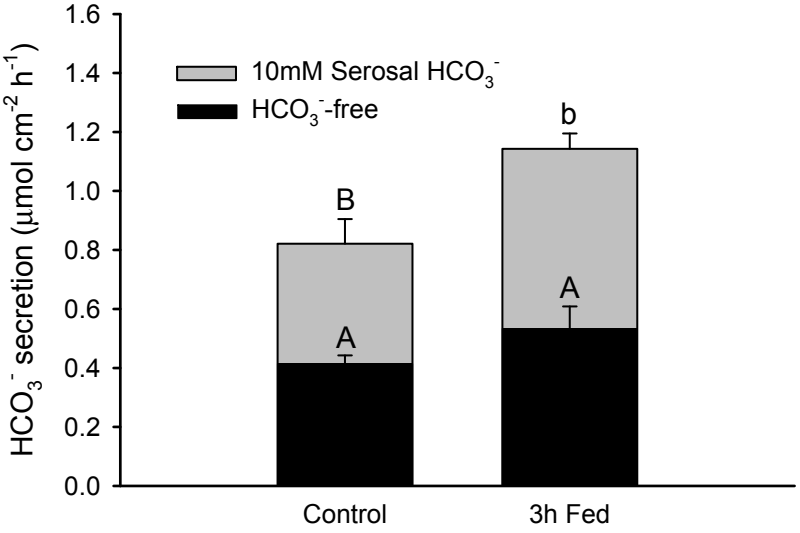

Table 6.2. Dependence of HCO_3^- secretion rates, TEP, and conductance (G) on serosal HCO_3^- in control and 3 h postprandial isolated epithelia. n = 6 for each set (control vs. 3h postprandial) of paired (HCO_3^--free vs. 10 mM serosal HCO_3^-) measurements, with statistically significant differences indicated by upper and lower case letters. Data are displayed as mean ± SEM.

	HCO_3^- secretion ($\mu mol\ cm^{-2}\ h^{-1}$)	TEP (mV)	G ($mS\ cm^{-2}$)
Control			
HCO_3^- -free	0.41 ± 0.03^A	-18.93 ± 2.42	17.28 ± 0.99
10 mM serosal HCO_3	0.82 ± 0.08^B	-16.17 ± 3.87	16.14 ± 1.10
3h Postprandial			
HCO_3^- -free	0.53 ± 0.08^A	-16.39 ± 1.16	16.66 ± 1.58
10 mM serosal HCO_3^-	1.14 ± 0.05^b	-19.84 ± 2.42	19.01 ± 0.35

O_2 consumption by isolated intestinal tissue

Initial experiments (n = 3) using this newly designed Ussing chamber tissue respirometer showed a significant decrease in total tissue O_2 consumption

when one half-chamber was deprived of O_2. During exposure to 0% air saturation, the mucosal and serosal salines had very minimal rates of O_2 appearance (0.031 ± 0.019 and 0.014 ± 0.008, μmol cm^{-2} h^{-1}, respectively). When exposed to 100% air saturation, the mucosal and serosal salines showed O_2 depletion at rates (0.359 ± 0.138 and 0.192 ± 0.022, μmol cm^{-2} h^{-1}, respectively) not significantly different than those measured during tissue exposure to symmetrical 100% air saturation. A representative trace of O_2 content in each half chamber during these experiments is shown in Fig. 6.5.

Fig. 6.5. A representative trace of O_2 depletion from mucosal and serosal half-chambers during exposure of control epithelia sequentially to (between 0 and 45 min) mucosal salines at 100% air saturation and serosal salines at 0% air (gassed with N_2), and (between 45 and 100 min) mucosal salines at 0% air saturation and serosal salines at 100% air.

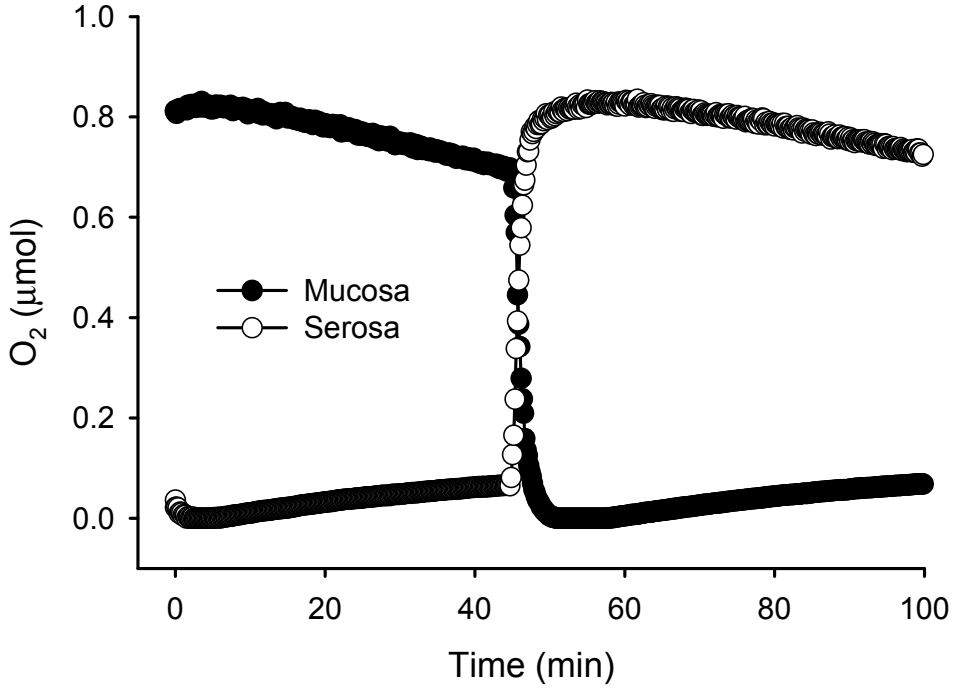

Substrate utilization.

No significant differences were observed between total tissue O_2 consumption between the different substrate combinations (Fig. 6.6), suggesting that the “standard” asymmetrical salines (Table 6.1) do not impose substrate limitations on isolated toadfish intestine. Furthermore, no significant difference in rates of O_2 depletion between the mucosal and serosal half-chambers were observed in any treatment when measurements in the serosal and luminal half-chambers were made in parallel between 90-95% air saturation (Fig. 6.6). Tissue metabolic rate was constant over the approx. 4 h experimental period used in the substrate utilization experiments. Based on these results, the “standard” asymmetrical mucosal and HCO_3^--free serosal (with 5mM glucose) salines was used for all subsequent measurements of tissue O_2 consumption.

Fig. 6.6. Isolated toadfish intestinal epithelia O_2 consumption shows no significant change between the sequential, randomized application of (1) mucosal + serosal (with 5 mM glucose), (2) mucosal + serosal (5 mM glucose + 5 mM glutamate), and (3) mucosal (5 mM glucose + 5 mM glutamate) + serosal (5 mM glucose + 5 mM glutamate) salines (n = 8). Separate epithelia (n = 5) show no significant difference in O_2 consumption on exposure to mucosal L-15 + serosal (5 mM glucose) salines. Furthermore, O_2 consumption is consistent between the mucosal and serosal half-chambers in all experimental treatments. Data are displayed as mean ± SEM.

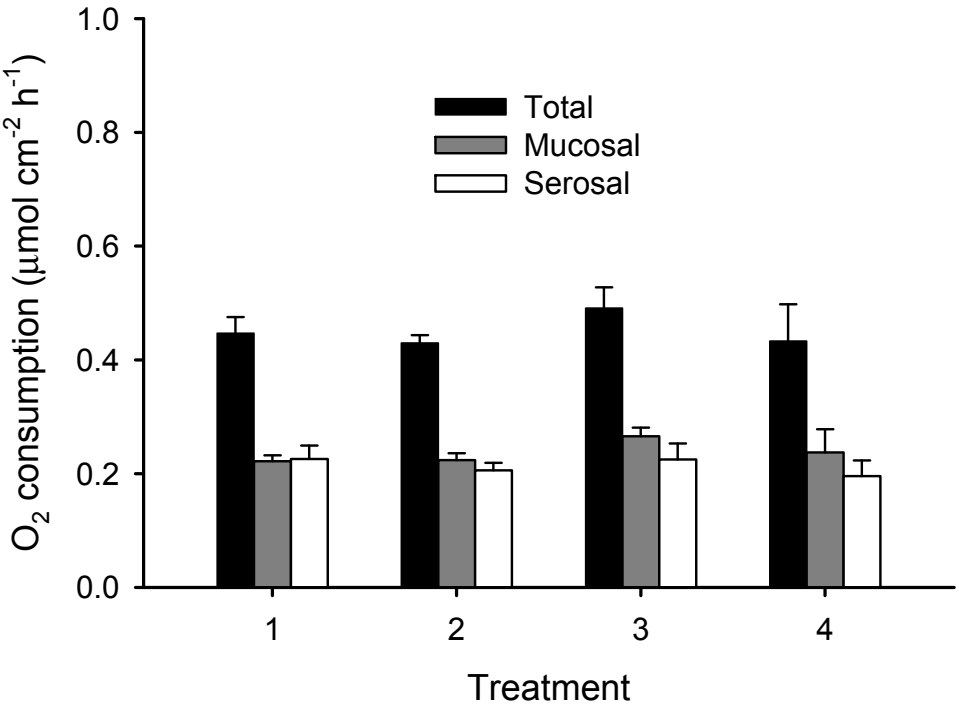

Constancy of O_2 consumption.

Results show that O_2 consumption by the isolated toadfish intestine occurs at significantly lower rates between 50-75% air saturation as compared to the highest rates which occur between 75 and100% air saturation (Fig. 6.7). No significant differences were observed among O_2 consumption recorded between 75 and 100% air saturation (Fig. 6.7). To ensure that measurements of O_2 consumption were not limited by PO_2, all subsequent measurements of O_2 consumption were performed at 90-95% air saturation.

Fig. 6.7. isolated toadfish intestinal epithelia show a marked decrease in O_2 consumption with % air saturation. Asterisks indicate statistical significance of this trend, with n = 8 with data displayed as mean ± SEM.

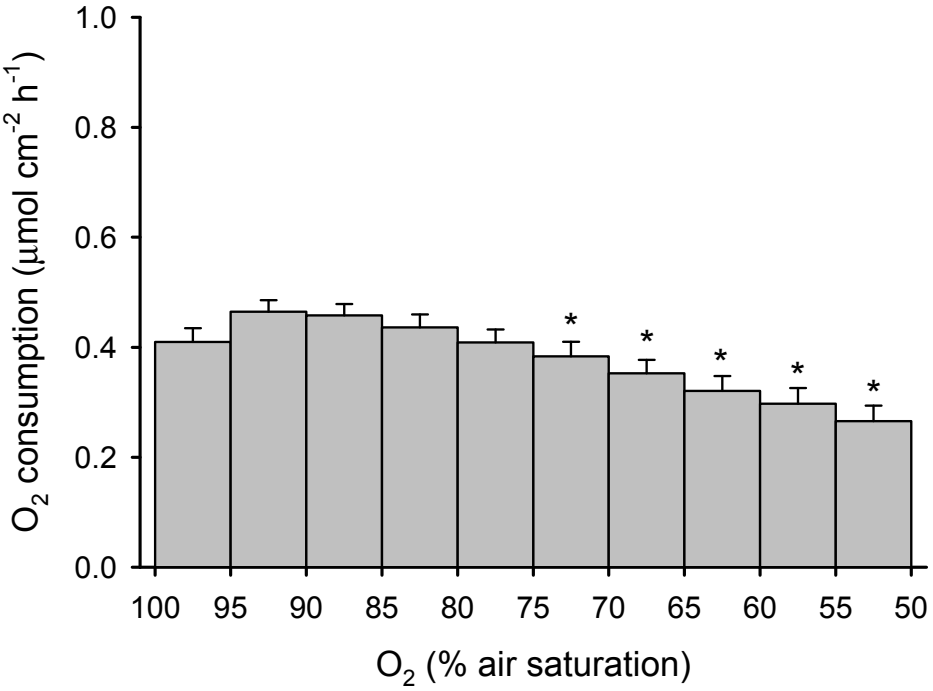

Specific dynamic action (SDA)

Isolated toadfish intestine is subject to a significant postprandial increase in O_2 consumption indicative of specific dynamic action (SDA) in this tissue. O_2 consumption is significantly elevated over control rates (0.47 ± 0.02 μmol cm^{-2} h^{-1}) between 3 (0.67 ± 0.04 μmol cm^{-2} h^{-1}) and 6 (0.88 ± 0.04 μmol cm^{-2} h^{-1}) h following feeding, with peak values at 6 h significantly greater than all other time points (Fig. 6.8). The application of L-15 media to the mucosa did not increase the SDA response by the isolated tissue. Mucosal application of L-15 gave no significant changes in 3 h postprandial O_2 consumption (0.51 ± 0.07 μmol cm^{-2} h^{-1}) as compared to glucose-containing mucosal saline, although these rates are significantly higher than those measured in control epithelia exposed to mucosal L-15 (0.43 ± 0.06 μmol cm^{-2} h^{-1}) as described above.

Fig. 6.8. Isolated toadfish intestinal epithelia show significant (*) elevation in O_2 consumption between 3-6 h postprandially, with a peak 6 h postprandially that is significantly greater than all other timepoints (**). n = 8 at each time point, with data displayed as mean ± SEM.

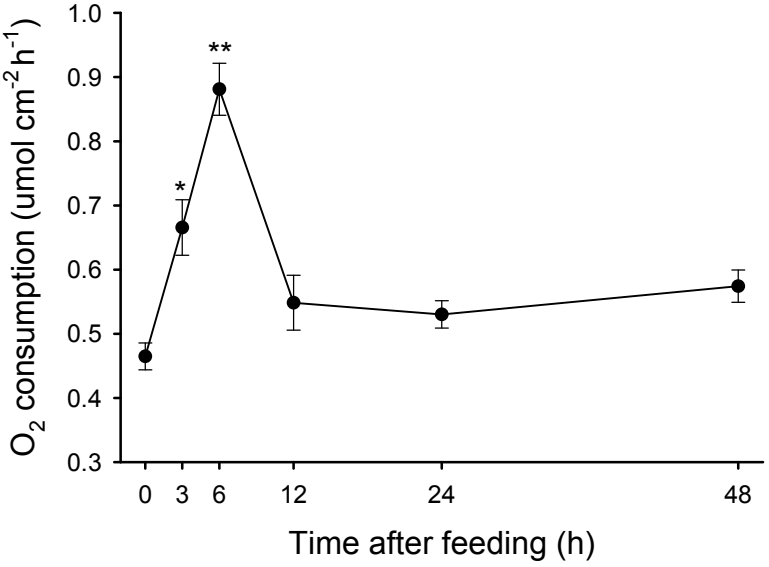

Conclusions

The present study suggests that the postprandial increases in intestinal fluid [HCO_3^-] measured in marine teleosts (Taylor and Grosell 2006b; Taylor *et al.* 2007) are attributable largely to increases in transepithelial HCO_3^- secretion. Measurements of epithelial HCO_3^- secretion suggest that adjustments in the contribution of endogenous CO_2 production by isolated toadfish intestine are minimal 3h after feeding (Fig. 6.4); however, epithelial O_2 consumption (Fig. 6.8) indicate a clear rise in tissue metabolic rate post feeding. This discrepancy can be explained in part by the peak postprandial HCO_3^- secretion preceding the peak postprandial metabolic response by the intestinal tissue. This temporal disparity has noteworthy implications for postprandial marine fish physiology. Specifically, with alkaline tide peaking 6-12 h after feeding in the teleost fish species showing this postprandial response (Bucking and Wood 2008; Cooper and Wilson 2008), an appropriately preceding peak in transepithelial intestinal HCO_3^- secretion may eliminate any measurable accumulation of blood HCO_3^-. The following estimates have provided insight to the feasibility of this hypothesis. Based on measurements of mass and surface area of isolated intestinal tissue (0.053 g tissue/cm^2), whole animal intestinal tract surface area was estimated to be 7.2 cm^2 (1.9% body mass x 20 g fish = 0.38 g intestinal tract tissue / 0.053 g tissue cm^{-2} = 7.2 cm^2 intestinal tract tissue) in a 20 gram fish. Assuming constant HCO_3^- secretion rates along the intestinal tract, the calculated intestinal tract surface area of 7.2 cm^2 and the difference in total HCO_3^- secretion between

postprandial and control epithelia (1.14 – 0.82 = 0.32 μmol cm^{-2} h^{-1}) indicate that whole animal postprandial base efflux to the intestinal fluids exceeds control base efflux by approx. 2.3 μmol h^{-1}. Extracellular fluid (ECF) volume in marine teleosts has been estimated to comprise approx. 20% body mass (Thorson 1961; Takei 2000), giving an ECF volume of approx. 4 ml in a 20 g toadfish. Considering equilibrium of HCO_3^- between the plasma and extracellular fluids, an alkaline tide of 2.5 mM HCO_3^- in 4 ml of ECF could be offset by a base efflux of 10 μmol. Simple division of this total by the observed increase in intestinal HCO_3^- secretion following feeding suggests that the 39% increase in base secretion by postprandial intestinal tissue would be sufficient to counteract an alkaline tide of this magnitude within 4-5 h. Based on the present results of significantly elevated postprandial intestinal HCO_3^- secretion peaking 3 h post-feeding but persisting over the entire 48 h postprandial period, the intestine certainly is capable of postprandial regulation of acid-base balance. Furthermore, while transepithelial HCO_3^- secretion contributes direct adjustments to plasma [HCO_3^-], any secretion of endogenously produced CO_2 as HCO_3^- into the intestinal fluids will also serve to acidify the plasma via basolateral H^+ extrusion (Fig. 6.9) serving cellular acid-base balance regulation (Grosell 2006).

Fig. 6.9. Schematic cellular model of the mechanism of HCO_3^- secretion by the marine teleost intestine. Hydration of endogenous CO_2 is facilitated by carbonic anhydrase (CA) and resultant HCO_3^- is exchanged across the apical membrane in exchange for Cl^-, while H^+ are extruded across the basolateral mechanism in exchange for Na^+, driven by the electrochemical gradient for Na^+ created by basolateral Na^+/K^+-ATPase (NKA). Alternatively, serosal HCO_3^- is taken up across the basolateral membrane via Na^+/HCO_3^- cotransport (NBC), also driven by the Na^+ electrochemical gradient. The Cl^- taken up from the luminal fluids leaves the cell through basolateral Cl^- channels. Note that this figure is limited to ion transport mechanisms pertaining to intestinal HCO_3^- secretion and is not inclusive of other important transport processes occurring across marine teleost intestinal epithelia.

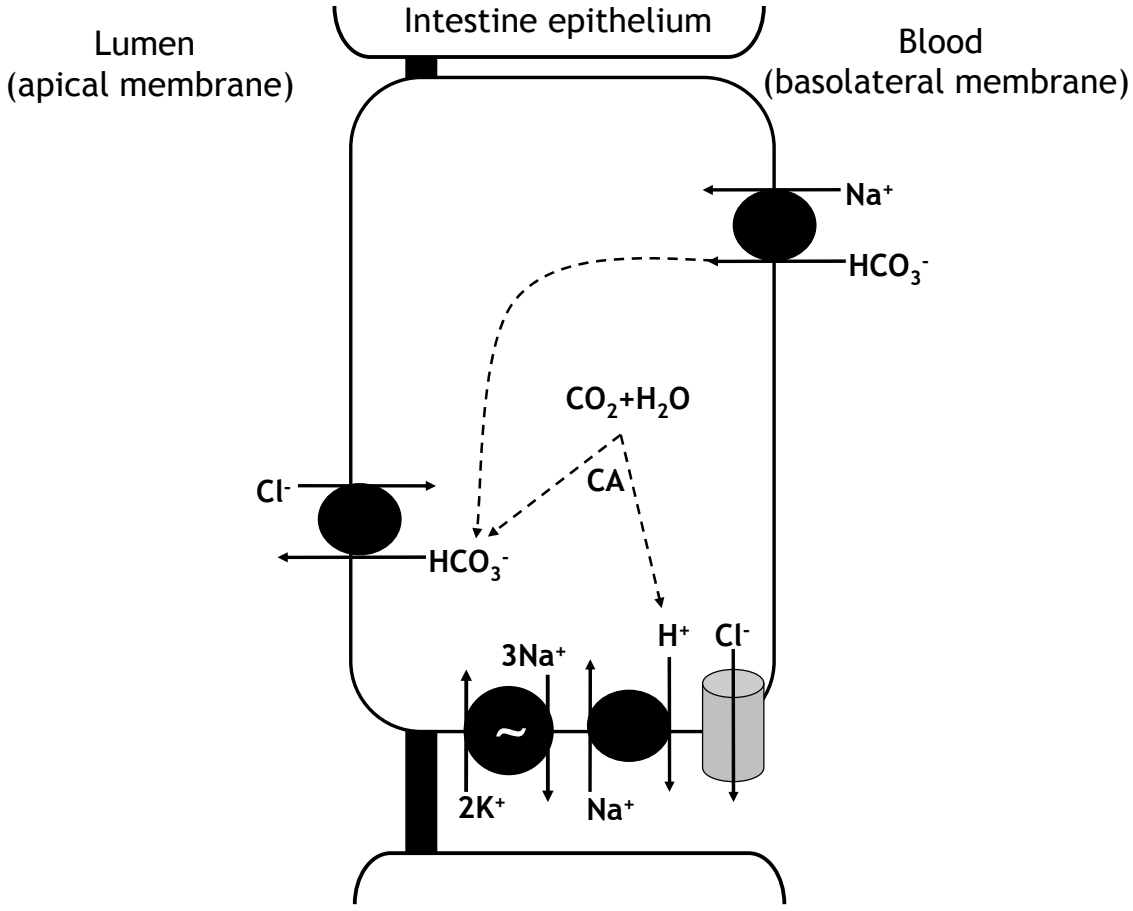

The focus of this study was to quantify any postprandial elevation in intestinal HCO_3^- secretion and deduce the source of postprandial high intestinal fluid [HCO_3^-] and thereby its possible contribution to dynamic regulation of acid-base balance after feeding. The present measurements of postprandial O_2 consumption (Fig. 6.8) used a novel technique to investigate largely unexplored intestinal tissue-specific metabolic rates post-feeding. Initial experiments showed very low rates of O_2 accumulation during O_2-free conditions, indicating a highly gas-tight system with minimal rates of back-flux of atmospheric O_2. The rates of O_2 consumption exceed the rate of O_2 appearance under O_2-free conditions by more than 100-fold demonstrating that O_2 back-flux was an insignificant source of error in these experiments. Rates of O_2 depletion during exposure of one half-chamber to 100% air saturation, with anoxic conditions in the opposing half-chamber, suggest that diffusion limitations occur at both the mucosal and serosal membranes of the epithelium and prevent O_2 consumption from one half-chamber from maintaining the whole tissue O_2 consumption. Diffusion limitations were expected at the serosal membrane due to the lack of perfusion of the often substantial muscle layer during these *in vitro* measurements.

The lack of constancy in O_2 consumption measured at levels of air saturation below 75% was unexpected in these experiments, largely because teleost plasma contains a much lower O_2 concentration than air (Krogh and Leitch 1919; Evans 1997), and thus should not be O_2-limited even in the 50-75% air saturation range tested. Application of several results has enabled further investigation of this apparent limitation to metabolic rate. Considering that

glucose appears to be a sufficient substrate for toadfish intestinal tissue, the possibility of glucose depletion during the relatively prolonged experiments examining the influence of O_2 availability on metabolic rate must be considered. An assumed relationship between O_2 consumption and glucose metabolism of 6 mol O_2/ mol of glucose suggests the isolated toadfish intestine depletes glucose from the tissue respirometer at maximal rates of 0.066 μmol h^{-1}. Thus the 5 mM serosal glucose (14.75 μmol in the half-chamber volume of 2.95 ml) used in all experiments is sufficient to sustain the carbohydrate metabolism of the epithelium for well past the experimental period (> 200 h).

By comparing tissue O_2 consumption with HCO_3^- secretion under HCO_3^- -free conditions (Fig. 6.4) as a proxy for endogenous CO_2 production, the respiratory quotient (moles of CO_2 produced/ moles of O_2 consumed; RQ) was calculated for control (RQ = 0.89) and 3 h postprandial (RQ = 0.80) epithelia. The high RQ in control tissue suggests the utilization of a carbohydrate-rich (carbohydrate RQ = 1.0), substrate. This result is in accordance with studies suggesting the intestine metabolizes predominantly carbohydrate and protein (RQ = 0.83) substrates (Duee *et al.* 1995) and that these macromolecules are also the predominant fuels for osmoregulation (Tseng and Hwang 2008), a process in which the marine teleost intestine plays a critical role (Grosell 2007). Furthermore, the high RQ under control conditions is in agreement with the observations of glucose alone being a sufficient metabolic substrate for toadfish intestinal tissue. The drop in RQ seen in postprandial epithelia can be explained by at least two theories, none of which are mutually exclusive. First, the

postprandial intestine may indeed metabolize a higher fraction of protein and/or lipid (RQ = 0.71) than that of an unfed fish. Second, as a caveat in both control and postprandial RQ calculations, CO_2 production may exceed that accounted for by measured HCO_3^- secretion. This could be attributable to simple diffusion of endogenously produced CO_2 out of the tissue, and/or the activity of an apical H^+-ATPase which could lead to titration of secreted HCO_3^- beyond that accounted for by the pH-stat methodology (i.e., an underestimation of intestinal HCO_3^- secretion rates) as illustrated in two recent studies (Grosell *et al.* 2009a; Grosell *et al.* 2009b). Furthermore, the possibility of endogenous amino acid metabolism by the isolated tissue has been considered. However, during substrate preference experiments, no significant decrease in O_2 consumption was seen when glucose (without glutamate) was applied as the final treatment as opposed to the first treatment. This result suggests that an experimental time of 4 h is not sufficient to deplete the tissue of any internal amino acid stores it may be metabolizing, and supports the former explanation of alternative CO_2 fates leading to a reduction in apparent RQ. In addition to the aforementioned implications, calculated RQ values validate the decision to investigate both glucose and glutamate as potentially limiting metabolic substrates. The high RQ suggests carbohydrate is an important metabolic substrate in isolated toadfish intestine, a result supported by substrate utilization experiments which suggest a carbohydrate substrate can sustain O_2 consumption by isolated epithelia. Calculations of glucose depletion from the respirometer indicate that carbohydrate substrate limitation was not a factor in the reduction of O_2

consumption with time. With respect to PO_2 dependence of O_2 consumption below 75% air saturation, the present results suggest that neither O_2 back-flux nor metabolic substrate limitation is likely to account for this unexpected outcome. Regardless of the reasons for significantly reduced O_2 consumption below 75% air saturation (Fig. 6.7), this experiment validates the use of 75-100% air saturation in these experiments, and also suggests that tissues subjected to pH-stat experiments conducted at 100% O_2 likely display the same metabolic rates as tissues exposed to air. Factors influencing the dependence of isolated tissue O_2 consumption on PO_2 are certainly a source of interest for future investigations.

Measurements of O_2 consumption by the isolated toadfish intestine also allow predictions to be made about the intestinal contribution to whole animal O_2 consumption and SDA. Results indicate unfed intestinal tissue consumes O_2 at rates approx. 3-fold higher than those measured by in whole toadfish (3.0 mmol kg^{-1} h^{-1}) (Gilmour *et al.* 1998). In a 20-g toadfish, intestinal O_2 consumption accounts for 3.4 μmol h^{-1}, or 5.6% of whole animal O_2 consumption. This is a surprisingly low fraction considering studies suggesting the non-fed, non-osmoregulating mammalian gastrointestinal tract to account for 20-25% of whole animal O_2 consumption (Duee *et al.* 1995). Peak postprandial intestinal O_2 consumption equates to 6.3 μmol h^{-1} for a 20-g toadfish, and this intestinal SDA response of a 2.9 μmol h^{-1} increase in O_2 consumption can account for approx. 4.8% of an assumed 60 μmol h^{-1} increase in metabolic rate of a 20-g toadfish as suggested by typical increases in fish O_2 consumption associated with SDA

(Jobling 1981; Mccue 2006; Secor 2009). These calculations suggest that the intestinal contribution to whole toadfish SDA is just over 2-fold higher than that suggested by its mass. This contribution of the intestinal tract to SDA is rather modest considering its location at “ground zero” with respect to nutrient absorption (requiring ATP-driven maintenance of a sodium gradient), but corresponds with the view that SDA is attributable predominantly to post-absorptive processes including protein synthesis, rather than pre-absorptive and absorptive processes (Secor 2009). Furthermore, L-15 data suggest that the presence of chyme in the lumen is not likely to further stimulate the intestinal SDA response. However, considering the remarkable variation in magnitude between studies of fish SDA (Secor 2009), comparison of tissue-specific and whole animal postprandial O_2 consumption is an important area for future study and would shed further light on the intestinal contribution to SDA.

The duration of whole animal SDA in fishes also varies greatly among studies, ranging from 1.3 to 390 h, and is dependent largely on meal mass and temperature (Jobling 1981; Mccue 2006; Secor 2009). The duration of the intestinal tissue SDA response in toadfish appears markedly shorter than that shown for whole fish SDA during acclimation to similar temperatures (Jobling 1981; Secor 2009). An estimated meal size of 9.5% body mass in the present experiments suggests an approximate meal energy of 6.3 kJ, based on measurements by Croxall and Prince (1982) of mean energy content in squid. For a meal of this energetic value, the gastric evacuation time of 24-48 h seen in the experimental animals is in line with that shown for other benthic fishes

acclimated to similar temperatures (Jobling 1981). The meal size in the present experimental animals was considerably larger than that used in other studies of postprandial fish physiology (Bucking and Wood 2008; Cooper and Wilson 2008; Secor 2009). Despite this relatively large meal size, data on postprandial gastrointestinal tract morphology showed little evidence of the intestinal hyperplasia (Lignot *et al.* 2005) or fluid engorgement (Wood *et al.* 2007b) that have been shown in digestive tissues of opportunistically feeding animals consuming similar rations. However, an increased contribution of the intestinal (rather than gastric) tissue to body mass was seen following feeding. This result is not surprising considering the prominent role of the intestinal tract in nutrient and water absorption, but the source of the postprandial intestinal mass increase deserves further attention as it appears to be more complicated than a simple increase in tissue perfusion.

Our data suggest that elevated postprandial intestinal HCO_3^- secretion occurs predominantly by transepithelial transport, rather than increased endogenous CO_2 production (i.e. SDA), and is capable of offsetting alkaline tide. Postprandial increases in basolateral NKA activity associated with SDA to fuel Na^+-driven nutrient uptake also act to strengthen the electrochemical gradient favoring basolateral NBC (Fig. 6.9). The serosal HCO_3^- substrate for NBC would be simultaneously increased during alkaline tide (Hersey and Sachs 1995; Niv and Fraser 2002), adding further driving force for transepithelial HCO_3^- secretion owing to the high affinity of basolateral NBC for serosal HCO_3^- in the physiological range (Taylor *et al.* 2009). Because intestinal HCO_3^- secretion has

been shown to be limited at the basolateral membrane rather than by apical Cl^- /HCO_3^- exchange (Taylor *et al.* 2009), postprandial elevation of the driving force(s) for basolateral NBC would facilitate intestinal base efflux and thereby form the basis of this mechanism for dynamic regulation of postprandial acid-base balance.

Acknowledgments

Jimbo's and Captain Ray Hurley and Debbie Fretz, Miami, FL, USA, for supplying us with toadfish; J.R. Taylor is supported by a University of Miami teaching assistantship. The present study was supported by an NSF award (IOB 0718460) and SGER to M. Grosell.

Chapter 7:

Discussion

This dissertation comprises a number of considerable contributions to the field of fish physiology and has prompted related investigations by several research groups. The assortment of techniques used herein to study an extensive selection of aquatic animals range from whole animal, to isolated tissue, to cellular and molecular levels including expression systems, and constitute an interdisciplinary approach that has also impacted tangential fields. This approach has furthermore conferred a broad base of knowledge, technical methodologies, and professional connections that will undoubtedly shape future scientific undertakings.

At the onset of this dissertation, the use of intestinal HCO_3^- secretion as an osmoregulatory strategy among marine teleosts was a relatively novel assertion in the literature, and its application beyond teleosts had become a source of curiosity amongst researchers but had not yet been ascertained. Results show a considerable gradient between extracellular and intestinal fluid [HCO_3^-] in all non-teleost species initially investigated (Chapter 2), thereby supporting the hypothesis that intestinal HCO_3^- secretion is not limited to marine teleosts but is more likely to be a mechanism linked to seawater ingestion across aquatic taxa. Due to the attention these initial investigations attracted from several research groups, preliminary data (Chapter 2) were quickly published and made available to the scientific community. However, the link between seawater ingestion and

intestinal HCO_3^- secretion as an essential mechanism by which ingested seawater is processed was continually investigated during the course of ensuing dissertation research as sampling opportunities permitted.

In addition to the sturgeon and elasmobranch species for which data have been shown and discussed (Chapter 2), similar measurements were made in progressively ancestral fish species including chimaera (*Hydrolagus colliei*), sea lamprey (*Petromyzon marinus*), and hagfish (*Eptatretus stoutii*). Furthermore, red rock crabs (*Cancer productus*) and Dungeness crabs (*Cancer magister*) were sampled as representative invertebrates thought to have some osmoregulatory ability based on seawater ingestion (Chu 1987; do Carmo Fernandes Santos 2002). Finally, green turtles (*Chelonia mydas*) were sampled as a representative tetrapod also shown to actively consume seawater as a means of osmoregulation (Holmes and McBean 1964; Prange 1985; Bennett *et al.* 1986). This comprehensive survey was made possible by access to these species via a number of visits to collaborating laboratories, as well as the shipment of lamprey plasma and intestinal fluids to RSMAS (University of Miami, FL) by J.M. Wilson (CIIMAR, Portugal). In osmoconforming species (chimaera, hagfish, and crabs), protocols mimicking those for elasmobranchs (Chapter 2) were used in which elevated salinity was employed to induce drinking. Drinking rates in these species were measured by addition of the relatively impermeant molecule polyethylene glycol-4000 (PEG-4000, Fluka) (Buxton *et al.* 1979) to the medium and subsequent quantification of its concentration in the intestinal fluids following

6-10 h exposure of animals to seawater (SW) or 120-140% SW (adjusted with Instant Ocean synthetic sea salt, Spectrum Brands, Inc.).

Plasma (or extracellular fluid in the case of hagfish, and haemolymph in crabs) chemistry (Table 7.1) and intestinal fluid chemistry (Table 7.2) are reported for these additional investigations, with more detailed ion analyses completed for species showing evidence of intestinal HCO_3^- secretion (lamprey and turtles) and also for hagfish. Hagfish were unique in showing a slight (although not statistically significant) increase in drinking rate (Table 7.2) on exposure to elevated salinity but having intestinal fluid [HCO_3^-] significantly lower than that of the extracellular fluids (Table 7.1). Of further curiosity, higher concentration of PEG in the intestinal fluids of salinity-challenged hagfish suggests that these fish are capable of intestinal water absorption without concomitant intestinal HCO_3^- secretion. In hagfish subjected to high salinity challenge the concentration of PEG in the intestinal fluids was 2.8 ± 0.4-fold greater than that of the 140% SW medium, while SW hagfish intestinal fluids contained PEG at 1.3 ± 0.1-fold greater concentration than ambient SW.

Table 7.1. Blood plasma (or extracellular fluid in hagfish, and haemolymph in crabs) chemistry in red rock crabs (n = 6 at each salinity), Dungeness crabs (n = 9 at each salinity), Hagfish (n = 12 at each salinity), lamprey (n = 3) and green turtle (n = 7), at indicated salinities. Data are reported as mean (SEM), with significant ($p < 0.05$) differences from seawater conditions indicated by asterisks in salinity challenged osmoconforming species.

	Red rock crabs		Dungeness crabs		Hagfish		Lamprey	Chimaera		Green turtle
	SW	130% SW	SW	130% SW	SW	140% SW	50% SW	SW	120% SW	SW
Osmolality ($mOsm\ l^{-1}$)					870 (8)	1021* (14)	301 (5)			337 (0.8)
pH	7.58 (0.09)	7.87* (0.02)	7.30 (0.04)	7.53* (0.03)	7.96 (0.02)	7.92 (0.02)	7.56 (0.04)	7.67 (0.03)	7.51* (0.04)	7.82 (0.16)
Total CO_2 (mM)	15.4 (1.1)	22.1* (1.0)	10.8 (0.5)	16.3* (0.5)	8.8 (0.5)	9.7 (0.4)	13.8 (0.8)	6.6 (0.3)	4.5* (0.3)	24.2 (2.7)
Cl^- (mM)					450.6 (4.8)	526.6* (12.8)	117.2 (4.5)			110.8 (3.0)
Na^+ (mM)					433.9 (5.3)	529.1* (8.1)	143.2 (17.8)			169.6 (3.6)
K^+ (mM)					9.3 (0.3)	10.6 (0.4)	4.2 (0.3)			2.1 (0.4)
Ca^{2+} (Mm)					4.1 (0.1)	4.6 (0.1)	2.4 (0.3)			1.6 (0.2)
Mg^{2+} (mM)					10.9 (0.4)	11.2 (0.7)	1.7 (0.1)			2.9 (0.5)
SO_4^{2-} (mM)					1.8 (0.3)	2.0 (0.3)	‡			‡

‡ Insufficient concentration for measurement

Table 7.2. Intestinal fluid chemistry and drinking rates of red rock crabs (n = 6 at each salinity), Dungeness crabs (n = 9 at each salinity), hagfish (n = 12 at each salinity), lamprey (n = 3) and green turtle (n = 4), at indicated salinities. Data are reported as mean (SEM), with significant ($p < 0.05$) differences from seawater conditions indicated by asterisks in salinity challenged osmoconforming species.

	Red rock crabs		Dungeness crabs		Hagfish		Lamprey	Chimaera		Green turtle
	SW	130% SW	SW	130% SW	SW	140% SW	50% SW	SW	120% SW	SW
Osmolality ($mOsm\ l^{-1}$)					934 (2)	1130* (14)	334 (22)			683 (†)
pH	7.20 (0.10)	6.98 (0.14)	6.96 (0.13)	7.08 (0.11)	7.31 (0.06)	7.08 (0.15)	8.34 (0.13)	7.36 (0.17)	6.92 (0.07)	8.03 (0.45)
Total CO_2 (mM)	7.6 (1.2)	7.6 (1.8)	9.4 (2.2)	10.3 (1.4)	0.9 (0.4)	1.1 (0.2)	38.5 (13.3)	12.7 (3.9)	5.4* (2.6)	51.8 (14.1)
Cl^- (mM)					482.2 (11.6)	594.8* (14.8)	127.7 (9.3)			52.0 (3.7)
Na^+ (mM)					394.5 (17.4)	454.5* (27.8)	38.2 (7.0)			266.9 (118.2)
K^+ (mM)					24.9 (2.9)	27.0 (2.0)	14.5 (2.5)			16.7 (4.0)
Ca^{2+} (mM)					9.6 (0.9)	15.1* (1.9)	13.6 (1.2)			2.6 (1.2)
Mg^{2+} (mM)					41.1 (3.7)	63.8* (7.0)	79.4 (15.5)			13.7 (9.8)
SO_4^{2-} (mM)					20.6 (2.4)	31.4* (2.5)	48.4 (7.5)			59.1 (7.3)
Drinking rate ($ml\ kg^{-1}\ h^{-1}$)	2.19 (0.99)	1.63 (0.40)	2.67 (0.46)	1.94 (0.33)	0.83 (0.37)	1.50 (0.51)		1.53 (0.58)	1.88 (0.39)	

† n = 1 due to small sample volume

Furthermore, some degree of intestinal NaCl absorption is indicated in salinity-challenged hagfish by approximately 21 and 18% reductions in intestinal fluid [Cl^-] and [Na^+] (Table 7.2) as compared to those of the 140% SW media (668 mM and 553 mM, respectively) used in these experiments. This result suggests that fluid absorption by the hagfish intestine could be coupled to NaCl absorption via NaCl and NKCC co-transporters, which prior to the recognition of anion exchange (AE) were considered to be principally responsible for the absorptive nature of the marine teleost intestine (Loretz 1995; Grosell 2007). Alternatively, it is possible that NaCl absorption could proceed via simple diffusion across the hagfish intestine into the extracellular fluids (Table 7.1) which also appear to maintain [NaCl] below that of the 120% SW media. However, with extracellular fluid osmolality (Table 7.1) lower than that of the intestinal fluids (Table 7.2) in these salinity-challenged hagfish, simple fluid diffusion is not likely to account for the curiously high concentration of PEG in the intestinal fluids. Clearly the mechanisms by which ion and fluid transport proceed in this ancestral vertebrate are deserving of future attention.

None of the osmoconforming species presented here (crabs and chimaera) were found to significantly increase their drinking rates (Table 7.2) on exposure to salinity challenge as was measured in several species of elasmobranchs (Anderson *et al.* 2001; Anderson *et al.* 2002) and also suggested in bamboo sharks (Chapter 2). This result indicates that the ability of the some elasmobranchs to use SW drinking and subsequent intestinal HCO_3^- secretion as a short-term osmoregulatory mechanism is unique amongst osmoconformers.

Meanwhile, lamprey and turtles both show significantly higher intestinal fluid [HCO_3^-] (Table 7.2) than that of the plasma (Table 7.1), suggestive of an active mechanism of intestinal HCO_3^- secretion. Intestinal fluid and plasma chemistry analyses show particularly low intestinal fluid [Cl^-] and high [Na^+] in turtles (Table 7.2), suggesting anion exchange to be a likely mechanism by which Cl^- and thereby fluid is absorbed by the sea turtle intestine. Conversely, lamprey show much lower intestinal fluid [Na^+] than [Cl^-] (Table 7.2), emphasizing the importance of more detailed species-specific studies of osmoregulatory mechanisms. Overall, these additional results underscore the use of intestinal HCO_3^- secretion as an osmoregulatory mechanism that is more universal amongst seawater animals than previously appreciated. Results suggest a close correlation between seawater ingestion and intestinal HCO_3^- secretion in all marine animals examined to date except hagfish. With the interest that these investigations have attracted from other research groups, it is likely that the specific mechanisms by which (and the extent to which) intestinal HCO_3^- secretion contributes to seawater processing and thereby osmoregulation in non-teleost animals will be deduced. Indeed, the mechanism(s) by which ingested seawater is processed in elasmobranchs have already been investigated in more detail during a collaborative effort (Anderson *et al.* 2007). Further collaborative investigations of lamprey and turtle intestinal morphology are also in progress, with immunohistochemical techniques likely to shed light on the intestinal mechanisms by which these species osmoregulate.

This dissertation has also contributed to the field of fish physiology the novel use of feeding as a tool to investigate osmoregulatory mechanisms in marine teleosts. With respect to physiology research, the (August) Krogh Principle states that, “For many problems there is an animal on which it can be most conveniently studied” (Krebs 1975). This principle often leads to investigations during which mechanistic studies are carried out on animals adapted to extreme environments where the mechanism in question is essential to the success of the animal. Accordingly, meal ingestion results in a range of physiological disturbances that require adjustments by mechanisms similar or identical to, but generally more extreme than, those used to maintain homeostasis. Specifically, (1) salt and water balance during digestion requires mechanisms analogous to, but of a greater magnitude than, those required to process the more moderate ion load to the gastrointestinal tract associated with seawater ingestion in osmoregulating marine animals; (2) acid/base balance regulation during digestion necessitates greater transport of acid/base equivalents than that generally required under unfed conditions, and (3) metabolic rate and thereby energy balance fluctuate to a greater degree than that expected in “control” animals. The homeostatic mechanisms by which each of these three categories of physiological disturbance is regulated are very much interrelated, as illustrated by the role of intestinal HCO_3^- secretion in each. This dissertation has examined the role of intestinal HCO_3^- secretion in postprandial (1) ion and thereby fluid absorption; (2) acid/base balance at both tissue and whole animal levels; and (3) oxygen consumption by the intestinal tissue.

The first of these postprandial disturbances to physiology investigated during this dissertation research was that of salt and water balance. Chapters 3 and 4 show significant challenges to salt and water balance in postprandial toadfish and flounder, and indicate that intestinal HCO_3^- secretion is likely up-regulated via anion exchange as a postprandial regulatory mechanism. Chapter 6 confirmed these results with quantification of postprandial HCO_3^- secretion rates in isolated toadfish intestine. While feeding resulted in dramatic changes to intestinal fluid chemistry in all fish sampled, accompanying changes in plasma chemistry were modest at best (Chapters 3 and 4). Neither toadfish nor flounder in freshwater or seawater, showed evidence of the significant postprandial blood alkalosis characterizing “alkaline tide” (Chapters 3 and 4). Interestingly, mechanisms of gastrointestinal ion absorption during digestion in fish have since become a topic of considerable interest, and a number of recent studies have shown a significant postprandial alkaline tide in both an elasmobranch (Wood *et al.* 2005; Tresguerres *et al.* 2007; Wood *et al.* 2007a; Wood *et al.* 2007b; Wood *et al.* 2008; Wood *et al.* 2009) and in freshwater trout (Bucking and Wood 2008; Cooper and Wilson 2008). Investigations of alkaline tide in seawater trout are ongoing but have not yet been published, but will undoubtedly be a source of interest with respect to salinity-specific (and possibly species-specific within seawater and freshwater) differences in postprandial acid-base balance regulation strategies.

Having gathered preliminary evidence for a role of intestinal HCO_3^- secretion in postprandial acid-base balance regulation (Chapters 3 and 4),

Chapter 5 served to characterize the basolateral HCO_3^- transport mechanism by which transepithelial base secretion is achieved. In light of the previously discussed investigations of this dissertation and a growing recognition of the importance of intestinal HCO_3^- secretion to marine teleost osmoregulation (Grosell *et al.* 2005; Marshall and Grosell 2005; Grosell and Genz 2006; Grosell 2006; McDonald and Grosell 2006; Taylor and Grosell 2006a; Grosell *et al.* 2007; Grosell and Taylor 2007; Grosell 2007; Genz *et al.* 2008), transepithelial intestinal HCO_3^- secretion has also attracted the interest of other research groups. As such, a basolateral Na^+/HCO_3^- co-transporter was characterized in a species of Japanese pufferfish commonly known as “mefugu” (*Takifugu obscurus*) in a timely study (Kurita *et al.* 2008) highlighting the mechanisms by which intestinal HCO_3^- secretion contributes to marine teleost osmoregulation. In addition to confirming the expression of an analogous basolateral NBCe1 in toadfish (tfNBCe1), Chapter 5 supports a rate-limiting role of basolateral NBC in intestinal HCO_3^- secretion, with a transport kinetics profile suggesting its ability to precisely regulate plasma acid/base balance.

With a better picture of the contribution of intestinal HCO_3^- secretion to postprandial regulation of salt/water (Chapters 3 and 4) and acid/base (Chapters 4 and 5) balance, the final postprandial physiological disturbance investigated during this dissertation was that of metabolic rate. Oxygen consumption by isolated toadfish intestinal tissue suggested that postprandial increases in endogenous CO_2 production were not adequate in either timeliness or magnitude to account for parallel increases in intestinal HCO_3^- secretion (Chapter 6). The

more considerable increase in postprandial transepithelial HCO_3^- secretion, as compared to endogenous CO_2 production and subsequent secretion, proved to be of sufficient timeliness and magnitude to offset a typical alkaline tide (Wood *et al.* 2005; Bucking and Wood 2008; Cooper and Wilson 2008), supporting a role of the marine teleost intestine in postprandial acid-base balance regulation (Chapter 6). To make an addendum to the Krogh Principle, this dissertation has shown that "For many problems there is a [situation in which] it can be most conveniently studied". Specifically, the use of feeding has provided a situation in which intestinal HCO_3^- secretion is up-regulated to a magnitude at which it could offset acid-base balance disturbances associated with digestion, by means independent of the metabolic disturbances also associated with digestion. The variability affiliated with meal ingestion does not by any means make feeding a "convenient" situation in which every physiological process can be investigated; however, the use of feeding in this instance has been instrumental in understanding the full breadth of function for this relatively newly recognized mechanism of intestinal ion transport in marine animals. The importance of these findings is emphasized by the recent assertion that the $CaCO_3$ excretion resulting from marine fish intestinal HCO_3^- secretion plays a significant role in the marine inorganic carbon cycle (Wilson *et al.* 2009).

As a whole, the collection of research included in this dissertation has led to considerable advancement in the field of fish physiology. Perhaps equally as important as the conclusions drawn from this dissertation, however, is the magnitude of interest they have attracted from a number of additional research

groups. This attention will undoubtedly stimulate further advancement in our knowledge of fish physiology and biology in general.

Acknowledgments:

Bamfield Marine Station (Vancouver Island, BC, CAN), particularly B. Cameron, for hagfish collection; I.J. McGaw (Univ. of Nevada, Las Vegas, NV, US) for crab collection; J.M. Wilson (CIIMAR, Portugal) for lamprey collection and sampling; D.R. Jones and C.J. Brauner labs (Univ. of British Columbia, CAN), particularly T.T. Jones, for green turtle access and laboratory facilities. Laboratory visits by J.R. Taylor to Bamfield Marine Station and UBC were supplemented by RSMAS (Univ. of Miami, FL, US) MSGSO student travel fund awards and also supported by an NSF award to M. Grosell.

Bibliography

1. **Alvarez, B. V. *et al.*** (2003). Direct extracellular interaction between carbonic anhydrase IV and the human NBC1 sodium/bicarbonate co-transporter. *Biochemistry* **42**, 12321-12329.

2. **Anderson, W. G., Takei, Y., and Hazon, N.** (2002). Osmotic and volaemic effects on drinking rate in elasmobranch fish. *J Exp Biol* **205**, 1115-1122.

3. **Anderson, W. G. *et al.*** (2007). Body fluid volume regulation in elasmobranch fish. *Comp.Biochem.Physiol.* **148**, 3-13.

4. **Anderson, W. G., Takei, Y., and Hazon, N.** (2001). The Dipsogenic Effect of the Renin-Angiotensin System in Elasmobranch Fish. *General and Comparative Endocrinology* **124**, 300-307.

5. **Ando, M., Mukuda, T., and Kozaka, T.** (2003). Water metabolism in the eel acclimated to seawater: from mouth to intestine. *Comp.Biochem.Physiol.B* **136**, 621-633.

6. **Andrade, D. V. *et al.*** (2004). Ventilatory compensation of the alkaline tide during digestion in the snake Boa constrictor. *J Exp Biol* **207**, 1379-1385.

7. **Beamish, F. W. H. and Thomas, E.** (1984). Effects of dietary protein and lipid on nitrogen losses in rainbow trout (*Salmo gairdneri*). *Aquaculture* **41**, 359-371.

8. **Bemis, W. E. and Kynard, B.** (1997). Sturgeon rivers: an introduction to acipenseriform biogeography and life history. *Environmental Biology of Fishes* **48**, 167-183.

9. **Bennett, J. M., Taplin, L. E., and Grigg, G. C.** (1986). Sea water drinking as a homeostatic response to dehydration in hatchling loggerhead turtles *Caretta caretta*. *Comp.Biochem.Physiol.* **83A**, 507-513.

10. **Britton, R. and Krehbiel, C.** (1993). Nutrient Metabolism by Gut Tissues. *J.Dairy Sci.* **76**, 2125-2131.

11. **Brown, D. *et al.*** (1996). Antigen retrieval in cryostat tissue sections and cultured cells by treatment with sodium dodecyl sulfate (SDS). *Histochem.Cell Biol.* **105**, 261-267.

12. **Brown, J. A. *et al.*** (2005). Activation of the newly discovered cyclostome renin-angiotensin system in the river lamprey (*Lampetra fluviatilis*). *J.Exp.Biol* **208**, 223-232.

13. **Bucking, C. and Wood, C. M.** (2006). Gastrointestinal processing of Na+, Cl-, and K+ during digestion: implications for homeostatic balance in freshwater rainbow trout. *Am J Physiol Regul Integr Comp Physiol* **291**, R1764-R1772.

14. **Bucking, C. and Wood, C. M.** (2008). The alkaline tide and ammonia excretion after voluntary feeding in freshwater rainbow trout. *J Exp Biol* **211**, 2533-2541.

15. **Buxton, T. B. *et al.*** (1979). Protein precipitation by acetone for the analysis of polyethylene glycol in intestinal perfusion fluid. *Gastroenterology* **76**, 820-824.

16. **Choe, K. P. and Evans, D. H.** (2003). Compensation for hypercapnia by a euryhaline elasmobranch: Effect of salinity and roles of gills and kidneys in fresh water. *Journal of Experimental Zoology Part A-Comparative Experimental Biology* **297A**, 52-63.

17. **Chu, K. H.** (1987). Sodium transport across the perfused midgut and hindgut of the blue crab *Callinectes sapidus*: the possible role of the gut in crustacean osmoregulation. *Comp.Biochem.Physiol.* **87A**, 21-25.

18. **Cobb, C. S. *et al.*** (2004). Angiotensin I-converting enzyme-like activity in tissues from the Atalntic hagfish (*Myxine glutinosa*) and detection of immunoreactive plasma angiotensins. *Comp.Biochem.Physiol.B* **138**, 357-364.

19. **Cooper, C. A. and Wilson, R. W.** (2008). Post-prandial alkaline tide in freshwater rainbow trout: effects of meal anticipation on recovery from acid-base and ion regulatory disturbances. *J.Exp.Biol* **211**, 2542-2550.

20. **Costa, D. P.** (1982). Energy, nitrogen, electrolyte flux and sea water drinking in the sea otter *Enhydra lutris*. *Physiol.Zool.* **55**, 35-44.

21. **Croxall, J. P. and Prince, P. A.** (1982). Calorific content of squid (Mollusca: Cephalopoda). *Br.Antarct.Surv.Bull.* **55**, 27-31.

22. **Dabrowski, K. *et al.*** (1986). Protein digestion and ion concentrations in Rainbow trout (*Salmo Gairdnerii* Rich.) digestive tract in sea- and fresh water. *Comp.Biochem.Physiol.A.* **83**, 27-39.

23. **Dahl, G.** (1992). The *Xenopus* oocyte cell-cell channel assay for functional analysis of gap junction proteins. In: *Cell-cell Interactions: A Practical Approach* (eds. Stevenson, B., Gallin, W., and Paul, D.), pp. 143-165. New York: Oxford University Press.

24. **Dascal, N.** (1987). The use of *Xenopus* oocytes for the study of ion channels. *CRC Crit.Rev.Biochem.* **22**, 317-387.

25. **do Carmo Fernandes Santos, M.** (2002). Drinking and osmoregulation in the mangrove crab Ucides cordatus following exposure to benzene. *Comparative Biochemistry and Physiology - Part A: Molecular & Integrative Physiology* **133**, 29-42.

26. **Dorwart, M. R. *et al.*** (2008). The solute carrier 26 family of proteins in epithelial ion transport. *Physiology* **23**, 104-114.

27. **Duee, P. H. *et al.*** (1995). Fuel Selection in Intestinal-Cells. *Proceedings of the Nutrition Society* **54**, 83-94.

28. **Evans, D. H.** (1997). The Physiology of Fishes, 2nd ed. pp. 1-544. CRC Press.

29. **Evans, D. H., Piermarini, P. M., and Choe, K. P.** (2005). The multifunctional fish gill: Dominant site of gas exchange, osmoregulation, acid-base regulation, and excretion of nitrogenous waste. *Physiol.Rev.* **85**, 97-177.

30. **Flik, G. and Verbost, P. M.** (1993). Calcium transport in fish gills and intestine. *J Exp Biol* **184**, 17-29.

31. **Fordtran, J. S. and Walsh, J. H.** (1973). Gastric acid secretion rate and buffer content of the stomachafter eating. *J.Clin.Invest.* **52**, 645-657.

32. **Frizzell, R. A. *et al.*** (1979). Coupled sodium-chloride influx across brush border of flounder intestine. *J.Membrane Biol.* **46**, 27-39.

33. **Garcia-Romeu, F. and Maetz, J.** (1964). The mechanism of sodium and chloride uptake by the gills of a freshwater fish, *Carassius auratus*. I. Evidence for an independent uptake of sodium and chloride ions. *J.Gen.Physiol.* **47**, 1195-1207.

34. **Genz, J., Taylor, J. R., and Grosell, M.** (2008). Effects of salinity on intestinal bicarbonate secretion and compensatory regulation of acid-base balance in *Opsanus beta*. *J.Exp.Biol* **211**, 2327-2335.

35. **Gilmour, K. *et al.*** (1998). Nitrogen excretion and the cardiorespiratory physiology of the gulf toadfish, *Opsanus beta*. *Physiol.Zool.* **71**, 492-505.

36. **Goss, G. G. *et al.*** (1998). Gill morphology and acid-base regulation in freshwater fishes. *Comparative Biochemistry and Physiology A-Molecular & Integrative Physiology* **119**, 107-115.

37. **Goss, G. G. *et al.*** (1992). Mechanisms of Ion and Acid-Base Regulation at the Gills of Fresh-Water Fish. *Journal of Experimental Zoology* **263**, 143-159.

38. **Grosell, M.** (2007). Intestinal transport processes in marine fish osmoregulation. *In: Fish osmoregulation, Eds Bernardo Baldisserotto, Juan Miquel Mancera, B.G.Kapoor.* 332-357.

39. **Grosell, M.** (2006). Intestinal anion exchange in marine fish osmoregulation. *J.Exp.Biol* **209**, 2813-2827.

40. **Grosell, M. and Genz, J.** (2006). Ouabain sensitive bicarbonate secretion and acid absorption by the marine fish intestine play a role in osmoregulation. *Am.J.Physiol.* **291**, R1145-R1156.

41. **Grosell, M. *et al.*** (2009a). The involvement of H^+-ATPase and carbonic anhydrase in intestinal HCO_3^- secretion in seawater acclimated rainbow trout. *J.exp.Biol.* **In Press**.

42. **Grosell, M., Gilmour, K. M., and Perry, S. F.** (2007). Intestinal carbonic anhydrase, bicarbonate, and proton carriers play a role in the acclimation of rainbow trout to seawater. *American Journal of Physiology-Regulatory Integrative and Comparative Physiology* **293**, R2099-R2111.

43. **Grosell, M. *et al.*** (2000a). A nose-to-nose comparison of the physiological effects of exposure to ionic silver versus silver chloride in the European eel (*Anguilla anguilla*) and the rainbow trout (*Oncorhynchus mykiss*). *Aquat.Toxicol* **48**, 327-342.

44. **Grosell, M. *et al.*** (2001). Intestinal HCO_3^- secretion in marine teleost fish: evidence for an apical rather than a basolateral Cl^-/HCO_3^- exchanger. *Fish Physiol.Biochem.* **24**, 81-95.

45. **Grosell, M., Mager E.M., and Williams, C.** (2009b). High rates of HCO_3^- secretion and Cl^- absorption against adverse gradients in the marine teleost intestine: the involvement of an electrogenic anion exchanger and H^+-pump metabolon? *J Exp Biol* ***In Press***.

46. **Grosell, M. *et al.*** (2004). Effects of prolonged copper exposure in the marine gulf toadfish (*Opsanus beta*). I. hydromineral balance and plasma nitrogenous waste products. *Aquat.Tox.* **68**, 249-262.

47. **Grosell, M., O'Donnell, M. J., and Wood, C. M.** (2000b). Hepatic versus gallbladder bile composition: in vivo transport physiology of the gallbladder in rainbow trout. *American Journal of Physiology-Regulatory Integrative and Comparative Physiology* **278**, R1674-R1684.

48. **Grosell, M. and Taylor, J. R.** (2007). Intestinal anion exchange in teleost water balance. *Comparative Biochemistry and Physiology A-Molecular & Integrative Physiology* **148**, 14-22.

49. **Grosell, M. *et al.*** (2005). Bicarbonate secretion plays a role in chloride and water absorption of the European flounder intestine. *Am.J.Physiol.* **288**, R936-R946.

50. **Gross, E. *et al.*** (2002). Regulation of the sodium bicarbonate cotransporter kNBC1 function: role of Asp986, Asp988 and kNBC1-carbonic anhydrase II binding. *The Journal of Physiology* **544**, 679-685.

51. **Herrin, R. C.** (1935). Chemical changes in blood and intestinal juice produced by the loss of intestinal juice. *J.Biol.Chem.* **108**, 547-562.

52. **Hersey, S. J. and Sachs, G.** (1995). Gastric acid secretion. *Physiol.Rev.* **75**, 155-189.

53. **Hickman, C. P. and Trump, B. F.** (1969). The Kidney. *Fish Physiology* **Hoar, W.S. and Randall, D.J. New York Academic Press**, 91-239.

54. **Hills, A. G.** (1973). Acid-base balance: chemistry, physiology, pathophysiology. Baltimore: Williams and Wilkins.

55. **Hogan, D. L.** (1994). Review article: gastroduodenal bicarbonate secretion. *Aliment.Pharmacol.Ther.* **8**, 475-488.

56. **Holmes, W. N. and McBean, R. L.** (1964). Some aspects of electrolyte excretion in the green turtle, *Chelonia mydas mydas*. *J.exp.Biol.* **41**, 81-90.

57. **Iwama, G. K. and Heisler, N.** (1991). Effect of environmental water salinity on acid-base regulation during environmental hypercapnia in the Rainbow trout (*Oncorhynchus mykiss*). *J.exp.Biol.* **158**, 1-18.

58. **Jobling, M.** (1981). The Influences of Feeding on the Metabolic-Rate of Fishes - A Short Review. *Journal of Fish Biology* **18**, 385-400.

59. **Kidder, G. W., Petersen, C. W., and Preston, R. L.** (2006). Energetics of osmoregulation: II. Water flux and osmoregulatory work in the euryhaline fish, Fundulus heteroclitus. *Journal of Experimental Zoology Part A-Comparative Experimental Biology* **305A**, 318-327.

60. **Kobayashi, H. and Takei, Y.** (1996). Berlin: Springer Verlag.

61. **Krebs, H. A.** (1975). The august Krogh Principle:"For many problems there is an animal on which it can be most conviniently studied.". *J.Exp.Zool.* **194**, 221-226.

62. **Kristiansen, H. R. and Rankin, J. C.** (2001). Discrimination between endogenous and exogenous water sources in juvenile rainbow trout fed extruded dry feed. *Aquat.Living Resour* **14**, 359-366.

63. **Krogh, A. and Leitch, I.** (1919). The respiratory function of the blood in fishes. *J Physiol* **52**, 288-300.

64. **Kurita, Y. *et al.*** (2008). Identification of intestinal bicarbonate transporters involved in formation of carbonate precipitates to stimulate water absorption in marine teleost fish. *American Journal of Physiology-Regulatory Integrative and Comparative Physiology* **294**, R1402-R1412.

65. **Kyte, J. and Doolittle, R. F.** (1982). A simple method for displaying the hydropathic character of a protein. *J.Mol.Biol.* **157**, 105-132.

66. **Li, H. C. *et al.*** (2007). Identification of a novel signal in the cytoplasmic tail of the Na^+:HCO_3^- cotransporter NBC1 that mediates basolateral targeting. *Am.J.Physiol.Renal physiol* **292**, F1245-F1255.

67. **Lignot, J. H., Helmstetter, C., and Secor, S. M.** (2005). Postprandial morphological response of the intestinal epithelium of the Burmese python (Python, molurus). *Comp.Biochem.Physiol.A* **141**, 280-291.

68. **Loretz, C. A.** (1995). Electrophysiology of ion transport in the teleost intestinal cells. *Cellular and Molecular Approaches to Fish Ionic Regulation, Fish Physiology Eds.C.M.Wood and T.J.Shuttleworth* **14**, 25-56.

69. **Lu, J. and Boron, W. F.** (2007). Reversible and irreversible interactions of DIDS with the human electrogenic Na/HCO_3 cotransporter NBCe1-A: role of lysines in the KKMIK motif of TM5. *Am.J.Physiol.Cell Physiol.* **292**, C1787-C1798.

70. **Lu, J. *et al.*** (2006). Effect of human carbonic anhydrase II on the activity of the human electrogenic Na/HCO3 cotransporter NBCe1-A in Xenopus oocytes. *Journal of Biological Chemistry* **281**, 19241-19250.

71. **Maetz, J. and Romeu, F. G.** (1964). The mechanism of sodium and chloride uptake by the gills of a fresh-water fish, *Carassius auratus*. II. Evidence for NH_4^+/Na^+ and HCO_3^-/Cl^- exchangers. *Journal of General Physiology* **47**, 1209-1227.

72. **Mandel, L. J. and Balaban, R. S.** (1981). Stoichiometry and coupling of active transport to oxidative metabolism in epithelial tissues. *Am J Physiol Renal Physiol* **240**, F357-F371.

73. **Mantel, L. H.** (1968). The foregut of Gecarcinus lateralis as an organ of salt and water balance. *Am.Zool.* **8**, 433-442.

74. **Marshall, W. S. and Grosell, M.** (2005). Ion transport, osmoregulation and acid-base balance. (eds. Evans, D. H. and Claiborne, J. B.),CRC press.

75. **Mccue, M. D.** (2006). Specific dynamic action: A century of investigation. *Comparative Biochemistry and Physiology A-Molecular & Integrative Physiology* **144**, 381-394.

76. **McDonald, M. D. and Grosell, M.** (2006). Maintaining osmotic balance with an aglomerular kidney. *Comparative Biochemistry and Physiology A-Molecular & Integrative Physiology* **143**, 447-458.

77. **McDonald, M. D. *et al.*** (2003). Branchial and renal handling of urea in the gulf toadfish, Opsanus beta: the effect of exogenous urea loading. *Comparative Biochemistry and Physiology A-Molecular & Integrative Physiology* **134**, 763-776.

78. **McMillan, D. N. and Houlihan, D. F.** (1998). The effect of refeeding on tissue protein synthesis in rainbow trout. *Physiol.Zool.* **61**, 429-441.

79. **McMurtrie, H. L. *et al.*** (2004). The bicarbonate transport metabolon. *Journal of Enzyme Inhibition and Medicinal Chemistry* **19**, 231-236.

80. **Morris, R.** (1958). General problems of osmoregulation with special reference to cyclosomes. *Symp.Zoo.Soc.Lond.* 1-16.

81. **Musch, M. W. *et al.*** (1982). Na^+-K^+-$2Cl^-$ co-transport in the intestine of a marine teleost. *Nature* **300**, 351-353.

82. **Nelson, L. E. and Sheridan, M. A.** (2006). Gastroenteropancreatic hormones and metabolism in fish. *Gen.Comp.Endocrinol.* **In press**.

83. **Niv, Y. and Fraser, G. M.** (2002). The Alkaline Tide Phenomenon. *Journal of Clinical Gastroenterology* **35**.

84. **Novak, I.** (2000). Keeping up with bicarbonate. *Journal of Physiology* **528**, 235.

85. **Ortiz, R. M.** (2001). Osmoregulation in marine mammals. *J Exp Biol* **204**, 1831-1844.

86. **Perry, S. F. and Wood, C. M.** (1989). Control and co-ordination of gas transfer in fishes. *Can.J.Zool.* **67**, 2961-2970.

87. **Pickering, A. D. and Morris, R.** (1973). Localization of ion-transport in the intestine of the migrating river lamprey, *Lametra fluviatilis* L. *J.xp.Biol.* **58**, 165-176.

88. **Piermarini, P. M., Kim, E. Y., and Boron, W. F.** (2007). Evidence against a direct interaction between intracellular carbonic anhydrase II and pure C-terminal domains of SLC4 bicarbonate transporters. *Journal of Biological Chemistry* **282**, 1409-1421.

89. **Prange, H. D.** (1985). Renal and Extra-renal mechanisms of salt and water regulation of sea turtles: A speculative perspective. *Copeia* **3**, 771-776.

90. **Ramkumar, D. and Schulze, K. S.** (2005). The pylorus. *Neurogastroenterol.Motil.* **17**, 22-30.

91. **Rankin, J. C.** (1997). In: *Ionic Regulation in Animals* (eds. Hazon, N., Eddy, F. B., and Flik, G.), pp. 50-69. Berlin: Springer.

92. **Rankin, J. C.** (2002). In: *Osmoregulation and Drinking in Vertebrates* (eds. Hazon, N. and Flik, G.), pp. 1-17. Oxford: BIOS Scientific Publishers Ltd.

93. **Rankin, J. C. *et al.*** (2004). Identification of Angiotensin I in a Cyclostome, Lampetra fluviatilis. *Zoological Science* **21**, 173-179.

94. **Rodriguez, A. *et al.*** (2002). Osmoregulation in juvenile Siberian sturgeon (Acipenser baerii). *Fish.Physiol.Biochem.* **26**, 345-354.

95. **Romero, M. F.** (2001). The electrogenic Na+/HCO3- cotransporter, NBC. *J.Pancreas* **2**, 182-191.

96. **Romero, M. F. and Boron, W. F.** (1999). Electrogenic Na^+/HCO_3^- cotransporters: cloning and physiology. *Annu.Rev.Physiol.* **61**, 699-723.

97. **Romero, M. F., Fulton, C. M., and Boron, W. F.** (2004). The SLC4 family of HCO_3^- transporters. *Pflügers Archieves - European Journal of Physiology* **447**, 495-509.

98. **Romero, M. F. *et al.*** (1997). Expression cloning and characterization of a renal electrogenic Na^+/HCO_3^- cotransporter. *Nature* **387**, 409-413.

99. **Rune, S. J.** (1965). The metabolic alkalosis following aspiration of gastric acid secretion. *Scand J Clin Lab Invest.* **17**, 305-310.

100. **Scott, G. R. *et al.*** (2008). Physiological and molecular mechanisms of osmoregulatory plasticity in killifish after seawater transfer. *J Exp Biol* **211**, 2450-2459.

101. **Scott, G. R., Schulte, P. M., and Wood, C. M.** (2006). Plasticity of osmoregulatory function in the killifish intestine: drinking rates, salt and water transport, and gene expression after freshwater transfer. *J Exp Biol* **209**, 4040-4050.

102. **Secor, S. M. and Diamond, J.** (1995). Adaptive responses to feeding in Burmese pythons: pay before pumping. *J Exp Biol* **198**, 1313-1325.

103. **Secor, S. M. and Diamond, J.** (1998). A vertebrate model of extreme physiological regulation. *Nature* **395**, 659-662.

104. **Secor, S.** (2009). Specific dynamic action: a review of the postprandial metabolic response. *Journal of Comparative Physiology B: Biochemical, Systemic, and Environmental Physiology* **179**, 1-56.

105. **Shehadeh, Z. H. and Gordon, M. S.** (1969). The role of the intestine in salinity adaptation of the rainbow trout, *Salmo gairdneri*. *Comp.Biochem.Physiol.* **30**, 397-418.

106. **Smith, H. W.** (1930). The absorption and excretion of water and salts by marine teleosts. *Am.J.Physiol.* **93**, 480-505.

107. **Smith, H. W.** (1931). The absorption and excretion of water and salts by the elasmobranch fishes. II. Marine elasmobranchs. *Am.J.Physiol.* **98**, 296-310.

108. **Smith, N. F., Talbot, C., and Eddy, F. B.** (1989). Dietary salt intake and its relevance to ionic regulation in freshwater salmonids. *J.Fish Biol.* **35**, 749-753.

109. **Sterling, D., Reitmeier, R. A. F., and Casey, J. R.** (2001). A transport metabolon. *J.Biol.Chem.* **276**, 47886-47894.

110. **Steward, M. C., Ishiguro, H., and Case, R. M.** (2005). Mechanisms of bicarbonate secretion in the pancreatic duct. *Annu.Rev.Physiol.* **67**, 377-409.

111. **Sugiura, S. H. and Hardy, R. W.** (2000). Environmentally friendly feeds. In: *Encyclopedia of Aquaculture* (ed. Stickney, R. R.), pp. 299-310. New York: John Wiley.

112. **Takei, Y.** (2000). Comparative physiology of body fluid regulation in vertebrates with special reference to thirst regulation. *Japanese Journal of Physiology* **50**, 171-186.

113. **Takei, Y. *et al.*** (1993). A novel angiotensin I isolated from an elasmobranch fish. *J Endocrinol* **139**, 281-285.

114. **Takei, Y. *et al.*** (2004). Identification of angiotensin I in several vertebrate species: its structural and functional evolution. *General and Comparative Endocrinology* **135**, 286-292.

115. **Taylor, J. R. and Grosell, M.** (2006a). Evolutionary aspects of intestinal bicarbonate secretion in fish. *Comparative Biochemistry and Physiology A-Molecular & Integrative Physiology* **143**, 523-529.

116. **Taylor, J. R. and Grosell, M.** (2006b). Feeding and osmoregulation: dual function of the marine teleost intestine. *J.Exp.Biol* **209**, 2939-2951.

117. **Taylor, J. R., Mager E.M., and Grosell, M.** (2009). Basolateral NBCe1 plays a rate-limiting role in transepithelial intestinal HCO_3^- secretion serving marine fish osmoregulation. *J Exp Biol* ***In review***.

118. **Taylor, J. R. *et al.*** (2007). Postprandial acid-base balance in freshwater and seawater-acclimated European flounder, *Platichthys flesus*. *J.Comp.Physiol.* **177**, 597-608.

119. **Thomas, M. A. and Machen, T. E.** (1991). Regulation of Cl/HCO_3 exchange in gastric parietal cells. *Cell Regul.* **2**, 727-737.

120. **Thorson, T. B.** (1961). The Partitioning of Body Water in Osteichthyes: Phylogenetic and Ecological Implications in Aquatic Vertebrates. *Biological Bulletin* **120**, 238-254.

121. **Tomasso, J. R. and Grosell, M.** (2004). Physiological basis for large differences in resistance to nitrite among freshwater and freshwater acclimated euryhaline fishes. *Environ.Sci.Technol.* **39**, 98-102.

122. **Tresguerres, M. *et al.*** (2007). V-H+-ATPase translocation during blood alkalosis in dogfish gills: interaction with carbonic anhydrase and involvement in the postfeeding alkaline tide. *Am J Physiol Regul Integr Comp Physiol* **292**, R2012-R2019.

123. **Tseng, Y. C. and Hwang, P. P.** (2008). Some insights into energy metabolism for osmoregulation in fish. *Comparative Biochemistry and Physiology Part C: Toxicology & Pharmacology* **148**, 419-429.

124. **Ussing, H. H. and Zerahn, K.** (1951). Active Transport of Sodium as the Source of Electric Current in the Short-circuited Isolated Frog Skin. *Acta Physiologica Scandinavica* **23**, 110-127.

125. **Verdouw, H., Van Echteld, C. J. A., and Dekkers, E. M. J.** (1978). Ammonia determination based on indophenol formation with sodium salicylate. *Water Research* **12**, 399-402.

126. **Vielma, J. and Lall, S. P.** (1997). Dietary formic acid enhances apparent digestibility of minerals in rainbow trout, *Oncorhynchus mykiss* (Walbaum). *Aquaculture Nutrition* **3**, 265-268.

127. **Vielma, J., Ruohonen, K., and Lall, S. P.** (1999). Supplemental citric acid and particle size of fish bone-meal influence the availability of minerals in rainbow trout *Oncorhynchus mykiss* (Walbaum). *Aquaculture Nutrition* **5**, 65-71.

128. **Walsh, P. J. *et al.*** (1991). Carbonate deposits in marine fish intestines: a new source of biomineralization. *Limnology and Oceanography* **36**, 1227-1232.

129. **Wang, J. J. *et al.*** (2007). Modulation of membrane channel currents by gap junction protein mimetic peptides: size matters. *American Journal of Physiology-Cell Physiology* **293**, C1112-C1119.

130. **Wang, T., Busk, H., and Overgaard, J.** (2001). The respiratory consequences of feeding in amphibians and reptiles. *Comparative Biochemistry and Physiology A-Molecular & Integrative Physiology* **128**, 535-549.

131. **Wilkie, M. P.** (2002). Ammonia excretion and urea handling by fish gills: Present understanding and future research challenges. *Journal of Experimental Zoology* **293**, 284-301.

132. **Wilson, R. W.** (1999). A novel role for the gut of seawater teleosts in acid-base balance. *Regulation of Acid-Base Status in Animals and Plants, SEB seminar series, Cambridge University Press, Cambridge* **68**, 257-274.

133. **Wilson, R. W. *et al.*** (1996). Intestinal base excretion in the seawater-adapted rainbow trout: a role in acid-base balance? *J.Exp.Biol* **199**, 2331-2343.

134. **Wilson, R. W. and Grosell, M.** (2003). Intestinal bicarbonate secretion in marine teleost fish - source of bicarbonate, pH sensitivity, and consequence for whole animal acid-base and divalent cation homeostasis. *Biochim.Biophys.Acta* **1618**, 163-193.

135. **Wilson, R. W. *et al.*** (2009). Contribution of fish to the marine inorganic carbon cycle. *Science* **323**, 359-362.

136. **Wilson, R. W., Wilson, J. M., and Grosell, M.** (2002). Intestinal bicarbonate secretion by marine teleost fish-why and how? *Biochim.Biophys.Acta* **1566**, 182-193.

137. **Wood, C. M.** (2001). Influence of feeding, exercise, and temperature on nitrogen metabolism and excretion. In: *Nitrogen Excretion* (eds. Wright, P. and Anderson, P.), pp. 201-238. New York: Academic Press.

138. **Wood, C. M. *et al.*** (2005). Alkaline tide and nitrogen conservation after feeding in an elasmobranch (Squalus acanthias). *J Exp Biol* **208**, 2693-2705.

139. **Wood, C. M. *et al.*** (2007a). The alkaline tide goes out and the nitrogen stays in after feeding in the dogfish shark, Squalus acanthias. *Respiratory Physiology & Neurobiology* **159**, 163-170.

140. **Wood, C. M. *et al.*** (2007b). Osmoregulation, ionoregulation and acid-base regulation by the gastrointestinal tract after feeding in the elasmobranch (Squalus acanthias). *J Exp Biol* **210**, 1335-1349.

141. **Wood, C. M. *et al.*** (2009). Using omeprazole to link the components of the post-prandial alkaline tide in the spiny dogfish, Squalus acanthias. *J Exp Biol* **212**, 684-692.

142. **Wood, C. *et al.*** (2008). Is the alkaline tide a signal to activate metabolic or ionoregulatory enzymes in the dogfish shark (*Squalus acanthias*)? *Physiological and Biochemical Zoology* **81**, 278-287.

143. **Zall, D. M., Fisher, D., and Garner, M. D.** (1956). Photometric determination of chlorides in water. *Anal.Chem.* **28**, 1665-1678.

144. **Zerahn, K.** (1956). oxygen consumption and active sodium transport in the isolated and short-circuited frog skin. *Acta Physiologica Scandinavica* **36**, 300-318.